Use Authorization

In presenting this thesis in partial fulfillment of the requirements for an advanced degree at Idaho State University, I agree that the Library shall make it freely available for inspection. I further state that permission to download and/or print my thesis for scholarly purposes may be granted by the Dean of the Graduate School, Dean of my academic division, or by the University Librarian. It is understood that any copying or publication of this thesis for financial gain shall not be allowed without my written permission.

Signature ___________________________________

Date _______________________________________

THE RELIABILITY OF A CIRCULAR REINFORCED CONCRETE BRIDGE PIER SUBJECT TO SEQUENTIAL VEHICULAR IMPACT AND BLAST LOADING

by

Kylie Steel

A thesis

submitted in partial fulfillment

of the requirements for the degree of

Master of Science in the Department of Civil and Environmental Engineering Idaho State University

Spring 2014

Committee Approval

To the Graduate Faculty:

The members of the committee appointed to examine the thesis of KYLIE STEEL find it satisfactory and recommend that it be accepted.

____

Major Advisor

Dr. Andrew Sorensen

____

Committee Member

Dr. Arya Ebrahimpour

____

Graduate Faculty Representative

Dr. Ken Bosworth

TABLE OF CONTENTS

LIST OF FIGURES

LIST OF TABLES

THE RELIABILITY OF A CIRCULAR REINFORCED CONCRETE BRIDGE PIER SUBJECT TO SEQUENTIAL VEHICULAR IMPACT AND BLAST LOADING

Thesis Abstract – Idaho State University (2014)

This study determines the structural reliability of circular reinforced concrete bridge piers that experience vehicular impact, blast loading, and sequential vehicular impact followed by blast loading. A numerical model is developed in MATLAB employing Monte Carlo simulation and a first order, second moment reliability analysis using the flexural capacity of the bridge pier as the limit state for the analysis. Several pier resistance and loading scenarios are considered and sensitivity analyses are carried out for the purpose of identifying the most influential parameters of the impact and blast loadings. The investigation of the sequential multi-hazard loading leads to the conclusion that multi-hazardous events are extremely detrimental to circular reinforced concrete bridge piers. Traditional methods of multi-hazard analysis do not adequately consider sequential loading and the structural resistance reduction methodology developed in this study is a better indicator of the reliability of the bridge pier subject to two hazardous, sequential loadings.

CHAPTER 1

INTRODUCTION

1.1 Background and Motivation

Human safety and asset protection has always been the priority of design engineers and as the level of technical knowledge in the structural engineering field advances, the necessity to provide economic designs with increased safety capacities against limited-duration, high- intensity loads, (e.g. seismic, hurricane, blast, etc.) intensifies. Loadings that structures are designed to support are typically continuous over time, such as dead and live loads, whereas hazardous loads are not typical or predictable and impose a force of great magnitude on the structure in a short duration of time.

Current design code allows for one peak hazardous loading to be applied to a structure at one time, but does not provide a method of analysis allowing for multiple high-intensity loadings (American Society of Civil Engineers (ASCE), 2010; Collins & Nowak, 2000). The analysis of loadings in sequence over time is especially important for hazardous loadings. Additionally, hazardous sequential loadings deal with the analysis of a structure whose load capacity may have been compromised by an initial load, and then immediately subjected to a second load. The investigation of multiple hazardous loadings on a structure is the main focus of this study.

Structures are susceptible to natural disasters, intentional hazards, and accidental hazards, due to their vulnerability to the public. Structural vulnerability includes the structure's accessibility and importance to the overall system. Natural disasters include events such as earthquakes, floods, and hurricanes. Intentional hazards include terrorist attacks, such as explosive events. Accidental hazards include man-made dangers that are unplanned or unintentional, such as fire or vehicle impact. The sequential hazardous loadings that are analyzed in this study include a vehicle impact event and an explosive event. Impact and blast are the loadings of interest because terrorists can cause lethal damage with these two hazards and the vulnerability of structures to these loadings is significant. Both accidental and intentional impact-loading events are analyzed; the difference lying in the vehicle velocity and acceleration. Accidental impact loadings most likely occur with a vehicle travelling at an acceptable speed, near the speed limit, and decelerating rather than accelerating. Both of these factors are considered in the analysis. Intentional events can include a greater impact force from heightened vehicle velocities and accelerations. Intentional blast events result in high blast pressure loadings on the bridge pier due to the intent to damage. With this information, different impact and blast forces are determined for each type of vehicle, and used as the loading random variables.

Buildings have typically been the focus of blast damage analysis, but it is valuable to extend the analysis to bridges to improve transportation infrastructure security (Galati et. al., 2007). Bridges are a vital part of any transportation infrastructure, especially in the United States' federal interstate system. Bridges have the potential for hazardous loadings, are frequently utilized, and can result in negative economical consequences if removed from service. Removal of a bridge, even if only temporarily, from a regional transportation system can cause disruption to the network resulting in potentially large economic losses.

Bridge piers are important load-bearing components of a bridge system, and local failure of these individual components could lead to progressive system failure. Bridge piers are susceptible to accidental vehicle impact or purposeful terrorist attack due to their vulnerability, specifically their accessibility and importance to the transportation system. Figures 1.1 and 1.2 display the vulnerability of a bridge pier to vehicles on the roadway. The objective of terrorism is to cause chaos or disruption, and as such the financial impact of a failed or damaged bridge can be significant. Because of the importance and vulnerability of bridges, understanding their response to this type of loading is critical and the necessity to provide economic designs with increased safety capacities against limited-duration, high-intensity loads, (e.g. seismic, hurricane, impact, etc.) is becoming a serious focus in structural design due to recent occurrences.

Figure 1.1: Accessible Bridge Piers

Figure 1.2: Damaged Bridge Pier

According to the U.S. Federal Highway Administration, vehicle impact is the third leading cause of bridge damage and/or failure (Agrawal & Chen, 2008). In a vehicular impact with a bridge pier event, damage simultaneously occurs in both the vehicle and the reinforced concrete bridge pier (El-Tawil, 2004). El-Tawil defines this type of impact event as a “soft” impact, which allows for the impact loading to be treated as a static loading due to similar failure mechanisms. In addition to this type of impact, the study considers an explosive resulting from a vehicle bomb. A vehicle bomb is a large terrorist explosive transported via car or truck. Public bridges are vulnerable to vehicle bomb attacks due to the accessibility to the general public and limited surveillance.

Progressive structural failure is typically the result of pier failure due to their role as the primary load carrying elements in a structure. "A better understanding of residual capacity in columns would aid in the prediction of the overall performance of buildings, its resistance to progressive collapse and determining the stability of damaged buildings" (Bao & Li, 2009, p. 1). Residual capacity, or strength, describes the loading that a structure or structural element can tolerate without experiencing failure. In this study, the residual strength of a concrete bridge pier subjected to impact and blast loading is determined using reliability analysis.

To assess the safety of a structure, engineers attempt to quantify the risk of damage or failure associated with the application of various loads to the structure. A structure's ability to resist structural damage and/or failure depends on both the strength of the structure and the different load combinations experienced by the structure (Ayyub & McCuen, 2011). In general, the resistance, or strength, of the structure needs to exceed the loading.

Structural reliability is a method that assesses the safety and reliability of a structure. In reliability analysis, the probability of failure is determined and used to estimate the reliability index, which is a parameter used to measure the reliability of a structure or structural element. Reliability is a primary consideration and ongoing focus area in structural engineering due to the necessity of safety of human life and the economy. Multi-hazard analysis is a reliability analysis of two or more hazardous loadings. When a structural element experiences one hazardous loading, it is assumed to start with its original design strength. If multi-hazard loading occurs, the above concept applies for the first loading, but not necessarily for the subsequent loading. The second loading occurs after the pier may already be damaged. That is, the residual strength of the pier will have decreased from the first hazardous loading, and then be further damaged from the second hazardous loading. The difficulty lies in accounting for the previous damage inflicted on the bridge pier from the first loading into the final probability of failure due to both loadings.

1.2 Problem Definition and Scope

Current research has been conducted regarding the structural effect from an impact loading or a blast loading by itself (Agrawal & Chen, 2008; Doege & Gebbeken, n.d.; El-Tawil, 2004; Longinow & Mniszewski, 1996), but there is insufficient research on examining the effect of sequential loading. This research study is interested in the determination of the probability of failure of a circular reinforced concrete bridge pier that experiences impact loading followed by blast loading. A detailed description of impact loading and blast loading is provided in Chapter 2. Therefore, the purpose of this study is to determine the probability of failure of a circular reinforced concrete bridge pier that experiences impact and blast loading successively. By better understanding the reliability of reinforced concrete bridge pierss, future bridge designs can be improved upon and made safer for the public and reduce potential economic loss. With increased reliability in structural design, the risk to human and structural lives can be decreased.

This thesis addresses the following questions in order to determine the probability of failure of a bridge pier that experiences both impact and blast loading:

(1) What is the probability of failure of a bridge pier that encounters an impact event? What are the impact loading factors that most contribute to high probabilities of failure?

(2) What is the probability of failure of a bridge pier that encounters a blast event? What are the blast loading factors that most contribute to high probabilities of failure?

(3) A reduction factor needs to be applied to the pier resistance after the first hazardous event has occurred. What reduction factor should be applied to the resistance aspect of the limit state equation to account for the already inflicted damage to the pier to be used in the reliability analysis of the second loading?

(4) What is the probability of failure of a bridge pier that encounters an impact and blast event successively?

(5) What are possible countermeasures to reduce probability of failure? What are the most cost-efficient countermeasures?

In addressing these questions, this thesis expands upon knowledge of structural reliability of a bridge pier subjected to an impact loading followed by a blast loading.

1.3 Objectives

In order to address the questions posed in the previous section, the objectives of this study are:

(1) Determine the probability of failure and residual strength of a bridge pier due to an impact event.

(2) Determine the probability of failure and residual strength of a bridge pier due to a blast event.

(3) Determine a range of resistance reduction factors corresponding to associated probabilities of failure to be used in the multi-hazardous reliability analysis after the impact event.

(4) Determine the probability of failure and residual strength of a bridge pier due to a blast load following an impact load.

(5) Perform a sensitivity analysis and develop sets of fragility curves corresponding to the impact, blast, and multi-hazardous loading imposed on different concrete bridge pier resistance scenarios.

(6) Identify the factors that most contribute to high probabilities of failure and identify countermeasures to reduce the probabilities of failure.

1.4 Research Tasks and Methodology

To achieve the objectives of this study, a numerical model using Monte Carlo simulation is created in the software package MATLAB to perform the reliability analysis utilizing the first-order, second-moment method. A summary of tasks carried out follows:

(1) System definition: define the bridge pier resistance equations and loading equations to form limit state functions for the impact event, blast event, and multi-hazardous event. Define the random variables in the performance equations. Gather statistical data on the random variables.

(2) Construct the MATLAB code, incorporating the Monte Carlo simulation. A simulation method, rather than physical testing, is used because it allows for the manipulation of a representative system rather than a real system, which is ideal for sensitivity analysis. The Monte Carlo method is a technique used to simulate random numbers and formulate results using randomly generated values without any or limited physical testing (Collins & Nowak, 2000).

(3) A range of typical vehicle masses and velocities are determined for this analysis. With this information, different impact forces are determined for each type of vehicle, and used as the impact random variable.

(4) The range of the blast charge weights is a function of the size of the vehicles. Smaller vehicles have a smaller charge weight capacity, because they have less room to store the explosive. Similarly, larger vehicles have a larger capacity for a larger explosive, but still have a maximum limit. A range of charge weights are defined by the US Department of Energy and used to determine the blast load random variable (US Department of Energy, 2012).

(5) The study contains several different values of the random variables. The simulation is completed for each scenario. An example of a possible scenario is a SUV/van travelling at an extremely high speed transporting the vehicle bomb. This is considered an intentional hazardous event. The random variables are applied to a combined stress equation defining the structural system, considering both the design loading, causing compression in the structure, and both of the hazardous loadings, causing bending in the structure (Al-Manaseer & Hassoun, 2012).

(6) The probabilities of failure due to just the impact load and blast load alone are determined using the above procedures outlined. The Monte Carlo simulation and first-order, second-moment reliability analysis is performed for each loading and resistance scenario.

(7) The probability of failure due to the multi-hazard loading is determined using the above procedures outlined. When the blast loading is applied to the pier, the pier

is already damaged from the first hazardous loading, the impact force. This results in an increased probability of failure of the concrete bridge pier from the already determined failure probabilities in the impact analysis. A second simulation for the combination is performed considering the blast loading in the limit state equation. The resilience in the limit state equation is reduced to include the already determined probability of failure of the weakened structure. The Monte Carlo simulation is performed twice due to the impact and blast load variables, one time after each of these loadings.

(8) Sensitivity analysis is carried out to identify the factors that most contribute to high probabilities of failure. Fragility curves are generated to provide a graphical representation of the sensitivity analysis.

(9) Identify possible countermeasures to reduce failure probabilities of bridge piers. Perform a cost analysis to identify the most efficient countermeasures.

1.5 Thesis Overview

This thesis is divided into six chapters. The introduction (Chapter 1) is followed by Chapter 2, which contains a literature review of existing research relevant to this study. A detailed description of the methodology, loading combination definition, and structural resistance determination is presented in Chapter 3. Chapter 4 includes impact analysis and the corresponding sensitivity analysis. The blast analysis and corresponding sensitivity analysis is presented in Chapter 5. Chapter 6 presents the results of the multi-hazard analysis and the corresponding sensitivity analysis. The thesis ends with conclusions, countermeasures, and suggestions for future work (Chapter 7). A bibliography is shown at the end of the thesis, and the developed MATLAB codes are included in the Appendices.

CHAPTER 2

LITERATURE REVIEW

This chapter presents a review of the literature relevant to the study of multi-hazard analysis of reinforced concrete bridge piers. The chapter is divided into five sections. The first section presents a description of vehicle impact force events, including AASHTO standards and pier capacity and demand. The second section discusses blast events and addresses vehicle explosives and the critical charge weight. The third section presents a discussion of reliability analysis and Monte Carlo Simulation. This section discusses the overview and intention of simulation methods, the general procedure, and the use of MATLAB to perform the simulation. Section four discusses multi-hazard and risk analysis. The last section provides a summary of the literature relevant to the study.

2.1 Impact Analysis

2.1.1 Transportation System and Vehicle Impact

Over 600,000 bridges are registered in the National Bridge Inventory of the Federal Highway Administration (Agrawal & Chen, 2008). As of the end of 2011, the Federal Highway Administration recorded approximately 251,500 concrete bridges and 142,500 prestressed concrete bridges registered to the National Bridge Inventory. According to the Federal Highway Administration, vehicle impact is the third leading cause of bridge damage and/or failure (Agrawal & Chen, 2008). Because of increasing bridge damage, the number of vehicle impacts to structural bridges is becoming an increasingly investigated issue. Vehicle impacts can result in the loss of lives and failure of the bridge system, which can lead to transportation system and economic loss (El-Tawil, 2004).

The transportation system consists of roads, bridges, and any other means the population uses to travel. The transportation system allows for employment and can result in the reduction of time and costs (Notteboom & Rodrigue, 2012). Bridges are used for the transport of goods and people, which are necessary constituents in the economic system. Because of the critical role the transportation system plays in the economy, failure of components of the system will result in economical loss.

In a study by Agrawal and Chen (2008), guidelines provided from bridge case studies have been created to analyze the damage caused by vehicle collisions to bridge structural elements, such as bridge girders. Damaged girder inspections resulted in 61 percent having minor damages, 25 percent having moderate damages, and 14 percent having severe damage, such as loss of a material section (Agrawal & Chen, 2008).

Impact loads are probabilistic in nature due to their randomness in occurrence and intensity. There is a gap in the research regarding impact loads and bridge substructures, which confirms the importance of a study (Cizmar et. al., 2008). The risk of vehicle impact on a bridge depends on the amount of traffic and possible consequences resulting from an impact event.

2.1.2 Vehicle Impact Force and AASHTO Standards

A vehicle impact event to a bridge can have severe consequences on human life, the transportation system, and economy. Several impact events have occurred, some devastating. A 2004 study by El-Tawil discusses a vehicle impact incident and described the consequential effects. The incident occurred in 1993 in Alabama, where a tractor with a large load collided with a bridge pier. The incident resulted in a partial bridge collapse and the death of two people. Among other accidents, this incident represents the importance of vehicle impact analysis on concrete bridge piers.

Vehicle collision with a concrete bridge pier can cause damage to both the vehicle and the bridge pier. Figure 2.1 shows a simulated model of a vehicle collision with a bridge pier prior to the collision and after the collision. It is evident from this figure that vehicle impact can cause structural deformation and possible permanent damage, resulting in decreased structural capacity.

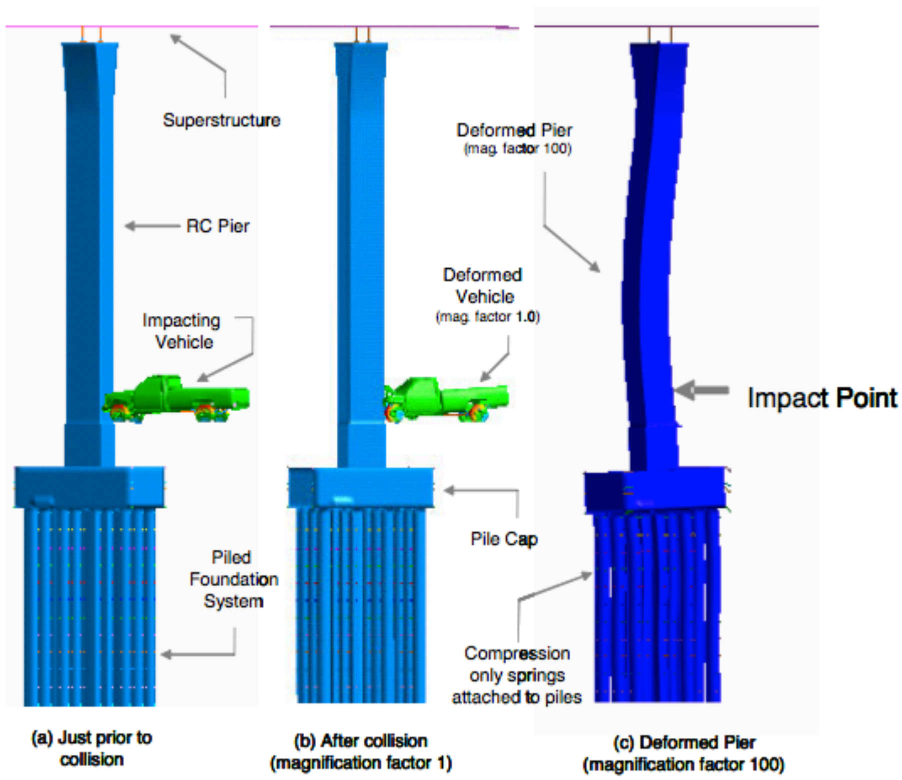

Figure 2.1: Model Representing Impact Simulation (El-Tawil, 2004)

The American Association of State Highway and Transportation Officials (AASHTO) is a design standard that specifies design requirements for transportation components. According to El-Tawil (2004), information regarding vehicle versus structural impact events is limited. AASHTO does require that a bridge pier be designed to withstand a lateral, static impact force of 1,800 kilownewtons (404.7 kips) (El-Tawil, 2004). AASHTO specifies that this force is 1.35 meters (4.4 feet) above the ground, which is an average height of a vehicle impact point. El-Tawil explains the weaknesses of the AASHTO standard regarding vehicle and structural collision as:

(1) The standard specifies a height of the impact force in the design force value. In addition to the height of the vehicle, the impact force will also be a function of the vehicle speed and attributes, such as stiffness and mass. An increased approach speed will affect the impact force differently than a lower speed and heavier or stiffer vehicle components will have a greater effect on the structure than weaker components. The AAHSTO code needs to specify the design force as a function of these factors, as well as height.

(2) The standard does not identify the dynamic interaction created by the impact force.

(3) The AASHTO code specifies a design impact force of 1,800 kilonewtons (404.7 kips) but does not indicate requirements for the detailing of the bridge pier. It simply states the design force. The standard should provide provisions regarding the detailing of the bridge pier to withstand this design force.

A relatively constant low force accompanied by a large, short-lived spike over the impact event duration characterizes the impact force (El-Tawil, 2004). El-Tawil identifies the spike as the peak dynamic force, which typically occurs at the beginning of the impact event duration. Due to the instant and intense loading implied by the peak dynamic force, the short demand is not representative of the structure demand experienced by the bridge pier. El-Tawil claims that instead, the peak dynamic force should be transformed to an equivalent static force, which should be used as the design demand force, by equating the deflection experienced at the impact force location. To determine the demand versus capacity of the impact event, the equivalent static force over time should be compared to the design force of 1,800 kilonewtons (404.7 kips) specified by AASHTO.

Simulations completed by El-Tawil (2004) indicated that the AASHTO capacity standards for vehicle and structural collision were lower than the design demand experienced by a bridge pier during a collision. This causes concern because if one of these vehicle-bridge pier impact events occurs, severe loss may be experienced. Also, El-Tawil's simulations referred to smaller trucks. If a vehicle impact event occurred with a larger vehicle, such as a semi-truck, the design demand on the bridge pier could increase significantly, resulting in more damage.

2.1.3 Pier Capacity and Demand

The impact event influence on a bridge pier depends on the capacity of the bridge pier and loading resulting from the vehicle collision. The limit state equation defines this relationship. A general limit state equation, also known as a performance function, is the resistance minus the load effect (Ayyub & McCuen, 2011). Cizmar and others (2008) state that the capacity of a reinforced concrete bridge pier is a function of the reinforcing steel, concrete section dimensions, and axial load applied to the bridge pier. The impact loading demand on a bridge pier is a function of vehicle mass, speed, stiffness, and acceleration. Cizmar and others define the performance function of a reinforced bridge pier exposed to vehicular impact loading using Equations 2.1 through 2.3:

$$M_{rd} - M_E = 0 \qquad \text{(Eq. 2.1)}$$

$$M_{rd} = \lambda_M \left(A_{s2} f_y y_2 + 2A_{s1} f_y \frac{y_2}{2} + N_{Ed} \frac{y_2}{2} \right) \qquad \text{(Eq. 2.2)}$$

$$M_{E_{impact}} = hF = h\sqrt{km(v^2 - 2ar)} \qquad \text{(Eq. 2.3)}$$

where: M_{rd} is the bending strength of the concrete bridge pier, M_E is the bending moment due to actions, λ_M is the resistance uncertainty, A_{s1} and A_{s2} are the steel reinforcement areas in the pier with yield strengths of f_y, y_2 is the moment arm, N_{Ed} is the non-factored axial load, *h* is the height of the impact force, *k* is the vehicle stiffness, *m* is the vehicle mass, *v* is the vehicle speed, *a* is the vehicle deceleration, and *r* is the distance from the original vehicle path to the point of impact. Figure 2.2 shows the cross-sectional and steel dimensions used in the resistance loading equation.

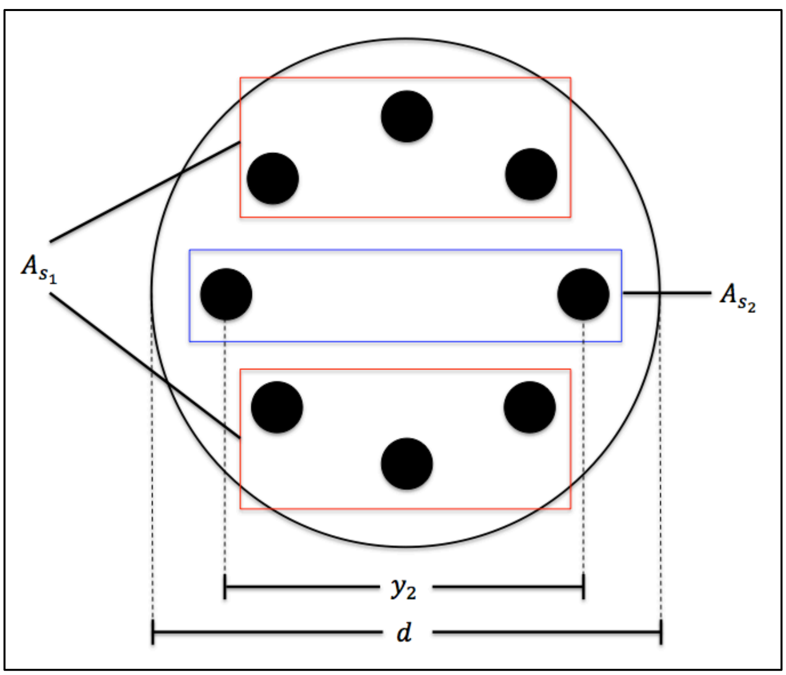

Figure 2.2: Cross-Section of Bridge Pier

2.2 Blast Analysis

2.2.1 Explosive Definition and Overview

Explosions can be defined as sudden release of energy in the form of light, heat, sound, and a shock wave. A shock wave is a high velocity mass of highly compressed air and typically the primary cause of damage (Gedeon, n.d.). Explosions produce pressures with extremely high-intensity and short-duration. Blast effects on structural and non-structural elements depend on the standoff distance and the magnitude of the explosive (Doege & Gebbeken, n.d.). The standoff distance is the distance between the explosive location and the affected structure. Structural elements include the piers, beams, and supporting elements of the structure. Nonstructural elements of a building include items such as interior walls and siding.

The magnitude of the explosive is typically equated to pounds of trinitrotoluene (TNT) or kilograms of TNT. If the charge weight, location of the explosion, and type of building construction are known, it is possible to estimate the level of damage a structure will experience (Doege & Gebbeken, n.d.). Blast pressures push both horizontally and vertically on a structure. Figure 2.3 provides a depiction of typical blast pressures on a structure. The figure shows that a blast can encompass a structure completely, applying pressures in several directions on the structure. This intense pressure loading can cause detrimental consequences to a structure (Gedeon, n.d.).

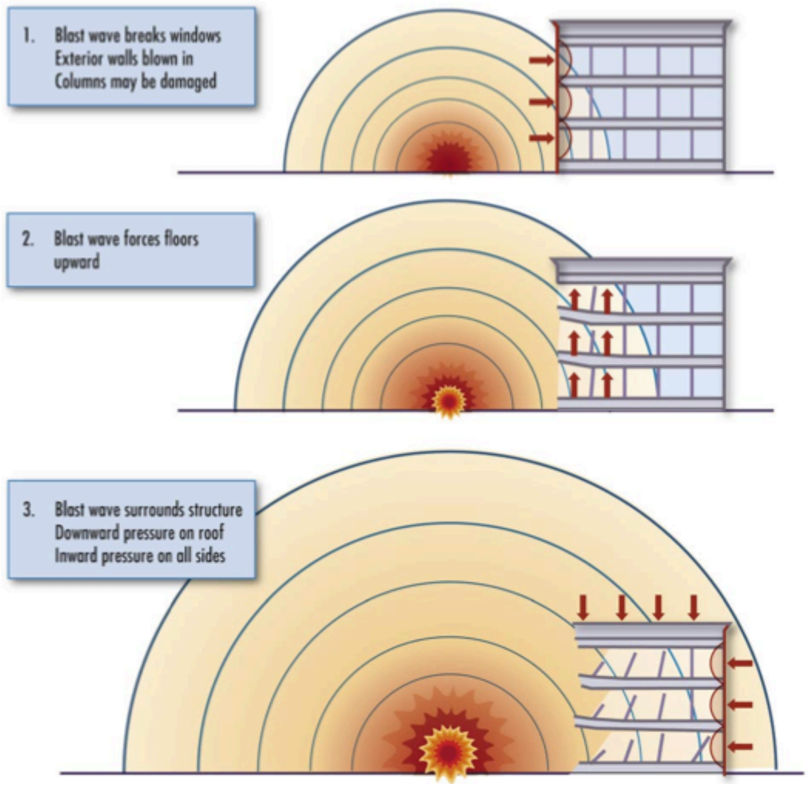

Figure 2.3: Blast Effects on a Structure (Gedeon, n.d.)

The blast pressure travels at high speed and can also be reflected off of surfaces, combing with direct pressure and resulting in elevated total pressure (Longinow & Mniszewski, 1996). Due to the elevated pressure, blast loading can exceed the building design loading by a great amount. Typical blast-resistant structures are mostly utilized by the military to protect against nuclear weapons. Designing and building civilian structures to resist blast loading is impractical in cost, function, and appearance.

One method to improve the structural system of a building is the application of a redundant framing system and consideration of vertical loads from both above and below floor systems (Longinow, & Mniszewski, 1996). Perimeter security or perimeter fences are other modes of protection against vehicle blasts that increase standoff distance. Longinow and Mniszewski state that perimeter boundaries can increase the distance from the explosive to the structure, decreasing the amount of possible structural and human damage.

2.2.2 Vehicle Explosions

Gedeon identifies different sizes of explosives using pipes, luggage, automobiles, vans, and trucks. The typical ranges of the explosive sizes for each transport item are: 1) Pipe Explosive, 5 pounds of TNT; 2) Luggage Explosive, 50 pounds of TNT; 3) Vehicle to Van Explosives, 500 – 4,000 pounds of TNT; 4) Truck Explosives, 10,000+ pounds of TNT (Gedeon, n.d.). These values can be used in the methodology to determine a range of the blast charge weights, which are a function of the size of the transport item.

2.2.3 Critical Charge Weight

Buildings have typically been the focus of blast damage analysis, but it is valuable to extend the analysis to bridges to improve transportation infrastructure security (Galati, Nanni, Quintero, & Wei, 2007). It is beneficial to explore different explosive magnitudes in contact or near bridge components and determine the corresponding structural damage.

Fragility and capacity curves can be used to identify the different levels of damage experienced by bridge components due to varying standoff distances and charge weights. Fragility curves are curves that express the probability of failure dependent on a given loading and capacity curves illustrate the remaining bridge component capacity associated with blast charge weights. A load demand curve can also be mapped on the capacity curve to determine the critical charge weight. The critical charge weight is the charge weight that corresponds with the damage point where the structural component cannot support any more static load. It is found by locating the intersection of the capacity curve and load demand curve and identifying the corresponding charge weight

(Galati, Nanni, Quintero, & Wei, 2007). As the load on a pier increases, the critical charge weight decreases.

2.3 Reliability Analysis and the Monte Carlo Method

"The reliability of a structure is its ability to perform its design purpose for some specified design lifetime" (Collins & Nowak, 2000, 2). Reliability analysis aids in identifying uncertainties in structural designs and analysis (Ching, 2011). The reliability analysis of a structure or structural element includes determining the reliability of a structure with different resistance and loading parameters.

2.3.1 Simulation

Simulation methods are used to understand and control systems with uncertainty. Simulation methods are preferred over analytical and numerical methods when complex systems are being analyzed (Haugh, 2004). Analytical models can examine several parameters with one execution, but are only effective with simple systems. Numerical methods involve repetitive computational runs for each parameter, but can handle more complex models than analytical methods. However, there are still limitations on numerical models when dealing with complex systems. Simulation techniques include repetitive computational runs, like numerical methods, but can handle realistic systems with high complexity.

Haugh (2004) defines the steps included in modeling a system as: identification, assumption definition and defense, input definition, desired objective of simulation, variable relationship identification, and simulation performance. It is important for the system to be understood and represented properly in the system identification and simulation process. This will cause greater accuracy in the estimated outcomes of the simulation.

The intention of simulation is to “numerically simulate some phenomenon and then observe the number of times some event of interest occurs” (Collins & Nowak, 2000, 69). The simulation process includes the generation of random numbers with values between zero and one to represent the probability of a particular event occurring. Random numbers are generated using computer software, such as *Microsoft Excel* or *Matlab*. The random variables are determined using the random numbers and are used in the component and/or system model.

With each case being analyzed, certain issues need to be addressed before and after the simulation is completed. The number of necessary random variables and their distributions need to be identified. Also, the method of generation of the random numbers needs to be determined. One of the steps included in a modeling system is the identification of the objective of the simulation. Along with this, the method of analysis of the output variables of the simulation needs to be determined.

2.3.2 Monte Carlo Method Overview

The reliability of a system can be modeled using the Monte Carlo method (Collins & Nowak, 2013). Decision making in several fields has transformed into using statistical tools and scientific analysis. If a considerable amount of data is collected, statistical based decisions can be very effective. The Monte Carlo method, developed in the 1940s, represents this statistical approach. “Monte Carlo analysis uses statistics to mathematically model a real-life process and then estimate the likelihood of possible outcomes” (Alexander, 2003, 91). In other words, the Monte Carlo method is an approach used to produce numerical results without having to perform any physical testing. The simulations performed with this method can assist in determining failure distributions and in improving the reliability of the components and the system as a whole.

Reliability problems inevitably include significant uncertainty due to the necessity to include multiple input random variables, which result in output random variables. The Monte-Carlo method is a simulation involving a parameters and random number generation to produce probability distributions. The parameters of interest can be determined using previous scientific data collection. Essentially, the simulation is repeated several times to generate a distribution of the defined parameters, providing statistical information for each. These probability distributions are then applied to the model and used to determine samples of the numerical data (Collins & Nowak, 2013).

2.3.3 Monte Carlo Simulation Process

The first phase in the Monte Carlo analysis is system definition. This includes defining the system's resistance and the loading of interest applied to the system. Collins and Nowak (2013) explain that the definition of these two components includes probability distribution type identification and the random variable identification for each. Once these factors are determined, the next phase is to complete the simulation. In the simulation, random numbers will be generated using computer software and applied to the statistical parameters of the variables. Once the simulation is complete, the numerical data produced can be applied to the system model, specifically the system's performance equation (Collins & Nowak, 2013). Collins and Nowak define the performance equation as the structural resistance minus the applied loading, using the equation:

$$Y = R - Q$$

where: Y is the structural performance, R is the structural resistance, and Q is the applied loading.

The probability of failure can be determined using the simulation values applied to the performance equation. In general, a negative performance value indicates a failure, whereas a positive performance value indicates a non-failure. These values can be plotted on a normal probability plot to graphically show failures and non-failures. The probability of failure can be determined by dividing the number of failures determined from the simulation by the total number of simulated performance values.

The reliability index is determined using the probability of failure. The reliability index is the inverse of the coefficient of variation and is used to measure the reliability of a structure or structural element. Mathematically, it is the shortest distance from the origin to the performance equation line on the normal probability plot created from the simulation. If R and Q are normally distributed, the reliability index can be determined using the following formula:

$$\beta = -\emptyset^{-1}\left(P_f\right)$$

where: β is the reliability index, $\emptyset$ is the normal distribution, and P_f is the probability of failure (Collins & Nowak, 2013).

2.3.4 Monte Carlo Simulation Advantages and Disadvantages

Advantages of the Monte-Carlo simulation method include flexibility, future development opportunities, and clarity (Applied R&M Manual for Defence Systems, 2011). The Monte-Carlo simulation is advantageous in flexibility because it contains the ability to adapt to several different situations. Fields of application include engineering, physical science, finance, and more. The Monte-Carlo simulation also allows for a reliability model to be extended and further developed. The variables included in the simulation computations can be adjusted to create more accurate results based on new findings or can be used in supplementary simulations. These simulations can also provide clarity for anyone, mathematician or non-mathematician, interpreting the data. The simulation allows for a complex situation to be simplified and can provide a better understanding of the system.

Disadvantages of the Monte-Carlo simulation method include the need for a computer, the process execution time required, and estimated results (Applied R&M Manual for Defence Systems, 2011). In order to complete the simulations necessary, a computer program is essential. This may pose a problem if a computer is not accessible. Analytical methods can be performed in a short amount of time. Simulation methods, however, include a repetitive process, which can result in a lengthy execution. Solutions resulting from the Monte-Carlo simulation are all estimates. The accuracy of the estimates depends on the number of simulation runs completed in the whole process. In order to increase the accuracy of the outputs, the simulation runs need to be increased, causing a longer execution process.

2.3.5 Monte Carlo Simulation Efficiency

The Monte Carlo method involves a repetitive process with a predetermined number of simulation runs. The number of simulation runs for a particular case needs to be determined and performed. Adjustment of the number of runs can be made to improve efficiency of the simulation. Along with this, other improvements can be made to the model to increase the simulation efficiency. One example of a possible improvement is the modification of the random input variables (Haugh, 2004). In general, the simulation efficiency can be increased by variance reduction techniques, which are dependent on the probability distributions of the variables in the model.

The Monte Carlo simulation is a valuable tool that uses mathematics to simplify a system. The simulation results can be used in the reliability analysis, which will lead to improvements in the reliability of the component and/or system of interest.

2.3.6 MATLAB

MATLAB is computer program constructed to perform and optimize engineering and scientific calculations. MATLAB is short for Matrix Laboratory and has evolved from a matrix mathematics program to an extensive computing program with several predefined functions (Chapman, 2008). With the use of the MATLAB programming language, almost any technical problem can be solved with efficiency using the computer program.

Some advantages of MATLAB include ease of use, predefined functions, and the graphical user interface (Chapman 2008). The programming language used in this computer platform is easier to learn and understand. MATLAB can handle simple calculations to large, complex programs. Chapman (2008) explains that the platform includes developmental tools, including editors, debuggers, and manuals, implemented into its system to increase the ease of use. The predefined functions are a major advantage of the program because it saves the user time in writing functions and subroutines. MATLAB provides a library of its predefined functions on the program platform, which is easy to access and understand. Chapman also identifies the plotting and graphing abilities of MATLAB and how they make the program a great tool for users to visualize their data and program output. MATLAB is also supported by several different computer systems, which results in increase accessibility of the program.

The disadvantages of MATLAB include the necessity to learn and implement the MATLAB programming language properly and the cost of the program (Chapman, 2008). Though the program supplies several tools to help users learn the programming language, the language is still meticulous and takes time to understand completely. This may be a disadvantage for users who do not have the time or desire to learn a new computer code language.

2.4 Multi-Hazard and Risk Analysis

2.4.1 Multi-Hazard Engineering

Multi-hazard engineering is a growing field as the possibility of multiple threats to structures becomes more apparent to structural engineers (Bell & Glade, 2004). Hazards produce intense demands on structures because of the different loading types and intensities. "Multi-hazard engineering is about simultaneously addressing all hazards as a problem of optimization under constraints, the criterion being life-cycle cost" (Multidisciplinary Center for Earthquake Engineering Research (MCEER), 2007,1). Multi-hazards affect both the general population and the surrounding structural elements. Multi-hazard analysis includes natural disasters, intentional hazards, and accidental hazards. Natural disasters include events such as earthquakes, floods, and hurricanes. Intentional hazards include terrorist attacks, such as explosive events. Accidental hazards include man-made dangers that are unplanned or unintentional, such as fire or vehicle impact. Multi-hazard analyses should be completed whenever possible and economical and includes risk analysis, risk management, and risk evaluation (Bell & Glade, 2004). Figure 2.4 demonstrates these three mains steps in multi-hazard analysis and how they are arranged in a continuous structure. In other words, the three steps in the analysis are never completed. Risk is a primary consideration and ongoing focus area in structural engineering due to the necessity of safety for human life and the economy.

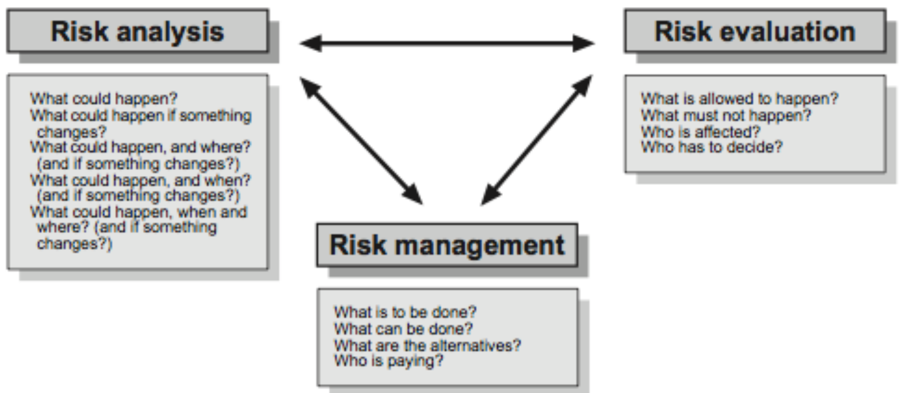

Figure 2.4: Concept of Risk Assessment (Bell & Glade, 2004)

2.4.2 Advantages and Disadvantages of Multi-Hazard Analysis

Multi-hazard analysis has several advantages including the possibility for more accurate estimation of structural resiliency, or recovery, from intense loading, a better prediction of lifecycle cost of the structure, and structural health monitoring to increase structural efficiency and economic analysis (Agrawal, et. al., 2007). The major disadvantage to multi-hazard analysis is the lack of possibility to fully quantify the risk associated with hazards or multi-hazards. However, multi-hazard analysis still assists engineers in awareness of the critical loadings a structure may be subjected to in its lifetime (Asprone, et. al, 2009).

2.4.3 Risk Management

Previous structural failures have taught engineers about structural material behavior and different loadings during a structure's lifetime. From these learning experiences, quality control systems have been formed and implemented. Prediction of material and structural behavior with experimental methods and tools has become essential in structural engineering. "Occurrence, intensity, and system response to natural and man-made hazards are uncertain" (Ellingwood, 2007, 2). Risk management strategies can either be used to reduce the frequency of hazardous events or increase the operations to reduce the consequences of a hazardous event (Ayyub, et.al., 2007).

Woo (2002) claims terrorism has joined natural hazards in the category of catastrophic risks in the United States. Woo explains that neither of the two event types can be predicted due to spontaneity, but their corresponding risk can be quantified using a probabilistic risk assessment. Risk is defined as "a product of hazard and vulnerability" (Woo, 2002, 7). The hazard is the event and the vulnerability is the consequential loss associated with the event. The difference between terrorist events and natural hazard events that must be considered is the human factor. Intentional hazards, having increased motivation, variable capabilities, and the ability to be countered, are complicated when attempting to quantify the risk associated with them (Woo, 2002). Ayyub and others (2007) describe intentional events as challenging because they result from human actions, which have the ability to adapt to a changing environment and produce innovative plans, and they can happen in any region. Ayyub and others explain that because there is uncertainty in intentional hazards and their characteristics, risk management must be implemented to reduce possible destruction.

2.4.4 Sabotage and Terrorism

Typical risk assessment procedure tasks include: scope definition, hazard identification, hazard analysis, consequence analysis, and risk calculation (Bell, & Glade, 2004). Sabotage and terrorism are in the category of "low-probability-high-consequence" events, which result in difficult analyses because there is a lot of uncertainty in both the occurrence of the event in the structure's lifespan and the cost of the event consequences (Melchers, 2002). "Low-probability-high-consequence" events are difficult to include in risk assessment procedures because they cannot be predicted rationally. Recent structural design has been taking defensive steps in security and reduced vulnerability to protect against sabotage and terrorism. There is a strong correlation between a substantial terrorist attack and financial market decline (Waugh, 2004). It is important to continue improving to quantify terrorism risk, as it may provide more security for economic and human life (Woo, 2002). Risk prevention and analysis deserve a primary emphasis in structural bridge design.

2.5 Summary

This chapter presents a review of the literature relevant to the study of reinforced concrete bridge piers exposed to subsequent impact and blast events. A summary of the significant points are presented:

1) It can be understood that vehicle impact on a bridge structure can be destructive to both human life and the bridge's structural life. The effect of vehicle impact on the structural integrity of bridges is becoming increasingly important. Engineering considers impact at reasonable speeds around the speed limit.

Intentional impact may not be considered, which can include a greater force due to an increased speed.

2) Vehicle explosives will be the focus of this research, as these will most likely be the methods of transport of an explosive on a bridge. With vehicle bombs, "the critical locations are considered to be at the closest point that a vehicle can approach on each side" (Gedeon, n.d., p. 14). This can help a structural designer to determine the minimum structural integrity a structure must have in order to endure an explosive at this distance.
3) Reliability analysis and Monte Carlo Simulations aid in the determination of the probability of failure and reliability index of a structure with different resistance and loading parameters.
4) The Monte Carlo method is a mathematical estimation process that uses several iterations in its process. The Monte Carlo simulation can be completed in MATLAB. MATLAB operations can be employed to simplify the Monte Carlo simulations. With MATLAB, several iterations can be performed and the uncertainty parameters can be varied to provide the best solution.
5) Multi-hazard analysis assists engineers in awareness of the critical loadings a structure may be subjected to in its lifetime.

CHAPTER 3

METHODOLOGY

The purpose of this study is to determine the probability of failure of a circular reinforced concrete bridge pier that experiences impact and blast loading successively. Previous research has been conducted regarding the structural effect from an impact loading or a blast loading by itself (Agrawal & Chen, 2008; Doege & Gebbeken, n.d.; El-Tawil, 2004; Longinow & Mniszewski, 1996), but there is insufficient research on examining the combined effect of sequential loading. In order to determine this effect, this research studies the probability of failure of a circular reinforced concrete bridge pier that experiences impact loading alone, blast loading alone, and multi-hazardous loading; specifically impact loading followed by blast loading.

It is important to recognize the difference in effect a structure experiences due to a single hazard load compared to two successive hazardous loadings (Banerjee & Prasad, 2011). When a structural element experiences one hazardous loading, it is assumed to start with its original design strength. In other words, the concrete pier is assumed to be in a healthy state, having only experienced loadings for which it was designed, when it is exposed to the impact loading or blast loading alone. If multi-hazard loading occurs, the above concept applies for the first loading, but not for the sequential loading. The second loading occurs after the pier may have already been damaged. That is, the residual strength of the pier will have been decreased from the first hazardous loading, and then be further decreased from the second hazardous loading.

There is a realistic probability that a structure will undergo multiple short-duration, high-intensity consecutive loadings. It is necessary to determine the probability of failure from the successive loadings in order to improve the structural integrity. If the probability of failure of a structure from successive loadings is determined, there is a possibility of a more accurate estimation of structural resiliency, or recovery, from intense loading. Knowledge of the structural resiliency will lead to a better prediction of lifecycle cost of the structure and structural health monitoring to increase structural efficiency and economic analysis (Agrawal, 2007).

3.1 Numerical Model Development

3.1.1 Relevant Data Collection

A numerical model is developed in the software package MATLAB to determine the probability of failure using the Monte Carlo simulation and a first order, second moment reliability analysis. The numerical model is designed for a nonspecific circular concrete bridge pier with vertical and spiral reinforcement. Statistical parameters concerning both material properties of reinforced concrete pierss and the loadings of interest are collected for use in the simulation analysis and are presented in Section 3.2.

3.1.1.1 Bridge Pier Data Collection

Pier resistance properties of interest in the analysis include the concrete pier dimensions, reinforcing area, yield strength of the reinforcement, and the axial load imposed on the bridge pier. In 2008, Cizmar and others studied the reliability of rectangular concrete piers under vehicle impact loading (Cizmar et. al., 2008). This study provides useful information about probabilistic and deterministic modeling of reinforced concrete piers subject to vehicle impact. However, their study only investigates square piers, whereas in the United States, round or circular piers are more frequently used. Additionally, their study considers only accidental impact or cases where the vehicles were decelerating to avoid crashing.   The study presented herein builds upon the previous work by considering: 1) circular instead of square piers, 2) terroristic intention (i.e. acceleration vs. deceleration), 3) strength reduction versus fault tree analysis and 4) sensitivity analysis to determine those design factors that most contribute to high probabilities of failure and as such can be modified to decrease probabilities of failure. Cizmar and others use the Joint Committee on Structural Safety (JCSS) Probabilistic Model Code to define a bridge pier resistance equation along with variable definitions and their corresponding statistical parameters. The defined equation and parameters serve as the foundation for this research study. Cizmar and others use SI units in their equations and corresponding variables. For this reason, SI units are used throughout this study.

3.1.1.2 Vehicular Impact Loading Data Collection

Statistical parameters for both the impact and blast loading are collected to account for the uncertainties that accompany a hazardous loading. The variables and their statistical parameters essential for the impact consideration are: vehicle mass, vehicle stiffness, vehicle speed, and vehicle acceleration. Cizmar and others also define an impact loading equation along with the impact variable definition and statistical parameters (Cizmar et. al., 2008). The defined equation and parameters serve as the foundation for the impact portion of this research study.

In addition to the properties and statistical parameters defined by Cizmar and others, vehicle size and mass figures are investigated and used in the difference impact analysis scenarios. The corresponding impact heights of different vehicle types are determined and sorted into realistic scenarios for the numerical analysis and shown in

Table 3.1.

Table 3.1: Vehicle Class, Mass, and Impact Height

Vehicle	Mass	Impact Height
Car	2,270 kg (5,000 lb)	0.61 m (2.0 ft)
SUV/Van	4,540 kg (10,000 lb)	0.91 m (3.0 ft)
Small Moving Van/Delivery Truck	8,170 kg (18,000 lb)	1.22 m (4.0 ft)
Moving Van/Water Truck	11,800 kg (26,000 lb)	1.5 m (4.9 ft)
Semi-Truck/Trailer	19,100 kg (42,100 lb)	1.8 m (5.9 ft)

3.1.1.3 Blast Loading Data Collection

Due to the limited information regarding blast loading, there are not statistical parameters regarding this loading. Because of this, statistical parameters are assumed for the blast loading moment and a sensitivity analysis is performed to determine the importance and probable value of these parameters. The maximum values of the blast charge weights considered in the analysis are shown in Figure 3.1 and correspond with the transport vehicle in the multi-hazardous event.

Similar to the impact-loading scenario, possible and likely blast charge weights are considered, paralleling charge weights with vehicle types. The charge weights provided in this figure are in pounds of trinitrotoluene (TNT) and are converted to kilograms of TNT for this study. There are 2.2 pounds of TNT in 1 kilogram of TNT. The different vehicle masses combined with varying charge weights ultimately provide several scenarios combining probabilistic combinations of impact and blast force on a bridge pier.

BOMB THREAT STAND-OFF CHART

Threat Description Improvised Explosive Device (IED)	Explosives Capacity[1] (TNT Equivalent)	Building Evacuation Distance[2]	Outdoor Evacuation Distance[3]
Pipe Bomb	5 LBS	70 FT	1200 FT
Suicide Bomber	20 LBS	110 FT	1700 FT
Briefcase/Suitcase	50 LBS	150 FT	1850 FT
Car	500 LBS	320 FT	1500 FT
SUV/Van	1,000 LBS	400 FT	2400 FT
Small Moving Van/ Delivery Truck	4,000 LBS	640 FT	3800 FT
Moving Van/ Water Truck	10,000 LBS	860 FT	5100 FT
Semi-Trailer	60,000 LBS	1570 FT	9300 FT

1. These capacities are based on the maximum weight of explosive material that could reasonably fit in a container of similar size.
2. Personnel in buildings are provided a high degree of protection from death or serious injury; however, glass breakage and building debris may still cause some injuries. Unstrengthened buildings can be expected to sustain damage that approximates five percent of their replacement cost.
3. If personnel cannot enter a building to seek shelter they must evacuate to the minimum distance recommended by Outdoor Evacuation Distance. These distance is governed by the greater hazard of fragmentation distance, glass breakage or threshold for ear drum rupture.

Figure 3.1: Vehicle Bomb Size (US Department of Energy, 2012)

3.1.2 Methodology Outline

Several multi-hazardous events are considered in this study. The bridge pier resistance variables are adjusted to provide the study with various pier resistance scenarios. Vehicle type, speed, and acceleration are also adjusted to provide various impact loading event scenarios. Similarly, blast charge weight and standoff distance are also adjusted to provide the study with various blast loading scenarios. The standoff distance is the distance between the explosive location and the affected structure. Blast effects on structural and non-structural elements depend on the standoff distance and the magnitude of the explosive (Doege & Gebbeken, n.d.).

This study strives to determine the effects of both impact and blast loadings on the structural element, both individually and simultaneously. To do this, each loading is analyzed by itself first and then combined to analyze the multi-hazardous loading effect.

The single hazardous loading scenarios are compared with the multi-hazardous loading scenarios.

Figures 3.2 and 3.3 outline the methodology used for the single hazardous event and multi-hazardous event reliability analyses, respectively.

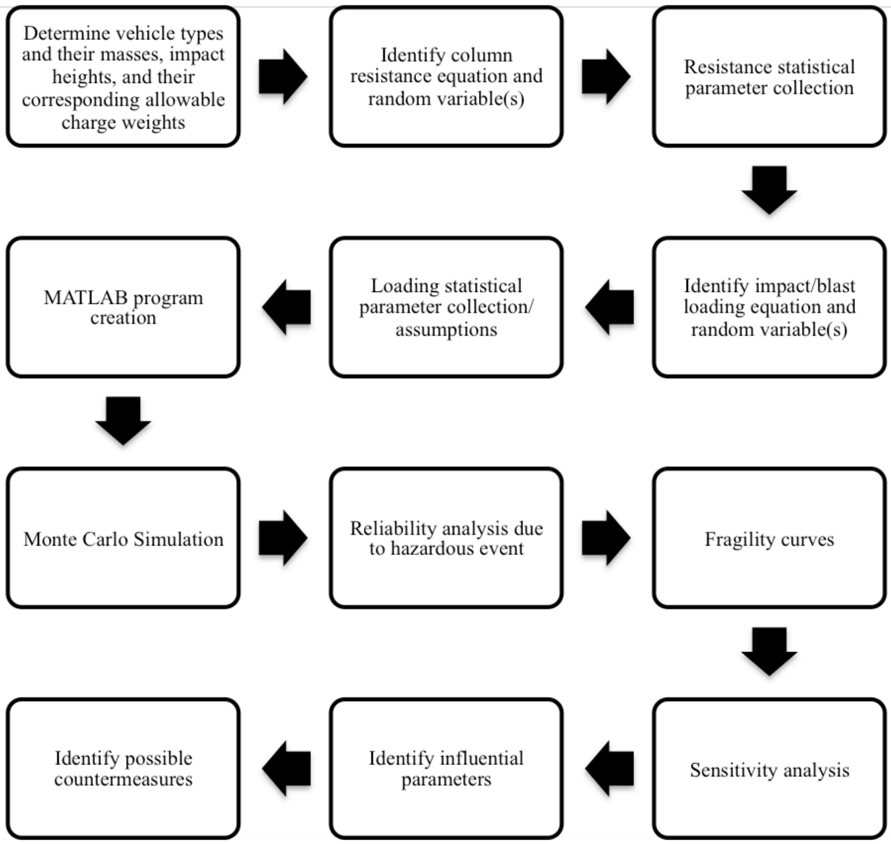

Figure 3.2: Single Hazardous Loading Methodology Outline

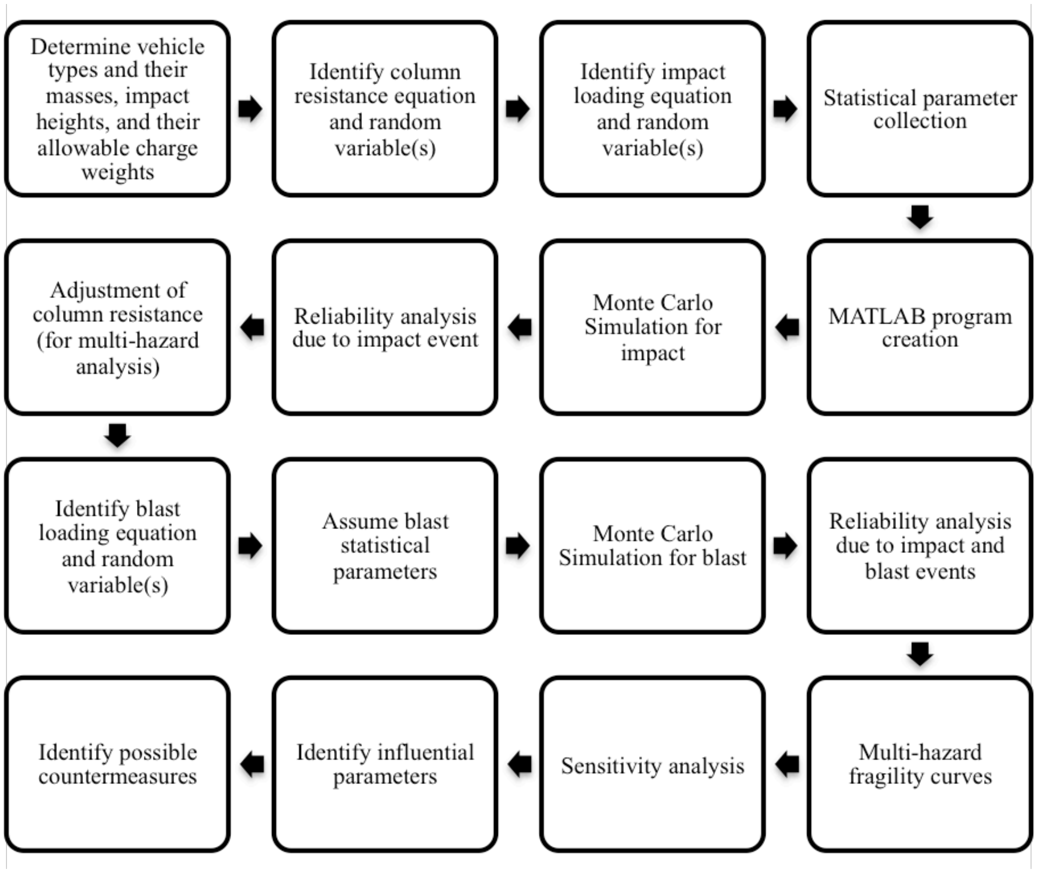

Figure 3.3: Multi-Hazardous Loading Methodology Outline

3.1.3 MATLAB Code

A MATLAB code is created to analyze the bridge pier and perform the reliability analysis according to the input resistance and loading parameters. Specifically, the MATLAB code is employed to determine the probability of failure of a bridge pier, with specified cross-sectional and reinforcing parameters, when exposed to different impact and blast loading events. The MATLAB code computes the probability of failure of the bridge pier from the impact alone, the blast alone, and from both impact and blast loading together. This allows for the severity of a multi-hazardous loading to be identified compared to just one hazardous loading. The MATLAB code allows for parameters to be adjusted, as desired by the user, for the Monte Carlo Simulation to assist in the sensitivity analysis.

3.2 Monte Carlo Method

The simulation method used in the first-order, second-moment reliability analysis of this study is the Monte Carlo method (Collins & Nowak, 2000). A simulation method, rather than a physical testing method, is used in this study because it allows for the manipulation of a representative system rather than a real system, which is ideal for sensitivity analysis. The Monte Carlo method is a technique used to simulate random numbers and formulate results using these random numbers without any or limited physical testing (Collins & Nowak, 2000). The steps involved in the Monte Carlo simulation are system definition, random variable identification, random number simulation, and data analysis.

3.2.1 System Definition

The first step in the Monte Carlo simulation is to define a limit state equation. A general limit state equation, also known as a performance function, is the resistance minus the load effect (Ayyub & McCuen, 2011). In this study, the resistance is identified as the flexural strength of the circular reinforced concrete bridge pier. The strength is determined based on pier section properties, steel reinforcing area, the yield strength of the reinforcing steel, and the axial load imposed on the bridge pier. The analysis is limited to bridge piers of circular cross-sections with spiral reinforcement, which is assumed to be adequate to support against shear. For simplicity, eight evenly spaced vertical reinforcing bars are specified for the vertical reinforcement in the bridge pier. A yield strength of 50 kN/cm^2 (72.5 ksi) is assumed for the steel reinforcement. The bridge pier is assumed to be fixed-fixed.

The reinforced concrete bridge pier is exposed to two different types of loadings, including an axial loading and the hazardous loadings. The axial loading includes the weight of the pier and the weight of the structural elements that the pier supports. The impact loading is a point load that will occur at some height near the bottom of the pier, with the height being dependent on the type and height of the vehicle. A point load is a concentrated force applied to the structure. The blast loading is a distributed load. A distributed load acts along some length of the structure, as opposed to a concentrated point. Identifying and applying these different types of loading are essential in the analysis of the reinforced concrete bridge pier because they cause different behaviors of the structural element. The different types of loading are considered in the combined axial and flexure equation identified later in this chapter.

The general limit state equation for the bridge pier is:

$$M_{rd} - M_E = 0 \qquad \text{(Eq. 3.1)}$$

where: M_{rd}, is identified as the bending strength of the concrete bridge pier and the load effect, M_E, is identified as the bending moment due to actions, such as the impact and blast loads. The resistance of the reinforced bridge pier is:

$$M_{rd} = \lambda_M \left(A_{s2} f_y y_2 + 2A_{s1} f_y \frac{y_2}{2} + N_{Ed} \frac{y_2}{2} \right) \qquad \text{(Eq. 3.2)}$$

where: λ_M is the resistance uncertainty and is taken as one in the resistance equation, A_{s1} and A_{s2} are the steel reinforcement areas in the pier with yield strengths of f_y, y_2 is the moment arm, and N_{Ed} is the non-factored axial load. Figure 3.4 shows the cross-sectional and steel dimensions used in the resistance loading equation. The compressive strength is not included in the moment resistance of the bridge pier because it is assumed that the concrete does not contribute to the tensile strength of the pier. The reinforcing steel is assumed to provide the tensile strength of the bridge pier.

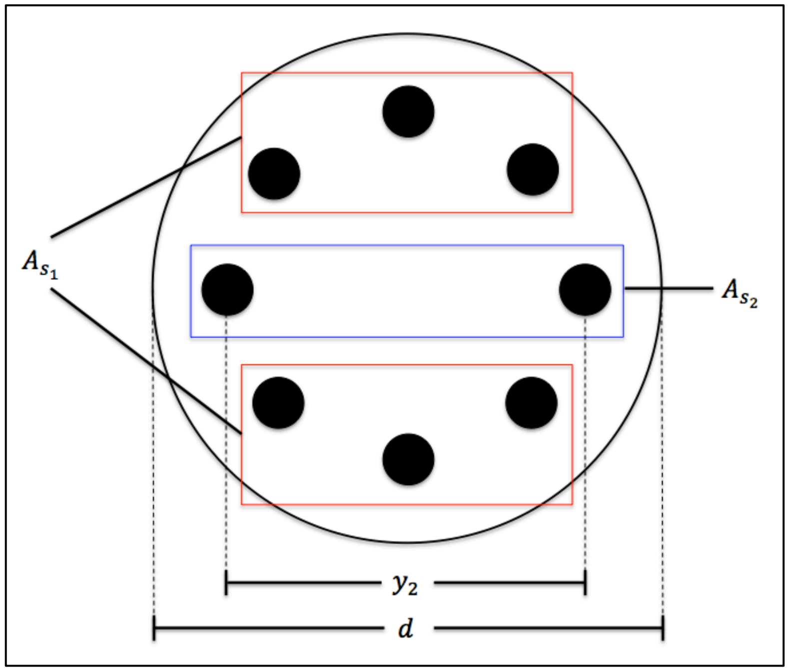

Figure 3.4: Cross-Section of Bridge Pier

3.2.1.1 Impact Loading

The load effect includes the impact loading and blast loading subjected to the bridge pier. In the single hazardous loading scenarios, the Monte Carlo simulation and reliability analysis is performed once per resistance and loading scenario. In the multi-hazardous scenario, the Monte Carlo simulation and reliability analysis is performed twice due to the two loadings.

According to the U.S. Federal Highway Administration, vehicle impact is the third leading cause of bridge damage and/or failure (Agrawal & Chen, 2008). In a vehicular impact event with a bridge pier, damage simultaneously occurs in both the vehicle and the reinforced concrete bridge pier (El-Tawil, 2004). El-Tawil defines this type of impact event as a “soft” impact, which allows for the impact loading to be treated as a static loading due to similar failure mechanisms. The equations and variable provided by Cizmar allows for the assumption of “soft” impact to be applied. The demand of the reinforced bridge pier due to the impact force is:

$$M_{E_{impact}} = hF = h\sqrt{km(v^2 - 2ar)} \qquad \text{(Eq. 3.3)}$$

where: *h* is the height of the impact force, *k* is the vehicle stiffness, *m* is the vehicle mass, *v* is the vehicle speed, *a* is the vehicle acceleration, and *r* is the distance from the original vehicle path to the point of impact. As previously discussed, the study by Cizmar and others (2008) consider an accidental impact event on the bridge pier, while the main focus of this study is a terroristic, intentional impact event. For this reason, the variable *a* is taken as the acceleration, rather than a deceleration, and put into the equation as a negative value to make the adjustment. Figure 3.5 displays a simplified depiction of the impact-loading event.

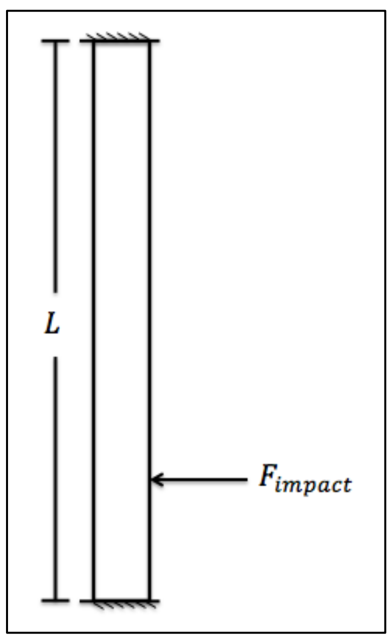

Figure 3.5: Impact Loading Event

3.2.1.2 Blast Loading

Explosions produce pressures with extremely high-intensity and short-duration. Blast effects on structural elements depend on the standoff distance and the magnitude of the explosive (Doege & Gebbeken, n.d.). The standoff distance is the distance between the explosive location and the affected structure. Different blast charge weights and standoff distances are chosen for each of the analyses. The blast over pressure due to the charge weight and standoff distance is determined using Equation 3.4 (Brode, 1955):

$$P_{so} = \frac{6.7W}{R^3} + 1 \qquad \left(\frac{kp}{cm^2}\right) \tag{Eq. 3.4}$$

where: W is the charge weight in kilograms of TNT and R is the standoff distance. A kilopond (kp) is a unit of force used in the "old" metric system that comes from gravity. The kilopond is used to represent pressure when divided by "cm.^{2}" Brode provides a conversion for the overpressure:

$$1\ \frac{kp}{cm^2} = 9.80665\times10^4\ Pascals \tag{Eq. 3.5}$$

It is assumed that the blast pressure is applied to the bridge pier in a trapezoidal shape. Specifically, the maximum pressure on the bridge pier is at the bottom, whereas the minimum pressure on the bridge pier is at the top. In between the two extremes, the blast pressure is assumed to be linear. Figure 3.6 displays a simplified depiction of the blast-loading event.

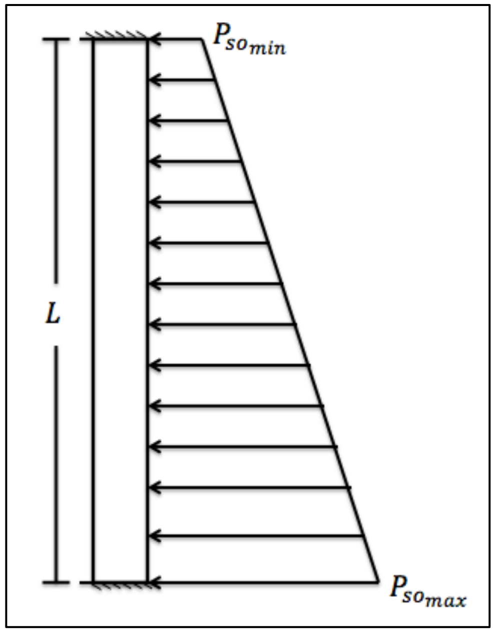

Figure 3.6: Blast Loading Event

Since the bridge pier is assumed to be fixed-fixed, the maximum moment due to the blast loading occurs at the bottom of the bridge pier. Utilizing the method of superposition and assuming the maximum moment location at the bottom of the pier length, the demand of the reinforced bridge pier due to the blast pressure is:

$$M_{E_{blast}} = \frac{\left(P_{so_{min}} d\right)L^2}{12} + \frac{\left(P_{so_{max}} - P_{so_{min}}\right)dL^2}{20} \qquad \text{(Eq. 3.6)}$$

where: $P_{so_{min}}$ is the blast-induced overpressure at the top of the pier, $P_{so_{max}}$ is the blast-induced overpressure at the bottom of the pier, d is the diameter of the pier, and L is the length of the pier.

In the blast analysis, the steel yield strength is multiplied by a dynamic increase factor (DIF) of 1.23, as specified by TM 5-1300 for reinforcing steel, to determine the dynamic yield strength (f_{ds}). Using the above capacity and demand equations, Equations 3.7 and 3.8 identify the bridge pier limit state equations for the impact and blast events, respectively.

$$\lambda_M \left(A_{s2} f_y y_2 + 2A_{s1} f_y \frac{y_2}{2} + N_{Ed} \frac{y_2}{2}\right) - h\sqrt{km(v^2 - 2ar)} = 0 \qquad \text{(Eq. 3.7)}$$

$$\lambda_M \left(A_{s2} f_{ds} y_2 + 2A_{s1} f_{ds} \frac{y_2}{2} + N_{Ed} \frac{y_2}{2}\right) - \left[\frac{\left(P_{so_{min}} d\right) L^2}{12} + \frac{\left(P_{so_{max}} - P_{so_{min}}\right) d L^2}{20}\right] = 0 \qquad \text{(Eq. 3.8)}$$

3.2.1.3 Multi-Hazard Loading

The multi-hazard analysis includes the limit state equations defined in Equations 3.7 and 3.8. The vehicular impact analysis is performed and the corresponding probability of failure is determined. Based on this probability of failure, the moment resistance of the bridge pier is reduced and used in the reliability analysis with the blast loading. The resistance reduction factors are determined using the standard deviation of the resistance moment as a whole. Figure 3.7 presents the statistical parameters of the resistance moment (Ellingwood et. al., 1980).

Table 3.2
Typical Resistance Statistics for Concrete Members

Designation	$\bar{R}/R_n$	V_R
Flexure, Reinforced Concrete, Grade 60	1.05	0.11
Flexure, Reinforced Concrete, Grade 40	1.14	0.14
Flexure, Cast-in-Place Pretensioned Beams	1.06	0.08
Flexure, Cast-in-Place Post-Tensioned Beams	1.04	0.095
Short Columns, Compression Failure, f'_c = 3 ksi	1.05	0.16
Short Columns, Tension Failure, f'_c = 3 and 5 ksi	1.05	0.12

Figure 3.7: Moment Resistance Statistical Parameters (Ellingwood, 1980)

The moment resistance is assumed to have a normal distribution (Ellingwood et. al., 1980). This study is concerned with reinforced concrete, with Grade 60 steel, in flexure so the coefficient of variation is taken as 0.11. Thus, the standard deviation (σ) used in the resistance reduction is defined as the moment resistance found in the impact reliability analysis multiplied by the coefficient of variation defined by Ellingwood.

Based on the parameters given by Ellingwood, this thesis develops reduction factors that correspond to the ranges of probabilities of failure of the bridge pier subject to the impact loading. Table 3.2 defines the assumed resistance reduction values for the probabilities of failures determined in the impact analysis. The statistical parameters of the blast are used in the reduction process to best represent the variation in the data and provide understandable decreases in bridge pier resistance. The variation spread corresponding to a range of failure probabilities is evenly distributed for ease of evaluation.

Table 3.2: Pier Resistance Reduction

Probability of Failure from Vehicle Impact	Reduction
$0\% < P_f \leq 12\%$	1σ
$12\% < P_f \leq 24\%$	2σ
$24\% < P_f \leq 36\%$	3σ
$36\% < P_f \leq 48\%$	4σ
$48\% < P_f \leq 60\%$	5σ
$60\% < P_f \leq 72\%$	6σ
$72\% < P_f \leq 84\%$	7σ
$84\% < P_f \leq 100\%$	8σ

Traditionally, a fault tree analysis has been used to analyze the structural reliability of a system. A fault tree analysis shows failure paths that can result in the defined top event. In this study, the top event is defined as the flexural failure of the reinforced concrete bridge pier (Ayyub & McCuen, 2011). Figure 3.8 shows the fault tree representing this study.

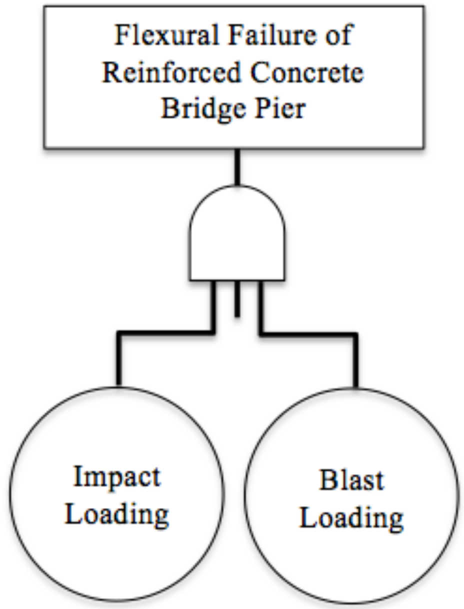

Figure 3.8: Fault Tree

Equation 3.9 shows the probability of failure of the system for the independent failure events (Ayyub & McCuen, 2011):

$$P(E) = 1 - [1 - P(E_1)][1 - P(E_2)] \dots [1 - P(E_{n-1})][1 - P(E_n)] \qquad \text{(Eq. 3.9)}$$

where: *P(E)* is the probability of failure of the system and $P(E_i)$ is the probability of failure of the individual event. Equation 3.10 shows the probability of failure of the reinforced concrete bridge pier for the impact and blast events:

$$P(f) = 1 - \left[1 - P\left(f_{impact}\right)\right][1 - P(f_{blast})] \qquad \text{(Eq. 3.10)}$$

where: *P(f)* is the probability of flexural failure of the bridge pier, $P(f_{impact})$ is the probability of failure due to the impact event, and $P(f_{blast})$ is the probability of failure due to the blast event. The results from both the newly proposed method and the fault tree analysis are compared.

3.2.2 Random Variables

When an engineer designs a concrete structure, they must first define the properties of the concrete and reinforcement the structure will be composed of (Darwin, Dolan, & Nilson, 2010). These parameters are then used in design equations to verify the structure is designed according to the design code established (ASCE, 2010). With all civil engineering designs and material properties, there is uncertainty in exactly how a structure or material will behave (Ayyub & McCuen, 2011). For this reason, the resistance and loading portions of the performance equation will contain one or more random variable(s).

Once the exact performance equation is identified, the random variables are identified. The resistance random variables in this study are: the concrete pier dimensions, specifically the moment arm, reinforcing area, yield strength of the reinforcement, and the axial load imposed on the bridge pier. The yield strength of the steel reinforcement is taken as 50 kN/cm^2 (72.5 ksi) for all event scenarios (Cizmar, et. al., 2008), while the remaining three random variables are user input values. The resistance random variables and their corresponding statistical parameters are shown in Table 3.3.

Table 3.3: Resistance Random Variable Parameters (Cizmar, et. al., 2008)

Variable	Variable Distribution	Units	Mean	Standard Deviation (% of mean)
y_2	Normal	cm	User Input	5%
A_s	Normal	cm^2	User Input	5%
f_y	Lognormal	kN/cm^2	50	5%
N	Lognormal	kN	User Input	10%

3.2.2.1 Impact Loading

The impact loading random variables in this study are: vehicle mass, vehicle stiffness, vehicle speed, and vehicle acceleration. The vehicle stiffness is taken as 300 kN/m (1,710 lb/in) for all event scenarios (Cizmar, et. al., 2008), while the vehicle speed and acceleration are user input values. The vehicle mass values are defined in Table 3.1 in Section 3.1.1.2. Each vehicle class has an average mass and an average impact height. The reliability analysis is carried out for all five classes of vehicles, in order to consider the significance in vehicle type on the failure probability of the bridge pier subject to the impact event. The value for the mass defined in Table 3.1 is taken as the value of the vehicle mass random variable for each vehicle class event. The impact height affects the moment applied to the bridge pier, which renders it an important parameter of each vehicle class. The impact loading random variables and their corresponding statistical parameters can be seen in Table 3.4.

Table 3.4: Impact Loading Random Variable Parameters (Cizmar, et. al., 2008)

Variable	Variable Distribution	Units	Mean	Standard Deviation (% of mean)
m	Normal	kg	See Table 3.1	33%
k	Lognormal	kN/m	300	20%
v	Lognormal	kmh/h	User Input	15%
a	Lognormal	m/s^2	User Input	32.5%

The force on the structure resulting from the vehicle impact is a function of the mass of the vehicle and the speed and acceleration of the vehicle. Both accidental and intentional events are analyzed, the difference lying in the vehicle speed and acceleration. Accidental impact loadings will most likely occur with a vehicle travelling at an acceptable speed, near the speed limit, and a deceleration. These factors are considered in the analysis. Intentional events can include a greater impact force from heightened vehicle speeds and accelerations. In order to satisfy various types of analyses, the user inputs the vehicle speed and acceleration into the MATLAB code.

3.2.2.2 Blast Loading

The blast loading random variable in this study is the charge weight (CW). The charge weight is a user input value. The blast loading random variables and their corresponding statistical parameters are shown in Table 3.5.

Table 3.5: Blast Loading Random Variable Parameters

Variable	Variable Distribution	Units	Mean	Standard Deviation (% of mean)
CW	Normal	kg of TNT	User Input	33%

Gedeon (n.d.) identifies different sizes of explosives using pipes, luggage, automobiles, vans, and trucks, shown in Table 3.6. The range of the blast charge weights is a function of the size of the vehicles. Smaller vehicles have a smaller charge weight capacity because they have less room to store the explosive. Similarly, larger vehicles have a larger capacity for a larger explosive, but still have a maximum limit. The values and ranges of charge weights defined in by Gedeon are used as a guide to determine the blast load random variable.

Table 3.6: Vehicle Bomb Charge Weights (US Department of Energy, 2012)

Vehicle	Blast Charge Weight (lbs of TNT)
Car	500
SUV/Van	1,000
Small Moving Van/Delivery Truck	4,000
Moving Van/Water Truck	10,000
Semi-Truck/Trailer	60,000

It is important to recognize that the values provided in Table 3.6 represent the explosive capacities of the different vehicle classes. Since the primary concern of this thesis is an explosive loading at a small standoff distance, the charge weights considered are less than 1,000 pounds of TNT. Table 3.7 defines all the non-random variables (i.e. deterministic values) used in the analysis, along with their means and standard deviations.

Table 3.7: Variable Parameters

Variable	Units	Mean	Standard Deviation (% of mean)
λ_M	-	1	0 (Deterministic)
r	m	23	0 (Deterministic)
h	m	See Table 3.1	0 (Deterministic)
R	m	User Input	0 (Deterministic)

3.2.3 Random Number Simulation

A critical step in the Monte Carlo Simulation is random number generation. The random numbers are generated within the MATLAB code. Each load or resistance random variable includes its own set of random numbers, using the same count of numbers for each variable to ensure consistency. The study contains several different combinations of the random variables. One example of this is an impact event including an SUV travelling at high speeds and the corresponding blast load from the explosive carried by the SUV.

For each scenario, a Monte Carlo simulation is completed for each random variable. Specifically, the resistance portion of the event includes four Monte Carlo simulations per scenario, the impact loading portion of the event includes four Monte Carlo simulations per scenario, and the blast loading portion of the event includes one Monte Carlo simulation per scenario. In the multi-hazardous scenarios, the Monte Carlo simulations are completed first for the resistance and impact portions of the performance function, and then again for the reduced resistance and blast portions of the performance function.

In the Monte Carlo simulations, the means and standard deviations of the random variables, collected in the relevant data collection phase and identified in Section 3.2.2, are first normalized from their original distributions. The moment arm, reinforcing steel area, vehicle mass, and charge weight have normal distributions, so the means and standard deviations are already normalized. The steel yield strength, axial load, vehicle stiffness, vehicle speed, and vehicle acceleration are lognormal, so the means and standard deviations are normalized using Equations 3.11 and 3.12 (Collins & Nowak, 2000):

$$\sigma^2_{\ln(X)} = \ln(V_X^2 + 1) \qquad \text{(Eq. 3.11)}$$

$$\mu_{lnX} = \ln(\mu_X) - \tfrac{1}{2}\sigma^2_{lnX} \qquad \text{(Eq. 3.12)}$$

where: $\sigma^2_{\ln(X)}$ is the variance of ln(X), V_X is the coefficient of variation, μ_{lnX} is the mean value of ln(X), and μ_X is the mean value of the variable X.

Once the random variables and their corresponding random number sets and normalized parameters are determined, Equation 3.13 is used to transform the random numbers to the standard normal and Equations 3.14 and 3.15 are used for the normal and lognormal variables, respectively:

$$z_i = \phi^{-1}(p_i) \qquad \text{(Eq. 3.13)}$$

$$x_i = \mu_X + z_i\sigma_X \qquad \text{(Eq. 3.14)}$$

$$x_i = exp[\mu_{lnX} + z_i\sigma_{lnX}] \qquad \text{(Eq. 3.15)}$$

where: z_i is the standard normal random variable, ϕ^{-1} is the inverse of the standard normal cumulative distribution function, p_i is the random number in the specific set, and

σ_X is the standard deviation of the variable. The means of these random number sets are taken as the simulated Monte Carlo values for the random variables and used in the performance equations. The resulting simulated random number sets are used in the limit state equations to be used in the reliability analysis.

3.3 Reliability Analysis

3.3.1 Reliability Index

In general, failure occurs when this performance function results in a negative number and a success occurs when the performance function results in a positive number. The probability of failure is equal to the number of failures determined from the simulation divided by the total number of simulated equations.

The probabilities of failure due to the impact load alone, the blast load alone, and sequential impact and blast loads are determined using the above procedures outlined. In the singular loading scenarios, one round of simulation for the resistance-loading combination is performed. In the multi-hazardous scenario, two rounds of simulation for the resistance-loading combinations are performed; the first considering the impact loading and the second considering the sequential blast loading in the limit state equation. When the blast loading is applied to the pier in the multi-hazardous scenario, the pier will have already been damaged from the impact force. This results in an increased probability of failure of the concrete bridge pier from the already determined failure probability in the impact analysis. The resilience in the limit state equation is reduced to include the already determined probability of failure of the weakened structure using the reductions provided in Table 3.2 in Section 3.2.1.3.

After the simulations are completed, a first order, second moment reliability analysis to determine the reliability index for the structure is performed for each case of interest (Ayyub & McCuen, 2011). Ayyub and McCuen define the reliability index as a parameter used to measure the reliability of a structure or structural element. The procedure to determine a structure's reliability includes both the probability of occurrence, the likeliness that the hazardous loading will occur in the structure's lifetime, and the reliability index (Eamon, 2007). It is important to recognize that the reliability analysis completed in this study is only concerned with a one hundred percent chance that the hazardous loadings will occur. In other words, the probability of occurrence for the impact force, blast pressure force, or both is equal to one.

The reliability index (β) is the inverse of the coefficient of variation and is (Collins & Nowak, 2000):

$$g(X_1, X_2, \dots, X_n) = a_0 + a_1X_1 + a_2X_2 + \dots + a_nX_n = a_0 + \sum_{i=1}^{n} a_iX_i \qquad \text{(Eq. 3.16)}$$

$$\beta = \frac{a_0 + \sum_{i=1}^{n} a_i\mu_{X_i}}{\sqrt{\sum_{i=1}^{n}\left(a_i\sigma_{X_i}\right)^2}} \qquad \text{(Eq. 3.17)}$$

where: $g(X_1, X_2, \dots, X_n)$ is a general limit state function, a_i terms are constants, and X_i are uncorrelated random variables. The performance functions for both the impact and blast loading scenarios are nonlinear, so Equations 3.18 and 3.19 can be used to determine β. These equations use a Taylor series expansion to approximate β by linearizing the nonlinear performance function about the mean values of the variables (Collins & Nowak, 2000):

$$g(X_1, X_2, \dots, X_n) \approx g\left(\mu_{X_1}, \mu_{X_2}, \dots, \mu_{X_n}\right) + \sum_{i=1}^{n}\left(X_i - \mu_{X_i}\right) \frac{\partial g}{\partial X_i}\bigg|_{ev.\ at\ mean\ values} \qquad \text{(Eq. 3.18)}$$

$$\beta = \frac{g(\mu_{X_1}, \mu_{X_2}, \ldots, \mu_{X_n})}{\sqrt{\sum_{i=1}^{n}\left(a_i \sigma_{X_i}\right)^2}} \quad where\ a_i = \left.\frac{\partial g}{\partial X_i}\right|_{evaluated\ at\ mean\ values} \qquad \text{(Eq. 3.19)}$$

where: $g(\mu_{X_1}, \mu_{X_2}, \ldots, \mu_{X_n})$ is the limit state function evaluated at the mean values and $\frac{\partial g}{\partial X_i}$ is the partial derivative of the limit state function evaluated at the mean value of the random variable of interest.

The reliability model computes β for various resistance and loading scenarios and the different vehicle classes. The corresponding probability of failure is (Collins & Nowak, 2000):

$$P_f = 1 - \phi(\beta) \qquad \text{(Eq. 3.20)}$$

where: P_f is the probability of failure and ϕ is the standard normal cumulative distribution function. Applying the defined Equations, the probabilities of failure corresponding to each vehicle type and charge weight are calculated for the specified pier resistance and loading event.

3.3.2 Sensitivity Analysis

Using the simulation procedure and equations, several pier resistance and loading event scenarios are considered and sensitivity analysis is carried out for the purpose of identifying the most influential parameters of the impact, blast, and multi-hazardous events causing failure as defined by the limit state equations. Collins and Nowak (2000) identify a general procedure for performing sensitivity analysis as: 1) system definition and possible scenario identification, 2) scenario reliability determination, and 3) most sensitive parameter identification.

In the sensitivity analysis, one parameter is adjusted while the others stay constant to analyze the influence the changing parameter has on the reliability. Fragility curves are generated in Microsoft Excel to provide a graphical representation of the sensitivity analysis. Fragility curves are curves that express the probability of failure dependent on a given loading. Each curve developed includes the probability of failure or reliability index on its dependent axis, while the parameter of focus in that specific sensitivity analysis is the independent variable.

During the sensitivity analysis, one parameter is adjusted while the other parameters are held constant. Table 3.8 shows values of the constant parameters while another parameter is undergoing analysis in the intentional impact event.

Table 3.8: Constant Parameters in Sensitivity Analysis (Intentional)

Variable	Mean
Pier Radius	0.25 m (0.82 ft)
Pier Height	5 m (16.4 ft)
Bar Number	7
Axial Load	75%P_{allow} kN
Vehicle Velocity	110 kmh/hr (68.4 mph)
Vehicle Acceleration	3 m/s^2 (9.84 ft/s^2)

Table 3.9 shows values of the constant parameters while another parameter is undergoing analysis in the accidental impact event.

Table 3.9: Constant Parameters in Sensitivity Analysis (Accidental)

Variable	Mean
Pier Radius	0.25 m (0.82 ft)
Pier Height	5 m (16.4 ft)
Bar Number	7
Axial Load	75%P_{allow} kN
Vehicle Velocity	80 kmh/hr (49.7 mph)
Vehicle Acceleration	-3 m/s^2 (-9.84 ft/s^2)

Fragility curves are developed for the impact loading alone, blast loading alone, and multi-hazardous loading. A sensitivity analysis is completed for each variable shown in Tables 3.8 and 3.9 in all three loading type scenarios. This allows for the identification of the resistance, impact loading, and blast loading parameters that most contribute to high probabilities of failure.

3.4 Opportunities and Limitations

3.4.1 Comparison Opportunities

The above procedure and explanations are applied to different reinforced concrete parameters, as explained previously, and compared to determine the effect of adjusting material properties on the failure probabilities. It is beneficial to the study to determine as many factors that can affect the probability of failure of the bridge pier and the various fragility curves allow for the critical loading and resistance combination to be determined for both the solitary hazardous loading and the multi-hazardous loading scenarios.

3.4.2 Limitations

The major limitation is time and money. There is not adequate time or funds provided to do physical testing in this study. If more time and funds were available, reinforced concrete samples could be formed and subject to impact and blast loadings. This is a very expensive and complex process that is not possible at this point in the study.

3.5 Summary

This chapter outlines and describes the methodology of the study of circular reinforced concrete bridge piers exposed to subsequent impact and blast events. A summary of the significant points are presented:

(1) Collect relevant bridge pier material data and the corresponding statistical parameters. Pier properties of interest in the analysis include the concrete pier dimensions, reinforcing area, yield strength of the reinforcement, and the axial load imposed on the bridge pier.

(2) Collect relevant impact loading data and the corresponding statistical parameters. Vehicle size and mass figures and their statistical parameters are collected. The corresponding impact heights of different vehicle types are determined and sorted into realistic scenarios for the numerical analysis.

(3) Collect relevant blast loading data and assume statistical parameters. Possible and likely blast charge weights, and their statistical parameters, are considered, paralleling charge weights with vehicle types.

(4) Monte Carlo simulation and first order, second moment reliability analysis is performed for impact events and impact fragility curves are developed. Repeat the simulations for various combinations.

(5) Monte Carlo simulation and first order, second moment reliability analysis is performed for blast events and blast fragility curves are developed. Repeat the simulations for various combinations.

(6) Monte Carlo simulation and first order, second moment reliability analysis is performed for impact events. Adjust the pier resistance depending the first hazard and repeat the Monte Carlo simulation and first order, second moment reliability analysis for the sequential blast event. Develop the multi-hazard fragility curves. Repeat the simulations for various combinations.

(7) Perform sensitivity analysis based on generated fragility curves and determine resistance and loading parameters that most influence the probability of failure.

CHAPTER 4

IMPACT ANALYSIS

This chapter includes the analysis of the circular reinforced concrete bridge pier subject to vehicular impact. Impact loads are probabilistic in nature due to their randomness in occurrence and intensity. There is a gap in the existing literature regarding impact loads and bridge substructures, which confirms the importance of a study (Cizmar, Miculinic, & Mestrovic, 2008). The risk of vehicle impact on a bridge depends on the amount of traffic and possible consequences resulting from an impact event.

The reliability analysis of the bridge pier subject to the impact loading follows the methodology outline explained in Section 3.1.2. The first step, relevant data collection, for the impact analysis is completed using the equations, variables, and the statistical data provided in *Reliability of concrete columns under vehicular impact* by Cizmar and others; the study used as the foundation for this research study (2008). The equations used in this research study employ the assumption that the impact loading can be treated as a static loading due to similar failure mechanisms between the vehicle and the bridge pier (El-Tawil, 2004).

Using the procedures and equations defined in Sections 3.2 and 3.3, the reliability and sensitivity analyses are completed with a MATLAB code developed specifically for this study included in Appendix A, that analyzes a circular reinforced concrete bridge pier subject to intentional blast loading. Several pier resistance and loading event scenarios are considered and sensitivity analysis is carried out for the purpose of identifying the most influential parameters of the impact events causing failure as defined by the limit state equations. The results of the impact reliability and sensitivity analyses are presented hereafter.

4.1 Intentional and Accidental Vehicular Impact

The principal focus of this study is on intentional, or terroristic, vehicular impact. In order to completely understand vehicular impact, accidental impact is also considered. The difference between the intentional and accidental scenario lies in the vehicle speed and acceleration. The purpose of considering both types of vehicular impact is to allow for the severity and importance of understanding the effect of vehicular impact on reinforced concrete bridge piers, along with identifying the most influential parameters contributing to probabilities of failure for both loading types.

The variables and their corresponding statistical parameters used in the impact analysis are defined in Section 3.2.2 in Table 3.3. Tables 4.1 and 4.2 show values of the constant held parameters while the other parameter is varied in the intentional and accidental vehicular impact event, respectively.

Table 4.1: Constant Impact Parameters in Sensitivity Analysis (Intentional)

Variable	Mean
Pier Radius	0.25 m (0.82 ft)
Pier Height	5 m (16.4 ft)
Bar Number	7
Axial Load	75%P_{allow} kN
Vehicle Velocity	110 kmh/hr (68.4 mph)
Vehicle Acceleration	3 m/s^2 (9.84 ft/s^2)

Table 4.2: Constant Impact Parameters in Sensitivity Analysis (Accidental)

Variable	Mean
Pier Radius	0.25 m (0.82 ft)
Pier Height	5 m (16.4 ft)
Bar Number	7
Axial Load	75%P_{allow} kN
Vehicle Velocity	80 kmh/hr (49.7 mph)
Vehicle Acceleration	-3 m/s^2 (-9.84 ft/s^2)

4.1.1 Sensitivity Analysis of Reinforcement Ratio

The reinforcement ratio is defined as the ratio of the reinforcement steel area to the gross area of the bridge pier:

$$\rho = \frac{A_S}{A_C} = \frac{A_S}{\pi\left(\frac{d}{2}\right)^2} \qquad \text{(Eq. 4.1)}$$

where: ρ is the reinforcement ratio, A_s is the area of reinforcing steel, A_c is the area of concrete, and d is the diameter of the bridge pier.

As seen in Tables 4.1 and 4.2, the constant pier radius is taken as 0.25 meters (9.8 in) for both intentional and accidental impact. With this radius, the gross area of the bridge pier is calculated as 1,964 cm^2 (304.4 in^2). In the sensitivity analysis of the reinforcement ratio, the steel reinforcing area is increased while all other variables are kept constant. The bar size numbers and their corresponding cross-sectional areas can be seen in Table 4.3. The reinforcement ratio is increased by considering the eight reinforcing bars in the bridge pier and increasing the bar size number with each iteration.

Table 4.3: Reinforcing Bar Area

Bar Number	Area (in^2)	Area (cm^2)
3	0.11	0.71
4	0.20	1.29
5	0.31	2.00
6	0.44	2.84
7	0.60	3.87
8	0.79	5.09
9	1.00	6.45
10	1.27	8.19
11	1.56	10.06

The reliability curves for the sensitivity analysis of the reinforcement ratio due to intentional vehicular impact are displayed in Figures 4.1 and 4.2. The five curves demonstrate the analysis of the different vehicle types defined in Section 3.1.1. Each sensitivity analysis for the specific parameters is completed for each of the vehicles types and shown later in the Figures.

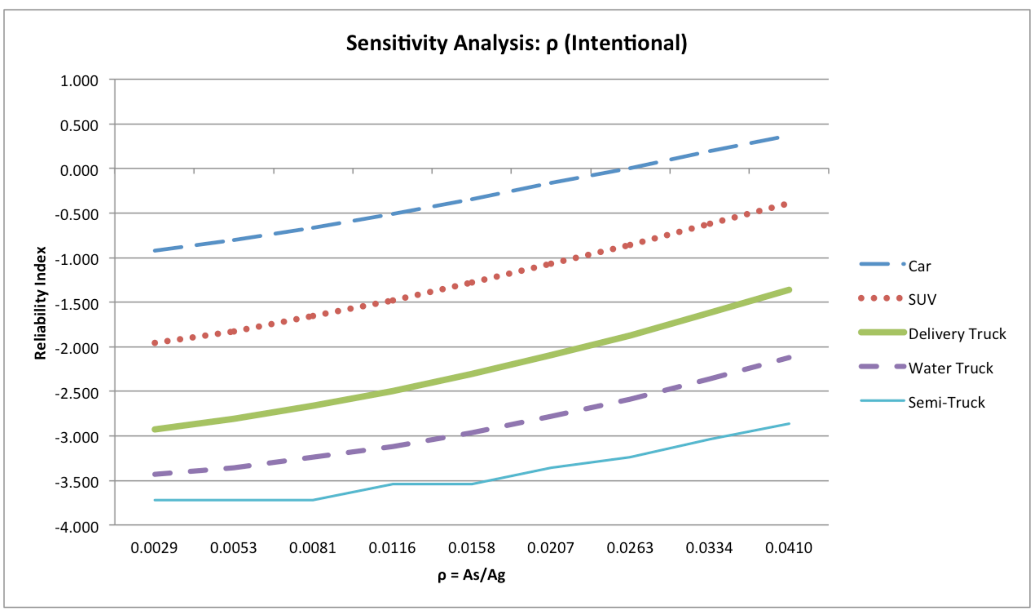

Figure 4.1: Reinforcement Ratio Reliability Index Curve - Intentional Impact

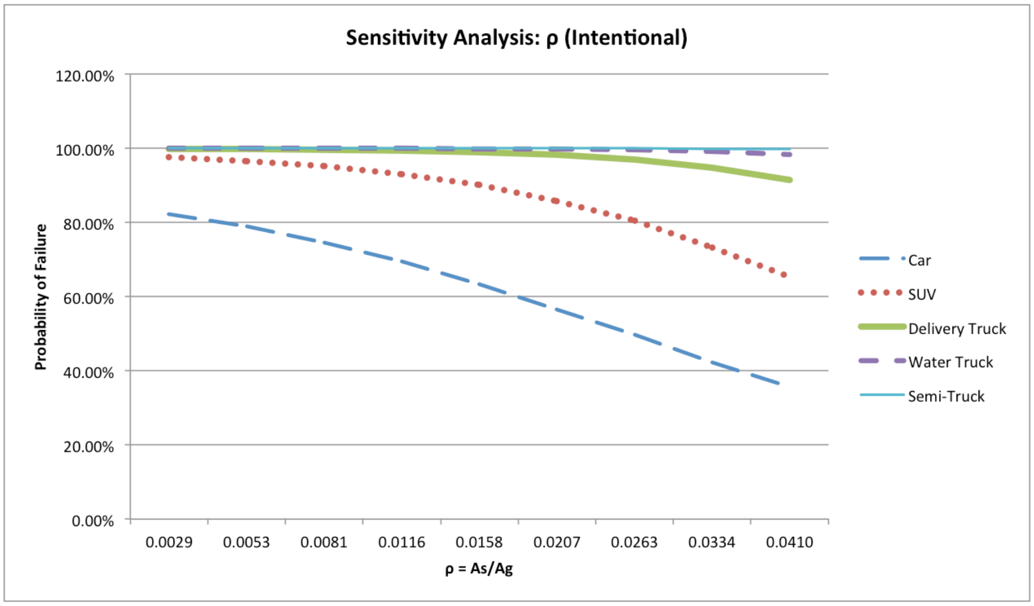

Figure 4.2: Reinforcement Ratio Fragility Curve – Intentional Impact

The reliability curves corresponding to the different vehicle types generally follow the same trend. The reliability index consistently increases as the reinforcement ratio increases, and therefore, the probability of failure consistently decreases as the reinforcement ratio increases. Table 4.4 provides the values of the largest decrease in the probability of failure for the different vehicle classes and at which change of reinforcement ratio the maximum decrease occurs (e.g. the maximum change in the failure probability occurs from the use of a number 11 bar rather than a number 10 bar).

Table 4.4: Reinforcement Ratio Incremental % Change – Intentional Impact

Reinforcement Ratio Incremental % Change			
Vehicle Class	**Maximum % Change**	**From:**	**To:**
Car	-15.77%	#10 Bar	#11 Bar
SUV	-10.90%	#10 Bar	#11 Bar
Delivery Truck	-3.50%	#10 Bar	#11 Bar
Water Truck	-0.80%	#10 Bar	#11 Bar
Semi-Truck	-0.09%	#10 Bar	#11 Bar

Table 4.4 demonstrates that the fragility curves get steeper as the bar numbers get higher. This means that the decrease of failure probability becomes larger with each increase in bar size. However, this is more evident in the smaller vehicles, as the larger vehicles display a much flatter curve. The percentages representing the largest decrease in failure probability, shown in Table 4.4, indicate that as the vehicle mass increases, the change in failure probability decreases and the fragility curves are flatter than that of a smaller mass vehicle. This is due to the probabilities of failure of the larger vehicles being very high, regardless of the reinforcement ratio.

Table 4.5 presents the percentage change in the probability of failure of the bridge pier with a percentage increase in the reinforcement ratio. Tables for each parameter undergoing a sensitivity analysis are provided to allow for the most influential resistance and loading parameters to be identified. For uniformity and ease of understanding, a percentage increase in the resistance and loading parameters will be held at ten percent.

Table 4.5: Reinforcement Ratio % Change in Failure Probability- Intentional Impact

Vehicle Class	% Change in Reinforcement Ratio	% Change in Probability of Failure
Car	10%	-0.43%
SUV	10%	-0.25%
Delivery Truck	10%	-0.06%
Water Truck	10%	-0.01%
Semi-Truck	10%	0.00%

The values in Table 4.5 demonstrate that the a ten percent increase in the reinforcement ratio can results in up to a 0.43% decrease in the probability of failure of the bridge pier subject to an intentional vehicular impact load. The values in the table indicate that the reinforcement ratio influences the probability of failure of the bridge pier, but very minimally for vehicle masses of 4,000 kilograms (8,800 pounds) and greater.

The reliability curves for the sensitivity analysis of the reinforcement ratio due to accidental vehicular impact are displayed in Figures 4.3 and 4.4.

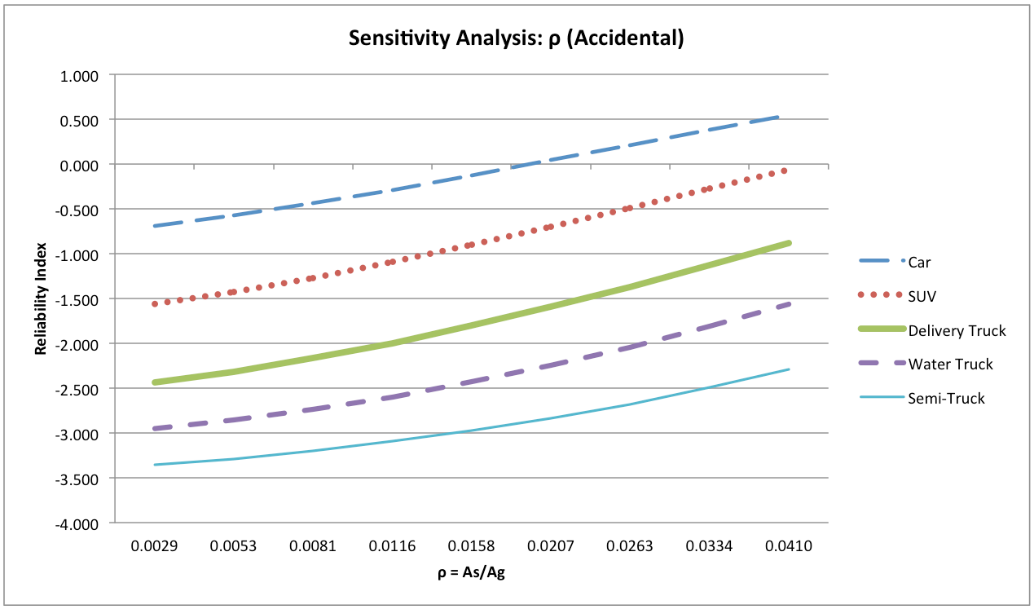

Figure 4.3: Reinforcement Ratio Reliability Index Curve – Accidental Impact

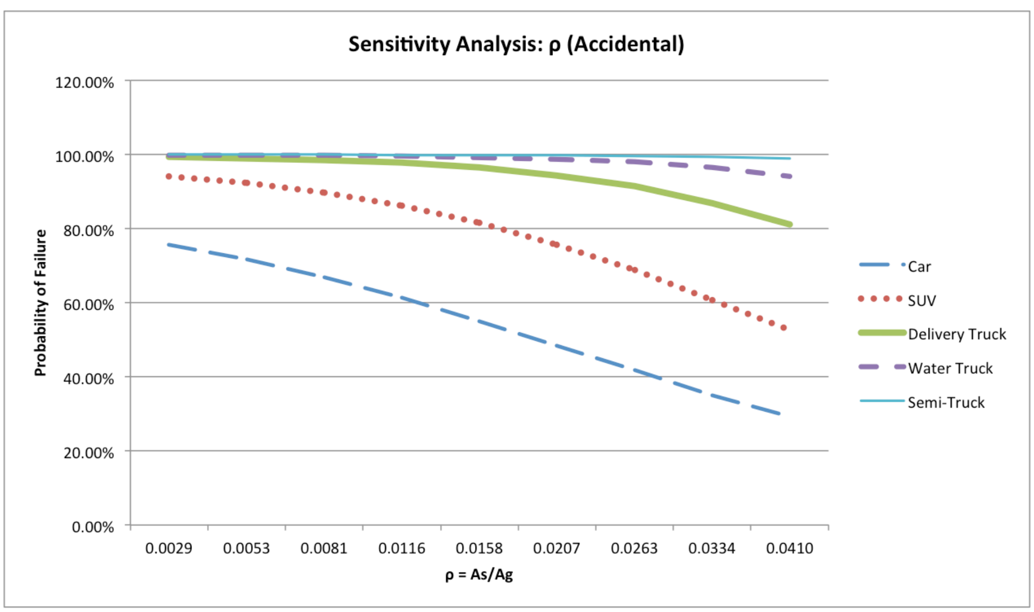

Figure 4.4: Reinforcement Ratio Fragility Curve – Accidental Impact

The reliability curves corresponding to the different vehicle types generally follow the same trend. The reliability index consistently increases as the reinforcement ratio increases, and therefore, the probability of failure consistently decreases as the reinforcement ratio increases. Table 4.6 provides the values of the largest decrease in the probability of failure for the different vehicle classes and at which change of reinforcement ratio the maximum decrease occurs.

Table 4.6: Reinforcement Ratio Incremental % Change – Accidental Impact

Reinforcement Ratio Incremental % Change			
Vehicle Class	**Maximum % Change**	**From:**	**To:**
Car	-16.65%	#10 Bar	#11 Bar
SUV	-13.29%	#10 Bar	#11 Bar
Delivery Truck	-6.66%	#10 Bar	#11 Bar
Water Truck	-2.47%	#10 Bar	#11 Bar
Semi-Truck	-0.47%	#10 Bar	#11 Bar

Like the intentional vehicular impact, the pattern of the curves demonstrates that the curve gets steeper as the bar numbers are increased. The percentages representing the largest decrease in failure probability, provided in Table 4.6, indicate that as the vehicle mass is increased, the change in failure probability is lesser and the fragility curves are flatter than that of a smaller mass vehicle.

Table 4.7 presents the percentage change in the probability of failure of the bridge pier with a ten percent increase in the reinforcement ratio.

Table 4.7: Reinforcement Ratio % Change in Failure Probability - Accidental Impact

Vehicle Class	% Change in Reinforcement Ratio	% Change in Probability of Failure
Car	10%	-0.47%
SUV	10%	-0.33%
Delivery Truck	10%	-0.14%
Water Truck	10%	-0.04%
Semi-Truck	10%	-0.01%

The values in Table 4.7 demonstrate that the a ten percent increase in the reinforcement ratio can results in up to a 0.47% decrease in the probability of failure of the bridge pier subject to an accidental vehicular impact load. The values in the table indicate that the reinforcement ratio influences the probability of failure of the bridge pier, but very minimally for vehicle masses of 5,000 kilograms (11,000 pounds) and greater.

The reinforcement ratio fragility curves are very similar for both the intentional and accidental vehicular impact loading scenarios. Both reliability index and failure probability curves followed the same trend. The accidental scenario displays steeper curves than the intentional scenario, which indicates the reinforcement ratio has greater influence when vehicles are travelling at lesser speeds and accelerations.

4.1.2 Sensitivity Analysis of Pier Radius

In the sensitivity analysis of the pier radius, the pier radius is increased from 0.15 meters (5.9 in) to 0.35 meters (13.8 in), in increments of 0.05 meters (2 in), while all other variables are kept constant. The reliability curves for the sensitivity analysis of the pier radius due to intentional vehicular impact are displayed in Figures 4.5 and 4.6.

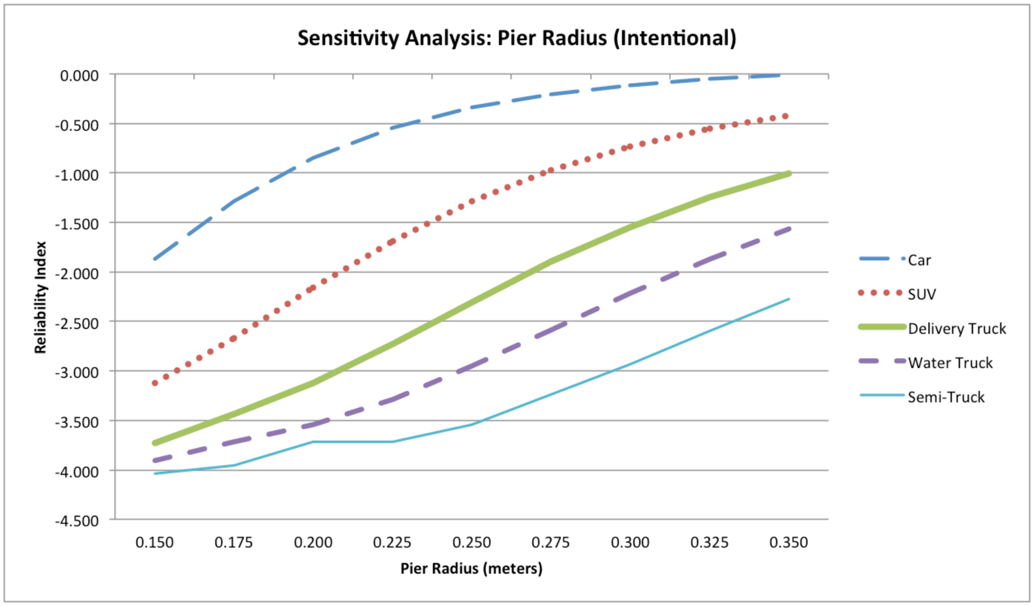

Figure 4.5: Pier Radius Reliability Index Curve – Intentional Impact

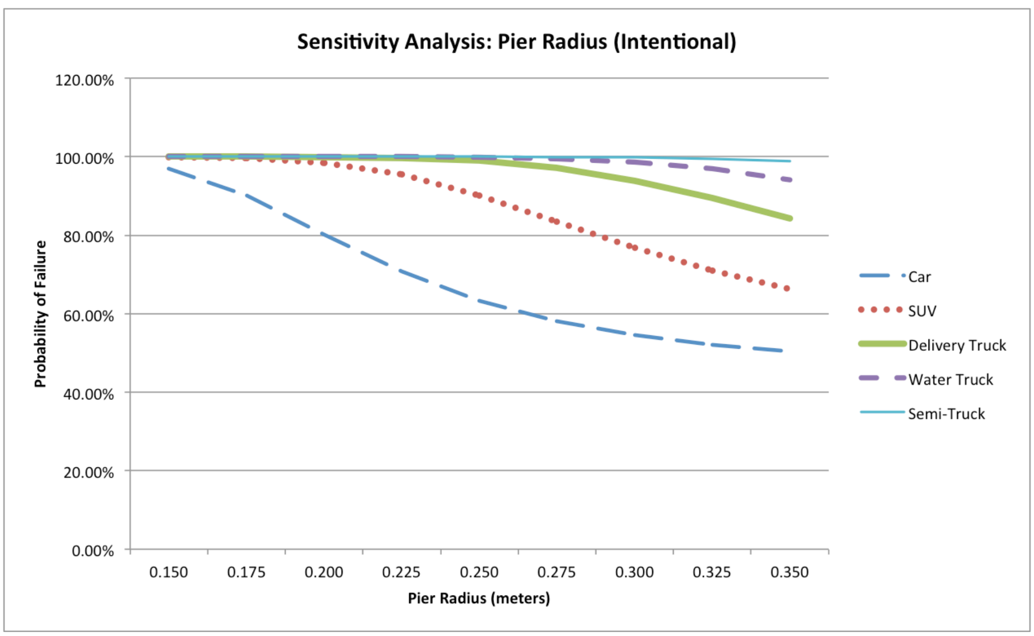

Figure 4.6: Pier Radius Fragility Curve – Intentional Impact

The reliability curves corresponding to the different vehicle types generally follow the same trend. The reliability index displays a steep increase at first and then levels as the pier radius reaches the larger values. This is the same for all vehicle classes, but the change is more dramatic in the smaller mass vehicles and more gradual with the larger mass vehicles. The probability of failure is extremely high, with some vehicle classes reaching 100% failure, at the lower pier radius values. As the pier radius is increased, the curve displays a steep decrease in probability of failure in the middle pier radius for the smaller vehicle classes. Like the reliability index, the failure probabilities level as the pier radius reaches the larger values. The larger vehicle classes display a fairly flat curve.

Table 4.8 provides the values of the largest decrease in the probability of failure for the different vehicle classes and at which change of pier radius the maximum decrease occurs.

Table 4.8: Pier Radius Incremental % Change – Intentional Impact

Pier Radius Incremental % Change			
Vehicle Class	**Maximum % Change**	**From:**	**To:**
Car	-11.76%	0.220 meters	0.225 meters
SUV	-8.09%	0.275 meters	0.300 meters
Delivery Truck	-5.76%	0.325 meters	0.350 meters
Water Truck	-2.91%	0.325 meters	0.350 meters
Semi-Truck	-0.68%	0.325 meters	0.350 meters

These values show that the lesser mass vehicles display a steeper decrease in failure probability at smaller pier radii. It can also be seen that the decreases in failure probability are larger for the smaller mass vehicles compared to that of the larger mass vehicles. Table 4.9 presents the percentage change in the probability of failure of the bridge pier with a ten percent increase in the pier radius.

Table 4.9: Pier Radius % Change in Failure Probability – Intentional Impact

Vehicle Class	% Change in Pier Radius	% Change in Probability of Failure
Car	10%	-3.60%
SUV	10%	-2.53%
Delivery Truck	10%	-1.18%
Water Truck	10%	-0.44%
Semi-Truck	10%	-0.09%

The values in Table 4.9 demonstrate that the a ten percent increase in the pier radius can results in up to a 3.60% decrease in the probability of failure of the bridge pier subject to an accidental vehicular impact load. The values in the table indicate that the pier radius significantly influences the probability of failure of the bridge pier for all vehicle classes.

The reliability curves for the sensitivity analysis of the pier radius due to accidental vehicular impact are displayed in Figures 4.7 and 4.8.

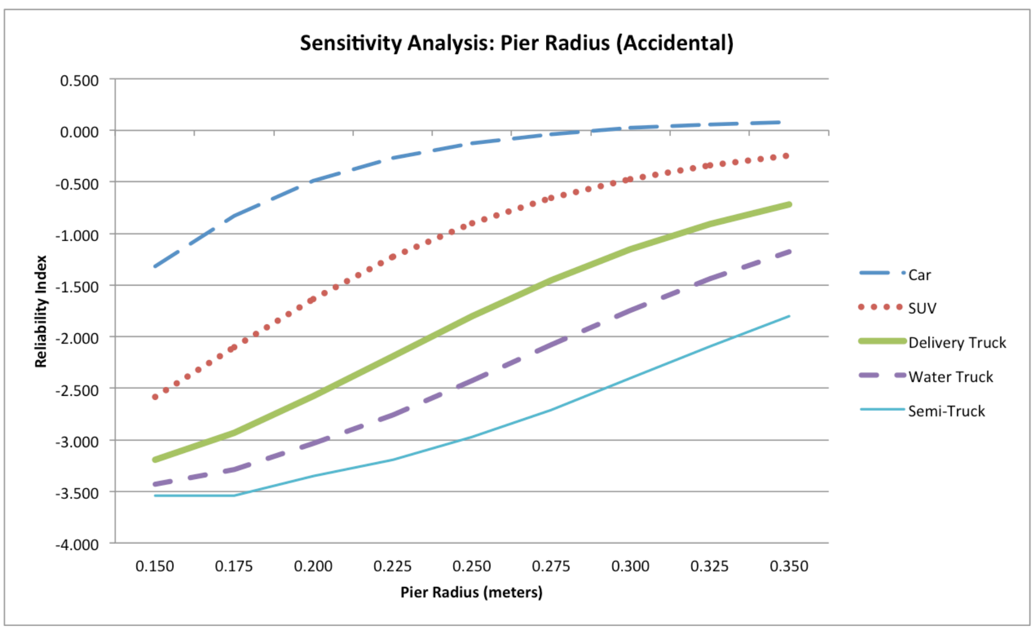

Figure 4.7: Pier Radius Reliability Index Curve – Accidental Impact

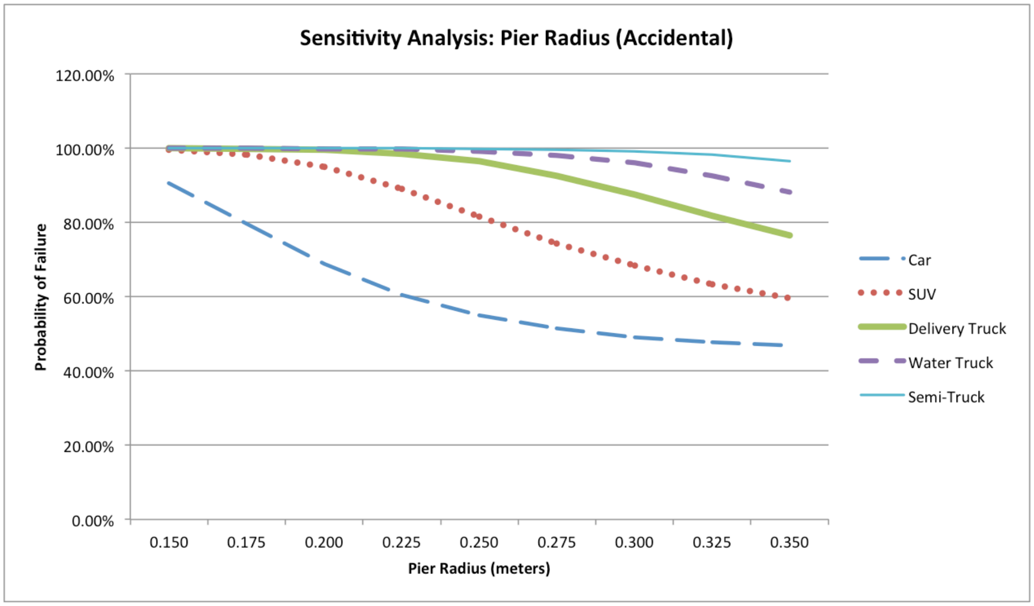

Figure 4.8: Pier Radius Fragility Curve – Accidental Impact

The reliability curves corresponding to the different vehicle types generally follow the same trend. Like the intentional impact scenario, the reliability index displays a steep increase at first and then levels as the pier radius reaches the larger values. This is the same for all vehicle classes, but the change is more dramatic in the smaller mass vehicles and more gradual with the larger mass vehicles. The probability of failure is extremely high, with some vehicle classes reaching almost 100% failure, at the lower pier radius values. As the pier radius is increased, the curve displays a steep decrease in probability of failure in the middle pier radius. Like the reliability index, the failure probabilities level as the pier radius reaches the larger values.

Table 4.10 provides the values of the largest decrease in the probability of failure for the different vehicle classes and at which change of pier radius the maximum decrease occurs.

Table 4.10: Pier Radius Incremental % Change – Accidental Impact

Pier Radius Incremental % Change			
Vehicle Class	**Maximum % Change**	**From:**	**To:**
Car	-13.65%	0.200 meters	0.175 meters
SUV	-8.75%	0.275 meters	0.300 meters
Delivery Truck	-6.66%	0.325 meters	0.350 meters
Water Truck	-4.76%	0.325 meters	0.350 meters
Semi-Truck	-1.81%	0.325 meters	0.350 meters

These values show that the lesser mass vehicles display a steeper decrease in failure probability at smaller pier radii. It can also be seen that the decreases in failure probability are larger for the smaller mass vehicles compared to that of the larger mass vehicles. Table 4.11 presents the percentage change in the probability of failure of the bridge pier with a ten percent increase in the pier radius.

Table 4.11: Pier Radius % Change in Failure Probability – Accidental Impact

Vehicle Class	% Change in Pier Radius	% Change in Probability of Failure
Car	10%	-3.63%
SUV	10%	-3.01%
Delivery Truck	10%	-1.77%
Water Truck	10%	-0.89%
Semi-Truck	10%	-0.27%

The values in Table 4.11 demonstrate that the a ten percent increase in the pier radius can results in up to a 3.63% decrease in the probability of failure of the bridge pier subject to an accidental vehicular impact load. The values in the table indicate that the pier radius significantly influences the probability of failure of the bridge pier for all vehicle classes.

The pier radius fragility curves were very similar for both the intentional and accidental vehicular impact loading scenarios. Both reliability index and failure probability curves followed the same shape. From the figures and tables presented, it can be seen that the pier radius is highly influential on the reliability of the bridge pier. The accidental scenario displays steeper curves than the intentional scenario, which indicates the reinforcement ratio has slightly greater influence when vehicles are travelling at lesser speeds and accelerations.

4.1.3 Sensitivity Analysis of Pier Height

In the sensitivity analysis of the pier height, the pier height is increased from 4.5 meters (14.8 ft) to 8.5 meters (27.9 ft), in increments of 0.50 meters (1.6 ft), while all other variables are kept constant. The reliability curves for the sensitivity analysis of the pier height due to intentional vehicular impact are displayed in Figures 4.9 and 4.10.

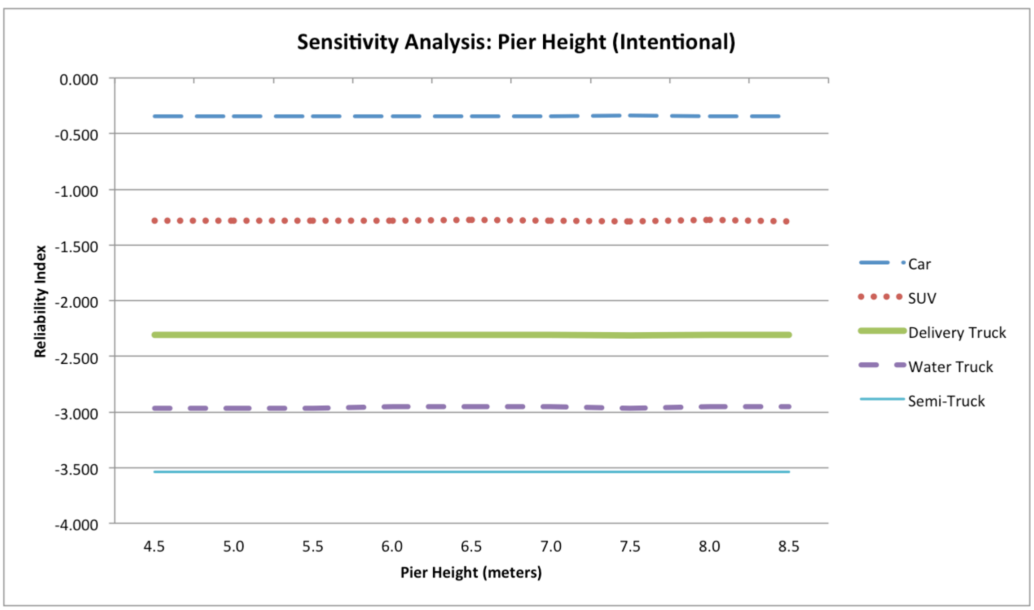

Figure 4.9: Pier Height Reliability Index Curve – Intentional Impact

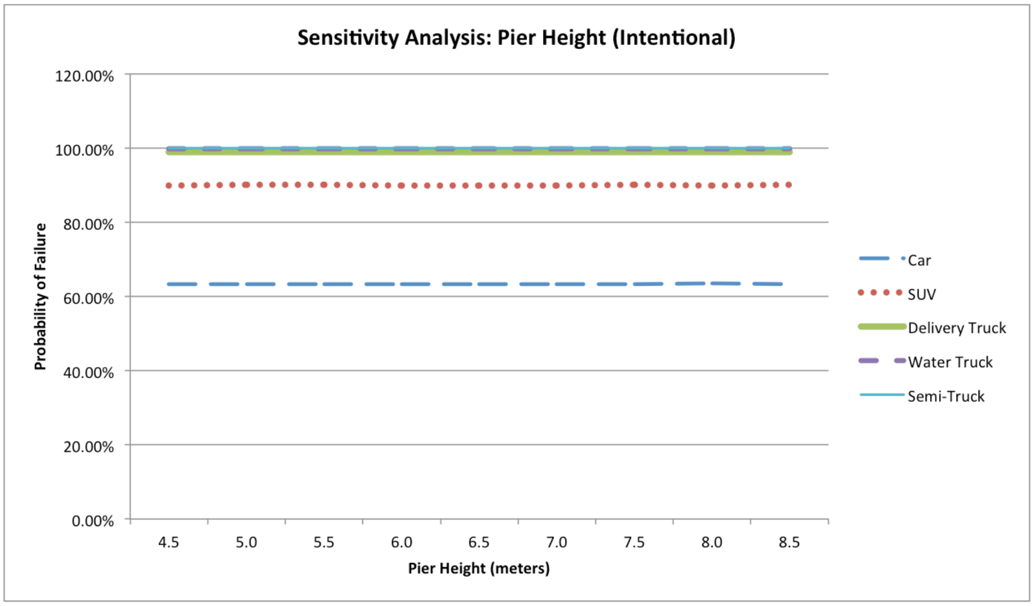

Figure 4.10: Pier Height Fragility Curve – Intentional Impact

The reliability curves corresponding to the different vehicle types generally follow the same trend. For all the vehicle classes, both the reliability index and probability of failure curves exhibit a horizontal line, indicating that the pier height has little to no influence on the reliability index and probability of failure of the reinforced concrete bridge pier.

Table 4.12 provides the values of the minimum and maximum changes in the probability of failure for the different vehicle classes with an incremental increase in pier height.

Table 4.12: Pier Height Incremental % Change – Intentional Impact

Pier Height Incremental % Change		
Vehicle Class	**Minimum % Change**	**Maximum % Change**
Car	-0.25%	0.32%
SUV	-0.20%	0.22%
Delivery Truck	-0.01%	0.02%
Water Truck	-0.01%	0.01%
Semi-Truck	0.00%	0.00%

The minimum and maximum values in Table 4.12 show that the incremental fluctuations are minimal, with the largest fluctuation barely exceeding 0.30%. These small values confirm that the pier height has little influence on the reliability of the bridge pier. Table 4.13 presents the percentage change in the probability of failure of the bridge pier with a ten percent increase in the pier height.

Table 4.13: Pier Height % Change in Failure Probability – Intentional Impact

Vehicle Class	% Change in Pier Height	% Change in Probability of Failure
Car	10%	0.01%
SUV	10%	0.02%
Delivery Truck	10%	0.00%
Water Truck	10%	0.00%
Semi-Truck	10%	0.00%

The values in Table 4.13 demonstrate that the a ten percent increase in the pier height can results in up to a 0.02% increase in the probability of failure of the bridge pier subject to an intentional vehicular impact load. The values in the table indicate that the pier height has little to no influence on the probability of failure of the bridge pier for all vehicle classes.

The reliability curves for the sensitivity analysis of the pier height due to accidental vehicular impact are displayed in Figures 4.11 and 4.12.

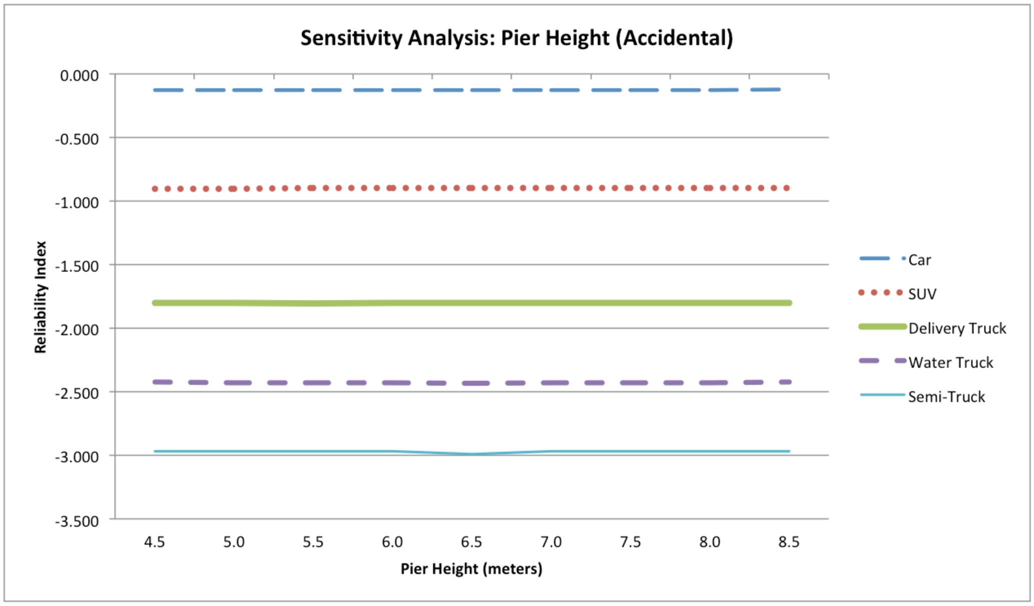

Figure 4.11: Pier Height Reliability Index Curve – Accidental Impact

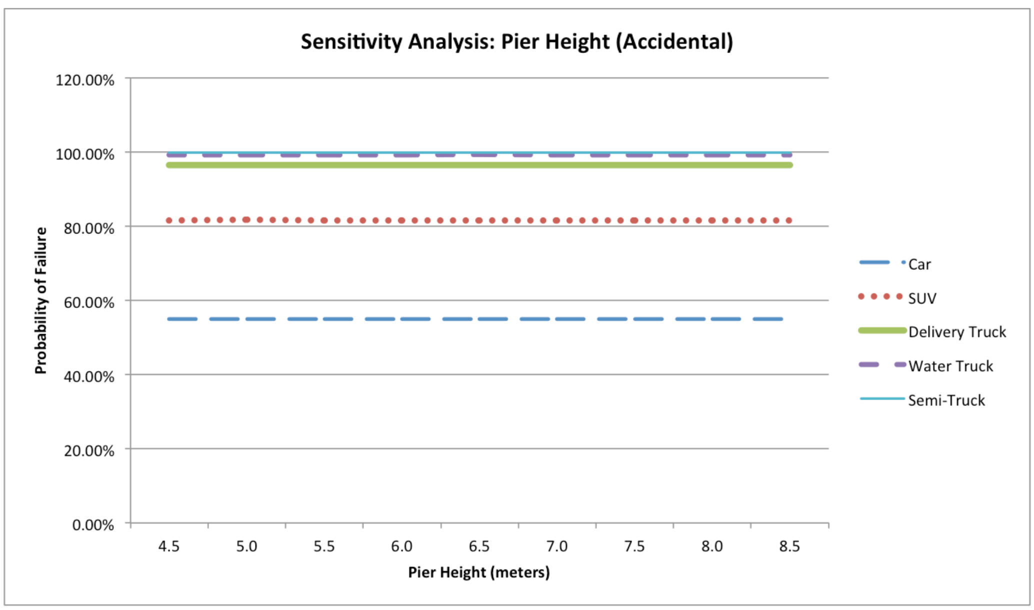

Figure 4.12: Pier Height Fragility Curve – Accidental Impact

The reliability curves corresponding to the different vehicle types generally follow the same trend. Like the intentional scenario, both the reliability index and probability of failure curves exhibit a horizontal line for all five vehicle classes, indicating that the pier height has little to no influence on the reliability index and probability of failure of the reinforced concrete bridge pier.

Table 4.14 provides the values of the minimum and maximum changes in the probability of failure for the different vehicle classes with an incremental increase in pier height.

Table 4.14: Pier Height Incremental % Change – Accidental Impact

Pier Height Incremental % Change		
Vehicle Class	**Minimum % Change**	**Maximum % Change**
Car	-0.11%	0.07%
SUV	-0.17%	0.10%
Delivery Truck	-0.03%	0.04%
Water Truck	-0.01%	0.01%
Semi-Truck	-0.01%	0.01%

The minimum and maximum values in Table 4.14 show that the incremental fluctuations are minimal, with the largest fluctuation barely exceeding -0.15%. These small values confirm that the pier height has little influence on the reliability of the bridge pier. Table 4.15 presents the percentage change in the probability of failure of the bridge pier with a ten percent increase in the pier height.

Table 4.15: Pier Height % Change in Failure Probability – Accidental Impact

Vehicle Class	% Change in Pier Height	% Change in Probability of Failure
Car	10%	-0.01%
SUV	10%	-0.02%
Delivery Truck	10%	0.00%
Water Truck	10%	0.00%
Semi-Truck	10%	0.00%

The values in Table 4.15 demonstrate that a ten percent increase in the pier height can results in up to a 0.02% decrease in the probability of failure of the bridge pier subject to an accidental vehicular impact load. The values in the table indicate that the pier height has little to no influence on the probability of failure of the bridge pier for all vehicle classes.

Both the intentional and accidental scenarios resulted in the same conclusion. Though there were slight variations in the reliability indices and failure probabilities, the incremental changes barely exceed 0.30% between both scenarios. Using this analysis, it can be seen that the pier height does not influence the reliability of a reinforced concrete bridge pier in neither an intentional vehicular impact event nor an accidental vehicular impact event.

4.1.4 Sensitivity Analysis of Axial Load

In the sensitivity analysis of the axial load, the axial load is increased from 15% of the allowable axial load to the 95% of the allowable axial load, in 10% increments, while all other variables are kept constant. The reliability curves for the sensitivity analysis of the axial load due to intentional vehicular impact are displayed in Figures 4.13 and 4.14.

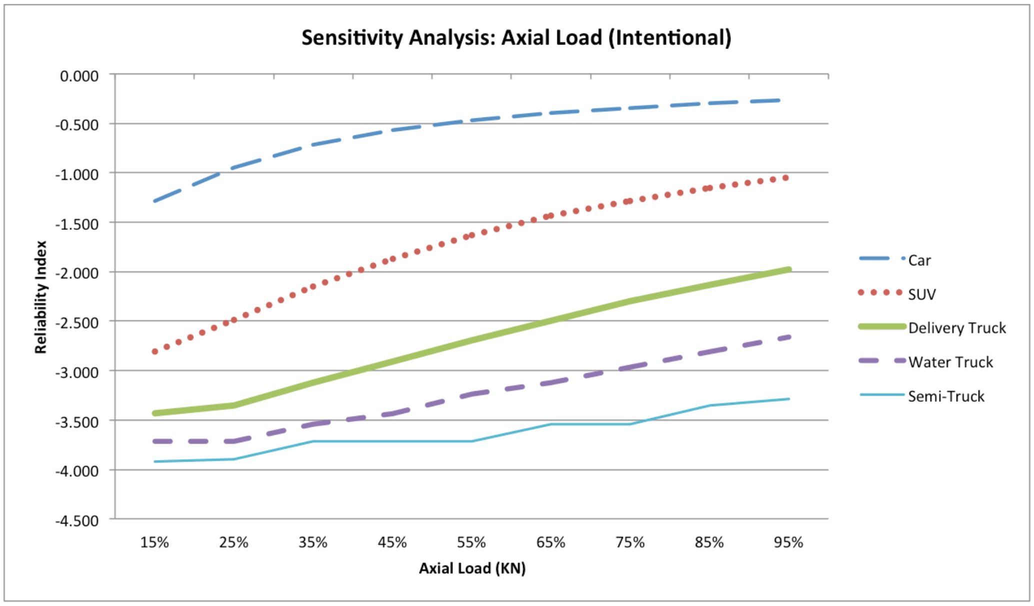

Figure 4.13: Axial Load Reliability Index Curve – Intentional Impact

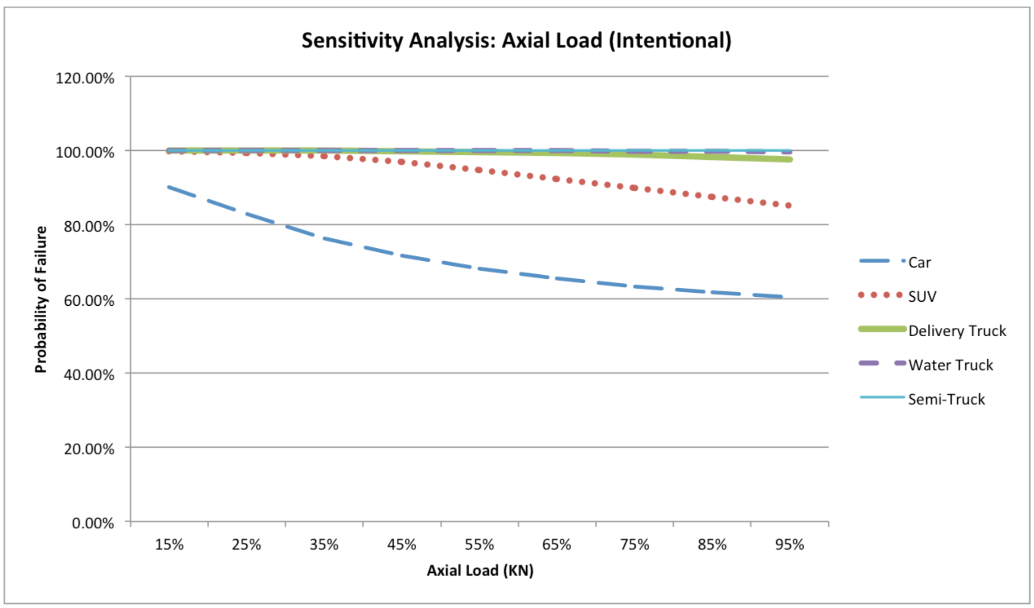

Figure 4.14: Axial Load Fragility Curve – Intentional Impact

The reliability curves corresponding to the different vehicle types generally follow the same trend, but show more variation than other parameters. The reliability index consistently increases, and therefore, the probability of failure consistently decreases as the axial load is increased. The fragility curves for the delivery truck, water truck, and semi-truck classes display a very flat trend, indicating extremely high failure probabilities for all axial load values. The smallest two vehicle classes demonstrate more variation as the axial load is increased.

Table 4.16 provides the values of the largest decrease in the probability of failure for the different vehicle classes and at which change of axial load the maximum decrease occurs.

Table 4.16: Axial Load Incremental % Change – Intentional Impact

Axial Load Incremental % Change			
Vehicle Class	**Maximum % Change**	**From:**	**To:**
Car	-8.10%	15%	25%
SUV	-2.78%	75%	85%
Delivery Truck	-0.77%	85%	95%
Water Truck	-0.14%	85%	95%
Semi-Truck	-0.02%	75%	85%

The values in Table 4.16 show that the lesser mass vehicles display a steeper decrease in failure probability at smaller axial loads. It can also be seen that the decreases in failure probability are larger for the smaller mass vehicles compared to that of the larger mass vehicles. Table 4.17 presents the percentage change in the probability of failure of the bridge pier with a ten percent increase in the axial load.

Table 4.17: Axial Load % Change in Failure Probability – Intentional Impact

Vehicle Class	% Change in Axial Load	% Change in Probability of Failure
Car	10%	-0.62%
SUV	10%	-0.27%
Delivery Truck	10%	-0.04%
Water Truck	10%	-0.01%
Semi-Truck	10%	0.00%

The values in Table 4.17 demonstrate that the a ten percent increase in the reinforcement ratio can results in up to a 0.62% decrease in the probability of failure of the bridge pier subject to an intentional vehicular impact load. The values in the table indicate that the axial load influences the probability of failure of the bridge pier, but very minimally for vehicle masses of 4,000 kilograms (8,800 pounds) and greater.

The reliability curves for the sensitivity analysis of the axial load due to accidental vehicular impact are displayed in Figures 4.15 and 4.16.

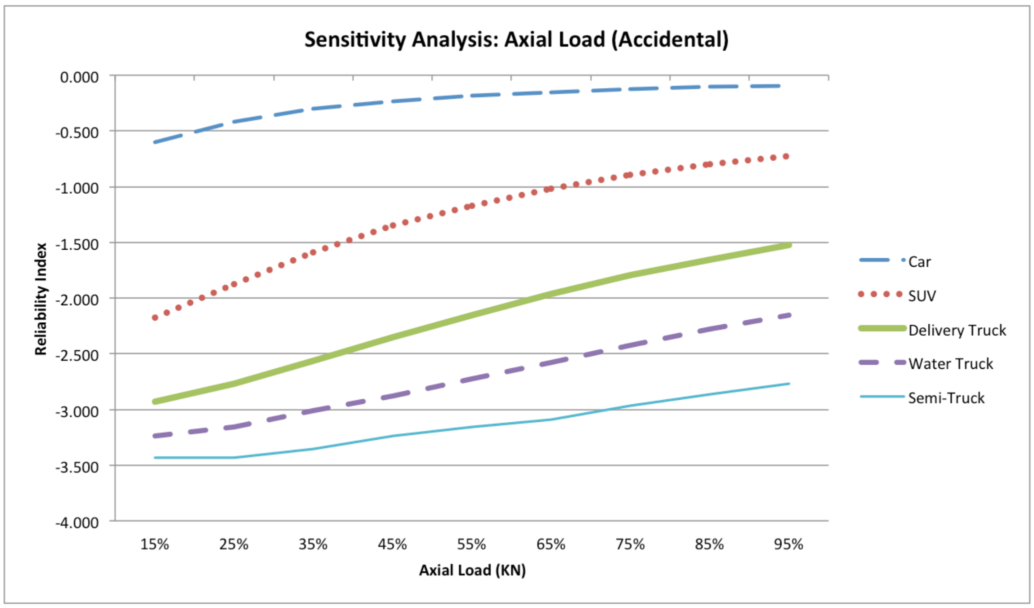

Figure 4.15: Axial Load Reliability Index Curve – Accidental Impact

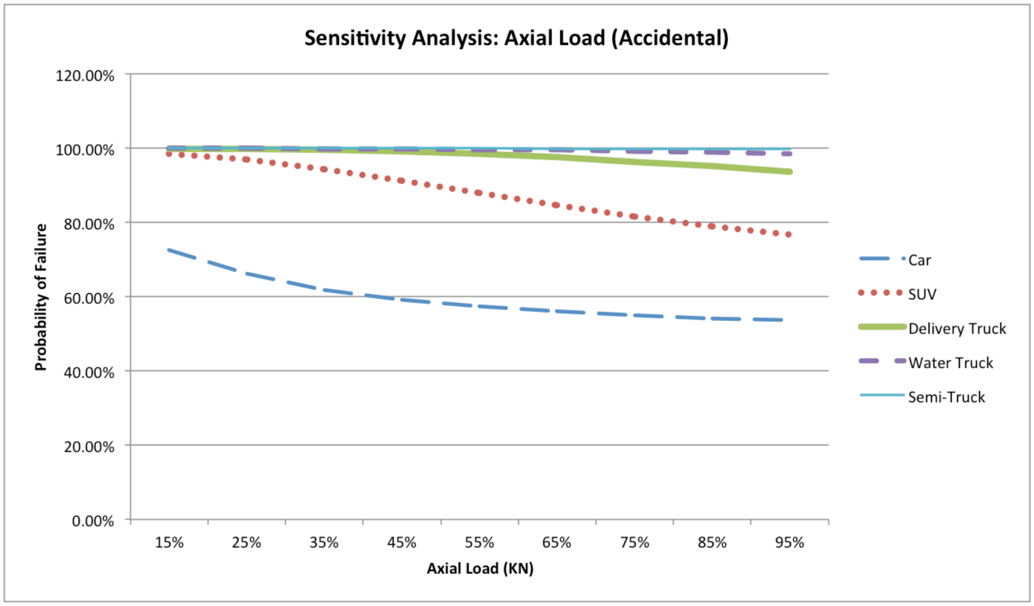

Figure 4.16: Axial Load Fragility Curve – Accidental Impact

The reliability curves corresponding to the different vehicle types generally follow the same trend, but show more variation than other parameters, similar to the intentional impact scenario. The reliability index consistently increases, and therefore, the probability of failure consistently decreases as the axial load is increased. Like the intentional scenario, the fragility curves for the delivery truck, water truck, and semi-truck classes display a very flat trend, indicating extremely high failure probabilities for all axial load values. The smallest two vehicle classes demonstrate more variation as the axial load is increased.

Table 4.18 provides the values of the largest decrease in the probability of failure for the different vehicle classes and at which change of axial load the maximum decrease occurs.

Table 4.18: Axial Load Incremental % Change – Accidental Impact

Axial Load Incremental % Change			
Vehicle Class	**Maximum % Change**	**From:**	**To:**
Car	-8.81%	15%	25%
SUV	-3.77%	55%	65%
Delivery Truck	-1.55%	85%	95%
Water Truck	-0.45%	85%	95%
Semi-Truck	-0.07%	85%	95%

The values in Table 4.18 show that the lesser mass vehicles display a steeper decrease in failure probability at smaller axial loads. It can also be seen that the decreases in failure probability are larger for the smaller mass vehicles compared to that of the larger mass vehicles. Table 4.19 presents the percentage change in the probability of failure of the bridge pier with a ten percent increase in the axial load.

Table 4.19: Axial Load % Change in Failure Probability – Accidental Impact

Vehicle Class	% Change in Axial Load	% Change in Probability of Failure
Car	10%	-0.49%
SUV	10%	-0.42%
Delivery Truck	10%	-0.12%
Water Truck	10%	-0.03%
Semi-Truck	10%	0.00%

The values in Table 4.19 demonstrate that the a ten percent increase in the axial load can results in up to a 0.49% decrease in the probability of failure of the bridge pier subject to an accidental vehicular impact load. The values in the table indicate that the axial load influences the probability of failure of the bridge pier, but very minimally for vehicle masses of 5,000 kilograms (11,000 pounds) and greater.

The axial load fragility curves were very similar for both the intentional and accidental vehicular impact loading scenarios. Both reliability index and failure probability curves followed the same shape. From the figures and tables presented, it can be seen that the axial load is influential on the reliability of the bridge pier. The accidental scenario displays steeper curves than the intentional scenario for the bigger vehicle classes, which indicates the axial load has greater influence when vehicles are travelling with higher masses and lesser speeds and accelerations. For the car vehicle class, the axial load has greater influence when vehicles are travelling at higher speeds and accelerations.

4.1.5 Sensitivity Analysis of Vehicle Velocity

In the intentional impact sensitivity analysis of the vehicle velocity, the vehicle velocity is increased from 90 kilometers per hour (55 miles per hour) to 170 kilometers per hour (105 miles per hour), in increments of 10 kilometers per hour (6 miles per hour), while all other variables are kept constant. The reliability curves for the sensitivity analysis of the vehicle velocity due to intentional vehicular impact are displayed in Figures 4.17 and 4.18.

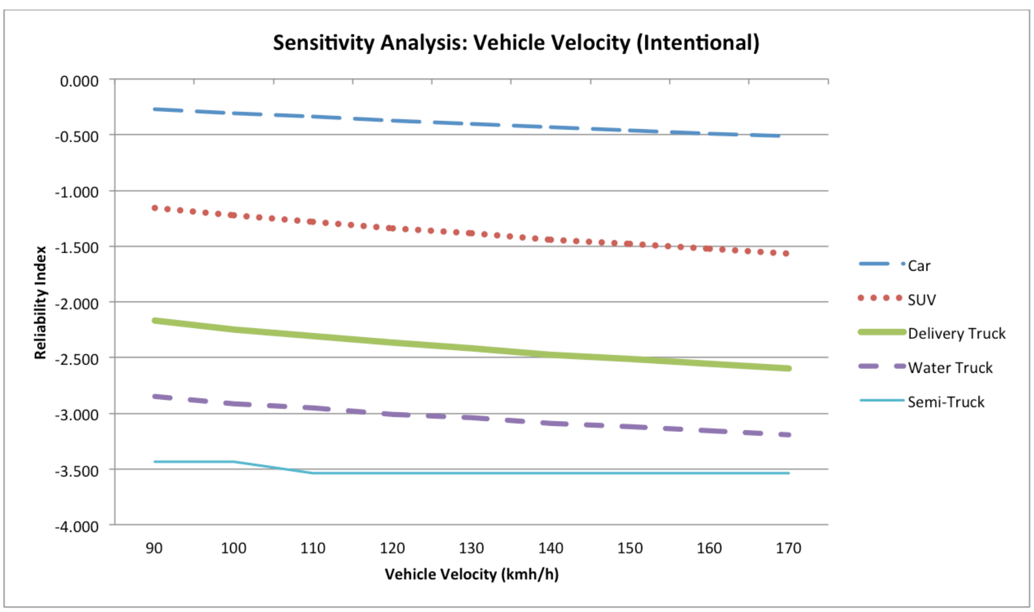

Figure 4.17: Vehicle Velocity Reliability Index Curve – Intentional Impact

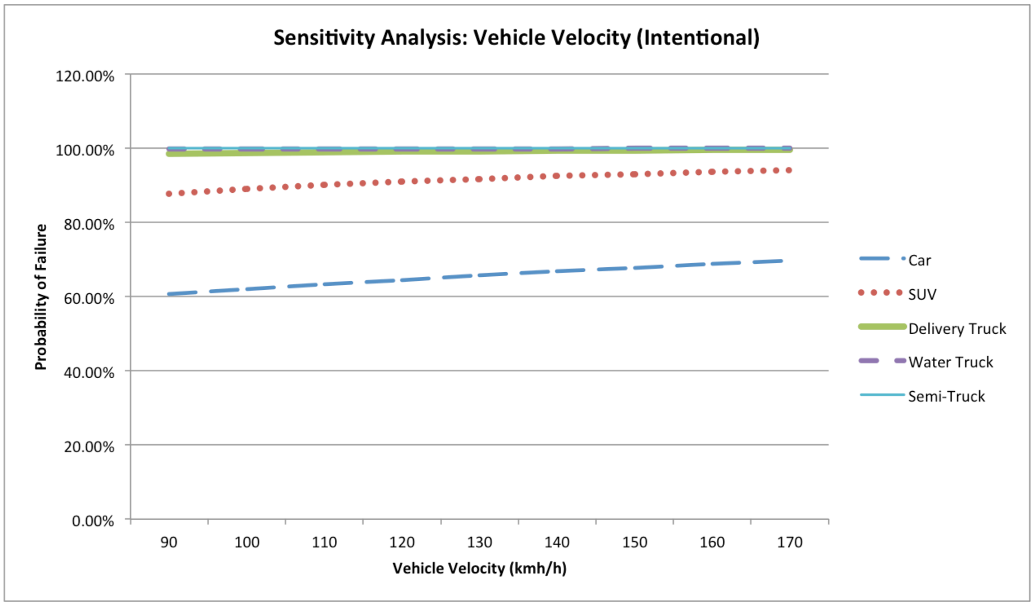

Figure 4.18: Vehicle Velocity Fragility Curve – Intentional Impact

The reliability curves corresponding to the different vehicle types generally follow the same trend. The reliability index consistently decreases as the vehicle velocity increases, and therefore, the probability of failure consistently increases as the vehicle velocity increases. Table 4.20 provides the values of the largest decrease in the probability of failure for the different vehicle classes and at which change of vehicle velocity the maximum decrease occurs.

Table 4.20: Vehicle Velocity Incremental % Change – Intentional Impact

Vehicle Velocity Incremental % Change			
Vehicle Class	**Maximum % Change**	**From:**	**To:**
Car	2.37%	90 kmh/h	100 kmh/h
SUV	1.44%	90 kmh/h	100 kmh/h
Delivery Truck	0.28%	90 kmh/h	100 kmh/h
Water Truck	0.04%	90 kmh/h	100 kmh/h
Semi-Truck	0.01%	100 kmh/h	110 kmh/h

The values in Table 4.20 demonstrate that the curves get flatter as the vehicle velocity gets higher. This means that the increase of failure probability becomes smaller with each increase in vehicle velocity. The percentages representing the largest increase in failure probability, provided in Table 4.20, indicate that as the vehicle mass is increased, the change in failure probability is lesser and the fragility curves are flatter than that of a smaller mass vehicle. The values above also indicate that the vehicle velocity has small influence on the reliability of the bridge pier.

Table 4.21 presents the percentage change in the probability of failure of the bridge pier with a ten percent increase in the vehicle velocity.

Table 4.21: Vehicle Velocity % Change in Failure Probability – Intentional Impact

Vehicle Class	% Change in Vehicle Velocity	% Change in Probability of Failure
Car	10%	1.68%
SUV	10%	0.83%
Delivery Truck	10%	0.12%
Water Truck	10%	0.02%
Semi-Truck	10%	0.00%

The values in Table 4.21 demonstrate that the a ten percent increase in the vehicle velocity can results in up to a 1.68% increase in the probability of failure of the bridge pier subject to an intentional vehicular impact load. The values in the table indicate that the vehicle velocity influences the probability of failure of the bridge pier, but very minimally for vehicle masses of 5,000 kilograms (11,000 pounds) and greater.

In the accidental impact sensitivity analysis of the vehicle velocity, the vehicle velocity is increased from 30 kilometers per hour (20 miles per hour) to 110 kilometers per hour (70 miles per hour), in increments of 10 kilometers per hour (6 miles per hour), while all other variables are kept constant. The reliability curves for the sensitivity analysis of the vehicle velocity due to accidental vehicular impact are displayed in Figures 4.19 and 4.20.

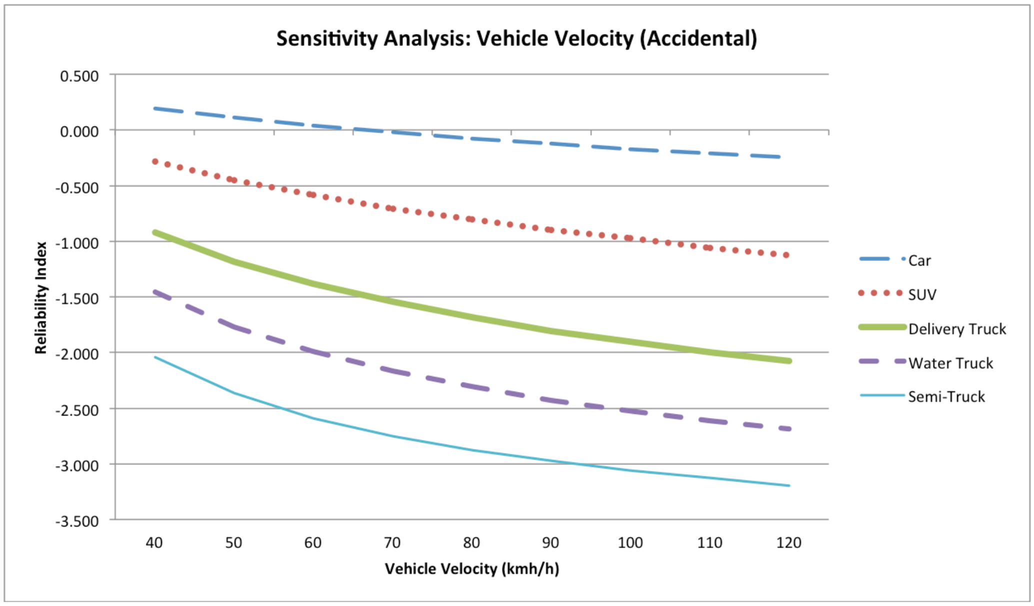

Figure 4.19: Vehicle Velocity Reliability Index Curve - Accidental Impact

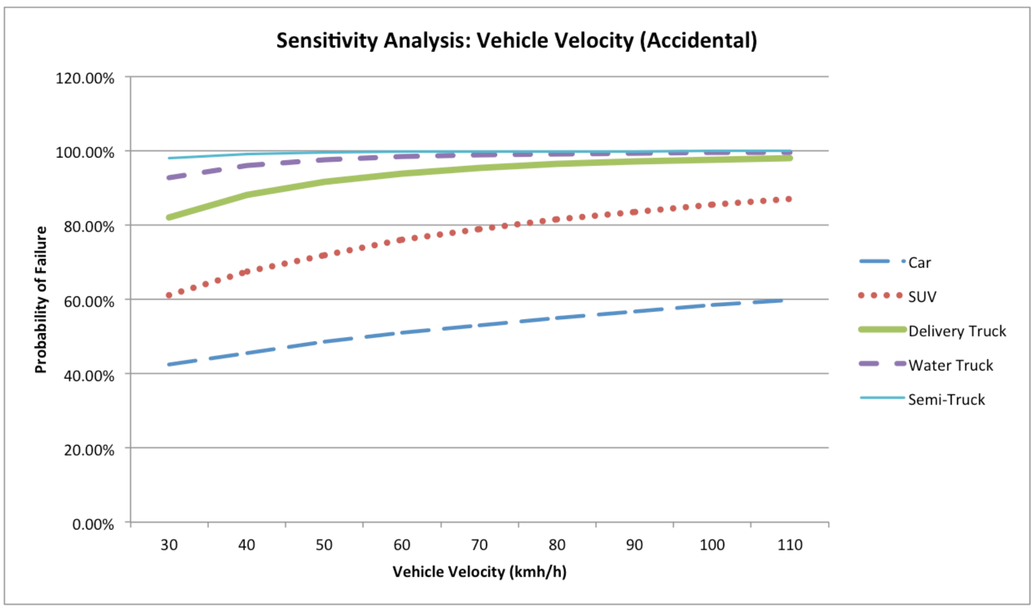

Figure 4.20: Vehicle Velocity Fragility Curve – Accidental Impact

The reliability curves corresponding to the different vehicle types generally follow the same trend. The reliability index consistently decreases as the vehicle velocity increases, and therefore, the probability of failure consistently increases as the vehicle velocity increases. Table 4.22 provides the values of the largest decrease in the probability of failure for the different vehicle classes and at which change of vehicle velocity the maximum decrease occurs.

Table 4.22: Vehicle Velocity Incremental % Change – Accidental Impact

Vehicle Velocity Incremental % Change			
Vehicle Class	**Maximum % Change**	**From:**	**To:**
Car	7.67%	50 kmh/h	40 kmh/h
SUV	10.52%	50 kmh/h	40 kmh/h
Delivery Truck	7.38%	50 kmh/h	40 kmh/h
Water Truck	3.73%	50 kmh/h	40 kmh/h
Semi-Truck	1.18%	50 kmh/h	40 kmh/h

The values in Table 4.22 demonstrate that the curves get flatter as the vehicle velocity gets higher. This means that the increase of failure probability becomes smaller with each increase in vehicle velocity. The percentages representing the largest increase in failure probability, provided in Table 4.22, indicate that the three smaller vehicle classes, with masses less than 4,500 kilograms (10,000 pounds), have similar changes in failure probability. With the larger vehicle classes, the change in failure probability dissipates as the vehicle mass is increased and the fragility curves are flatter than that of a smaller mass vehicle. The values above also indicate that the vehicle velocity has small influence on the reliability of the bridge pier.

Table 4.23 presents the percentage change in the probability of failure of the bridge pier with a ten percent increase in the vehicle velocity.

Table 4.23: Vehicle Velocity % Change in Failure Probability – Accidental Impact

Vehicle Class	% Change in Vehicle Velocity	% Change in Probability of Failure
Car	10%	1.55%
SUV	10%	1.60%
Delivery Truck	10%	0.73%
Water Truck	10%	0.28%
Semi-Truck	10%	0.08%

The values in Table 4.23 demonstrate that the a ten percent increase in the vehicle velocity can results in up to a 1.60% increase in the probability of failure of the bridge pier subject to an accidental vehicular impact load. The values in the table indicate that the vehicle velocity influences the probability of failure of the bridge pier for all vehicle classes.

The vehicle velocity fragility curves were very similar for both the intentional and accidental vehicular impact loading scenarios. Both reliability index and failure probability curves followed the same shape. From the figures and tables presented, it can be seen that the vehicle velocity is influential on the reliability of the bridge pier. The accidental scenario displays much larger increases in failure probability than the intentional scenario. This indicates that the vehicle velocity has greater influence when vehicles are travelling at lesser speeds and accelerations due to the high probabilities of failure regardless of the speed with the intentional impact.

4.1.6 Sensitivity Analysis of Vehicle Acceleration

In the intentional impact sensitivity analysis of the vehicle acceleration, the vehicle acceleration is increased from 1 m/s^2 (3.3 ft/s^2) to 5 m/s^2 (16.4 ft/s^2), in increments of 0.50 m/s^2 (1.6 ft/s^2), while all other variables are kept constant. The reliability curves for the sensitivity analysis of the vehicle acceleration due to intentional vehicular impact are displayed in Figures 4.21 and 4.22.

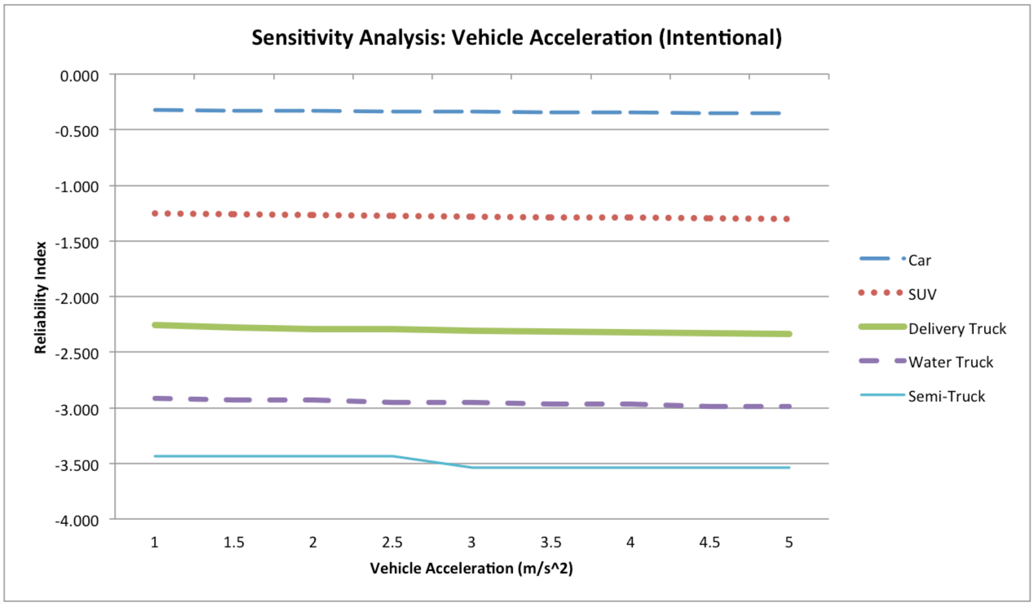

Figure 4.21: Acceleration Reliability Index Curve - Intentional Impact

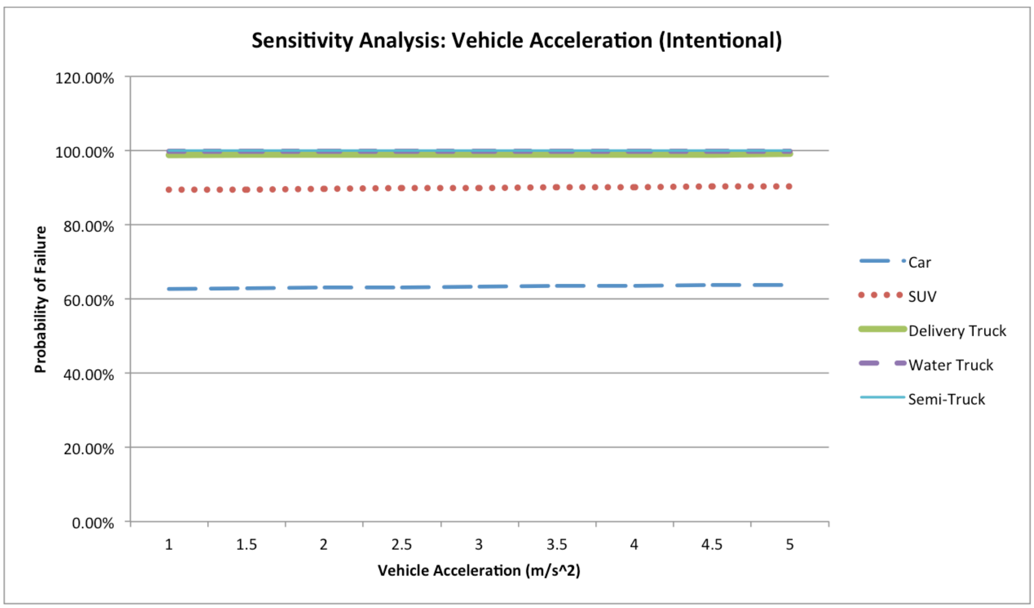

Figure 4.22: Acceleration Fragility Curve – Intentional Impact

The reliability curves corresponding to the different vehicle types generally follow the same trend. For all the vehicle classes, both the reliability index and probability of failure curves display a horizontal line, indicating that the vehicle acceleration has little to no influence on the reliability index and probability of failure of the reinforced concrete bridge pier.

Table 4.24 provides the values of the minimum and maximum changes in the probability of failure for the different vehicle classes with an incremental increase in vehicle acceleration.

Table 4.24: Acceleration Incremental % Change – Intentional Impact

Vehicle Acceleration Incremental % Change		
Vehicle Class	**Minimum % Change**	**Maximum % Change**
Car	0.06%	0.40%
SUV	0.03%	0.23%
Delivery Truck	0.01%	0.06%
Water Truck	0.00%	0.01%
Semi-Truck	0.00%	0.01%

The minimum and maximum values in Table 4.24 show that the incremental fluctuations are minimal, with the largest fluctuation not exceeding 0.40%. These small values confirm that the vehicle acceleration has little influence on the reliability of the bridge pier. Table 4.25 presents the percentage change in the probability of failure of the bridge pier with a ten percent increase in the vehicle acceleration.

Table 4.25: Acceleration % Change in Failure Probability – Intentional Impact

Vehicle Class	% Change in Vehicle Acceleration	% Change in Probability of Failure
Car	10%	0.05%
SUV	10%	0.03%
Delivery Truck	10%	0.01%
Water Truck	10%	0.00%
Semi-Truck	10%	0.00%

The values in Table 4.25 demonstrate that a ten percent increase in the vehicle acceleration can results in up to a 0.05% increase in the probability of failure of the bridge pier subject to an intentional vehicular impact load. The values in the table indicate that the vehicle acceleration has little to no influence on the probability of failure of the bridge pier for all vehicle classes.

In the accidental impact sensitivity analysis of the vehicle acceleration, the vehicle acceleration is decreased from -1 m/s^2 (-3.3 ft/s^2) to -5 m/s^2 (-16.4 ft/s^2), in increments of 0.50 m/s^2 (1.6 ft/s^2), while all other variables are kept constant. The negative implies that the vehicle is decelerating, unlike the positive acceleration in the intentional impact scenario. The reliability curves for the sensitivity analysis of the vehicle acceleration due to accidental vehicular impact are displayed in Figures 4.23 and 4.24.

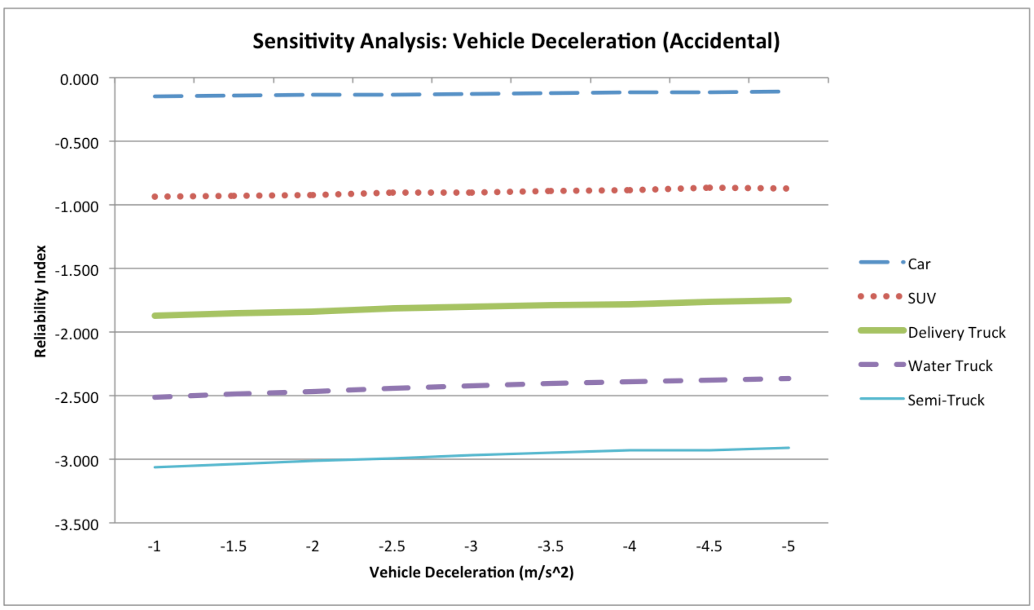

Figure 4.23: Deceleration Reliability Index Curve – Accidental Impact

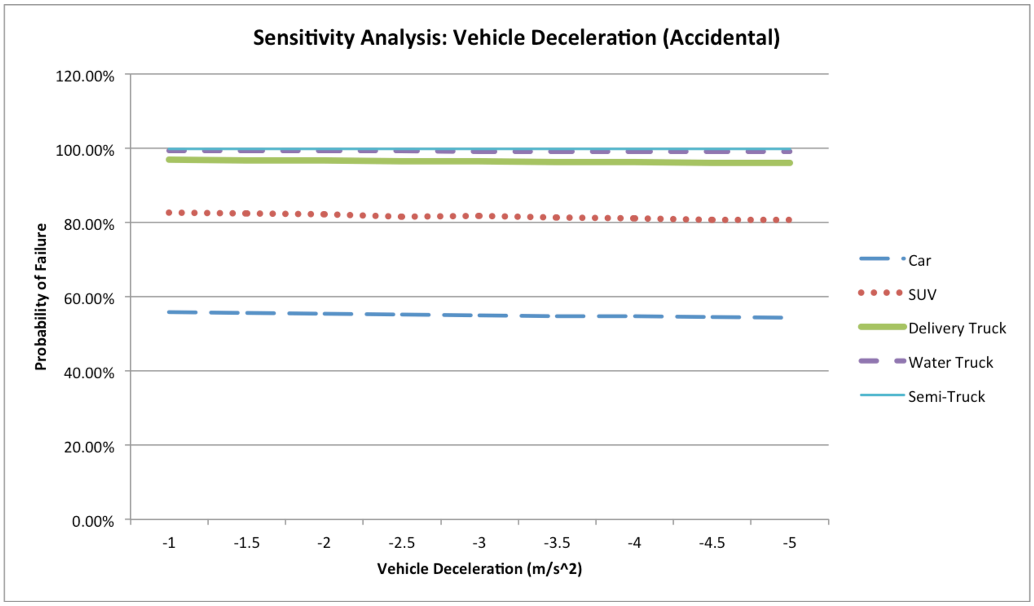

Figure 4.24: Deceleration Fragility Curve – Accidental Impact

The reliability curves corresponding to the different vehicle types generally follow the same trend. For all the vehicle classes, both the reliability index and probability of failure curves display a horizontal line, indicating that, like the intentional impact scenario, the vehicle deceleration has little to no influence on the reliability index and probability of failure of the reinforced concrete bridge pier.

Table 4.26 provides the values of the minimum and maximum changes in the probability of failure for the different vehicle classes with an incremental increase in vehicle deceleration.

Table 4.26: Deceleration Incremental % Change – Accidental Impact

Vehicle Deceleration Incremental % Change		
Vehicle Class	**Minimum % Change**	**Maximum % Change**
Car	-0.70%	-0.07%
SUV	-0.63%	0.07%
Delivery Truck	-0.16%	-0.06%
Water Truck	-0.05%	-0.03%
Semi-Truck	-0.01%	0.00%

The minimum and maximum values in Table 4.26 show that the incremental fluctuations are minimal, with the largest fluctuation barely exceeding 0.05%. These small values confirm that the vehicle deceleration has little influence on the reliability of the bridge pier. Table 4.27 presents the percentage change in the probability of failure of the bridge pier with a ten percent increase in the vehicle deceleration.

Table 4.27: Deceleration % Change in Failure Probability – Accidental Impact

Vehicle Class	% Change in Vehicle Deceleration	% Change in Probability of Failure
Car	10%	-0.07%
SUV	10%	-0.05%
Delivery Truck	10%	-0.02%
Water Truck	10%	-0.01%
Semi-Truck	10%	0.00%

The values in Table 4.27 demonstrate that a ten percent increase in the vehicle acceleration can results in up to a 0.05% decrease in the probability of failure of the bridge pier subject to an accidental vehicular impact load. The values in the table indicate that the vehicle deceleration has little to no influence on the probability of failure of the bridge pier for all vehicle classes.

Both the intentional and accidental scenarios resulted in the same conclusion. Though there were slight variations in the reliability indices and failure probabilities, the incremental changes do not exceed 0.70% amongst both scenarios. Using this analysis, it can be seen that the vehicle acceleration does not influence the reliability of a reinforced concrete bridge pier in neither an intentional vehicular impact event nor an accidental vehicular impact event.

4.1.7 Sensitivity Analysis of Vehicle Mass

In the impact sensitivity analysis of the vehicle mass, the vehicle masses correspond to the vehicle classes as seen in Table 4.28.

Table 4.28 Vehicle Class and Corresponding Mass

Vehicle Class	Mass (kg)	Mass (lb)
Car	2,270	5,004
SUV/Van	4,540	10,009
Small Moving Van/Delivery Truck	8,170	18,012
Moving Van/Water Truck	11,800	26,015
Semi-Truck/Trailer	19,100	42,108

The percentage change of the probability of failure between the different vehicle masses is calculated for each of the parameter's individual sensitivity analysis. For each analysis, the percentage changes in the probability of failure of the bridge pier are calculated and then averaged for a ten percent increase in vehicle mass. Tables 4.29 and 4.30 present the percentage change in the probability of failure of the bridge pier with a ten percent increase in the vehicle mass for the intentional and accidental impact scenarios, respectively.

Table 4.29: Vehicle Mass % Change in Failure Probability - Intentional

Vehicle Mass Incremental % Change		
Analysis	**% Change in Vehicle Mass**	**% Change in Probability of Failure**
Reinforcement Ratio	10%	1.02%
Pier Radius	10%	0.72%
Pier Height	10%	0.78%
Axial Load	10%	0.58%
Vehicle Velocity	10%	0.72%
Vehicle Acceleration	10%	0.78%

Table 4.30: Vehicle Mass Incremental % Change in Failure Probability - Accidental

Vehicle Mass Incremental % Change		
Analysis	% Change in Vehicle Mass	% Change in Probability of Failure
Reinforcement Ratio	10%	1.40%
Pier Radius	10%	0.95%
Pier Height	10%	1.10%
Axial Load	10%	0.93%
Vehicle Velocity	10%	1.25%
Vehicle Acceleration	10%	1.10%

The values in Tables 4.29 and 4.30 demonstrate that a ten percent increase in the charge weight can results in up to a 1.02% and 1.40% increase in the probability of failure of the bridge pier for the intentional and accidental impact scenarios, respectively. The intentional and accidental impact loading scenarios have a similar pattern in the probability of failure percentage changes. Tables 4.29 and 4.30 show that the vehicle mass has a greater influence on the probability of failure in the accidental impact loading scenario compared to the intentional impact loading scenario. The values in the tables indicate that the vehicle mass influences the probability of failure of the bridge pier.

4.2 Conclusions

A summary of the results from the intentional and accidental vehicular impact is presented in Tables 4.31 and 4.32, respectively. The tables present the percentage change in the probability of failure of the bridge pier with a ten percent increase in resistance and loading parameters. This allows for the parameters that most contribute to the probability of failure to be identified and arranged according to their level of influence.

Table 4.31A: Probability of Failure Overview for the Intentional Impact

Intentional Vehicular Impact Loading: Resistance Parameters		
% Change in Probability of Failure due to Impact Loading		
Reinforcement Ratio		
Vehicle Class	% Change in Reinforcement Ratio	% Change in Probability of Failure
Car	10%	-0.43%
SUV	10%	-0.25%
Delivery Truck	10%	-0.06%
Water Truck	10%	-0.01%
Semi-Truck	10%	0.00%
Pier Radius		
Vehicle Class	% Change in Pier Radius	% Change in Probability of Failure
Car	10%	-3.60%
SUV	10%	-2.53%
Delivery Truck	10%	-1.18%
Water Truck	10%	-0.44%
Semi-Truck	10%	-0.09%
Pier Height		
Vehicle Class	% Change in Pier Height	% Change in Probability of Failure
Car	10%	0.01%
SUV	10%	0.02%
Delivery Truck	10%	0.00%
Water Truck	10%	0.00%
Semi-Truck	10%	0.00%
Axial Load		
Vehicle Class	% Change in Axial Load	% Change in Probability of Failure
Car	10%	-0.62%
SUV	10%	-0.27%
Delivery Truck	10%	-0.04%
Water Truck	10%	-0.01%
Semi-Truck	10%	0.00%

Table 4.31B: Probability of Failure Overview for the Intentional Impact

Intentional Vehicular Impact Loading: Loading Parameters		
% Change in Probability of Failure due to Impact Loading		
Vehicle Velocity		
Vehicle Class	% Change in Vehicle Velocity	% Change in Probability of Failure
Car	10%	1.68%
SUV	10%	0.83%
Delivery Truck	10%	0.12%
Water Truck	10%	0.02%
Semi-Truck	10%	0.00%
Vehicle Acceleration		
Vehicle Class	% Change in Vehicle Acceleration	% Change in Probability of Failure
Car	10%	0.05%
SUV	10%	0.03%
Delivery Truck	10%	0.01%
Water Truck	10%	0.00%
Semi-Truck	10%	0.00%
Vehicle Mass		
Analysis	% Change in Vehicle Mass	% Change in Probability of Failure
Reinforcement Ratio	10%	1.02%
Pier Radius	10%	0.72%
Pier Height	10%	0.78%
Axial Load	10%	0.58%
Vehicle Velocity	10%	0.72%
Vehicle Acceleration	10%	0.78%

Table 4.32A: Probability of Failure Overview for the Accidental Impact

Accidental Vehicular Impact Loading: Resistance Parameters		
% Change in Probability of Failure due to Impact Loading		
Reinforcement Ratio		
Vehicle Class	% Change in Reinforcement Ratio	% Change in Probability of Failure
Car	10%	-0.47%
SUV	10%	-0.33%
Delivery Truck	10%	-0.14%
Water Truck	10%	-0.04%
Semi-Truck	10%	-0.01%
Pier Radius		
Vehicle Class	% Change in Pier Radius	% Change in Probability of Failure
Car	10%	-3.63%
SUV	10%	-3.01%
Delivery Truck	10%	-1.77%
Water Truck	10%	-0.89%
Semi-Truck	10%	-0.27%
Pier Height		
Vehicle Class	% Change in Pier Height	% Change in Probability of Failure
Car	10%	-0.01%
SUV	10%	-0.02%
Delivery Truck	10%	0.00%
Water Truck	10%	0.00%
Semi-Truck	10%	0.00%
Axial Load		
Vehicle Class	% Change in Axial Load	% Change in Probability of Failure
Car	10%	-0.49%
SUV	10%	-0.42%
Delivery Truck	10%	-0.12%
Water Truck	10%	-0.03%
Semi-Truck	10%	0.00%

Table 4.32B: Probability of Failure Overview for the Accidental Impact

Accidental Vehicular Impact Loading: Loading Parameters		
% Change in Probability of Failure due to Impact Loading		
Vehicle Velocity		
Vehicle Class	% Change in Vehicle Velocity	% Change in Probability of Failure
Car	10%	1.55%
SUV	10%	1.60%
Delivery Truck	10%	0.73%
Water Truck	10%	0.28%
Semi-Truck	10%	0.08%
Vehicle Deceleration		
Vehicle Class	% Change in Vehicle Deceleration	% Change in Probability of Failure
Car	10%	-0.07%
SUV	10%	-0.05%
Delivery Truck	10%	-0.02%
Water Truck	10%	-0.01%
Semi-Truck	10%	0.00%
Vehicle Mass		
Analysis	% Change in Vehicle Mass	% Change in Probability of Failure
Reinforcement Ratio	10%	1.40%
Pier Radius	10%	0.95%
Pier Height	10%	1.10%
Axial Load	10%	0.93%
Vehicle Velocity	10%	1.25%
Vehicle Acceleration	10%	1.10%

The investigation led to the identification of the following pier resistance factors, in descending order, that most likely contribute to failure in the intentional and accidental impact events: 1) pier radius 2) axial load in the pier 3) reinforcement ratio and 4) pier height.

The investigation also led to the identification of the following impact loading factors, in descending order, that most likely contribute to failure with the smaller vehicle classes: 1) vehicle speed 2) vehicle mass and 3) vehicle acceleration. For the larger vehicle classes, the following impact loading factors, in descending order, that most contribute to failure in the impact event are identified: 1) vehicle mass 2) vehicle speed and 3) vehicle acceleration.

Current countermeasures are typically intended to slow the vehicle or increase the distance between the roadway and pier. According to the results, this method of reducing the accessibility and vulnerability of the bridge pier lowers the probability of failure by a substantial amount. Design countermeasures to reduce the probability of failure include increasing the diameter of the pier radius to provide a larger gross area of concrete and increasing the reinforcement ratio by either adding more vertical reinforcing bars or increasing the bar size. Another countermeasure is to provide protection surrounding the bridge pier, such as barriers, to reduce the accessibility and vulnerability of the bridge piers.

CHAPTER 5

BLAST ANALYSIS

This chapter includes the analysis of a circular reinforced concrete bridge pier subject to intentional blast loading. Explosions produce pressures with extremely high-intensity that are short in duration. Blast effects on structural elements depend on the standoff distance and the magnitude of the explosive (Doege & Gebbeken, n.d.), where the standoff distance is the distance between the explosive location and the affected structure.

The reliability analysis of the bridge pier subject to the blast loading follows the methodology outline explained in Section 3.1.2. Using the procedures and equations defined in Sections 3.2 and 3.3, the reliability and sensitivity analyses are completed with the MATLAB code developed and inserted in Appendix B for the analysis of a circular reinforced concrete bridge pier subject to intentional blast loading. The results of the blast reliability and sensitivity analyses are presented next.

5.1 Intentional Blast Loading

The principal focus of this study is on intentional blast loading transported by a vehicle with a small standoff distance. Due to the objective of terrorism, to cause chaos or disruption, the standoff distance is taken as minimal to cause the largest pressure, resulting in the largest amount of damage. However, in order to completely understand blast loading, multiple standoff distances are also considered. The purpose of considering multiple standoff distances, along with multiple resistance-loading scenarios, is to allow for the severity and importance of understanding the effect of blast loading on reinforced concrete bridge piers to be determined, along with identifying the most influential parameters contributing to probabilities of failure.

The variables and their corresponding statistical parameters used in the blast analysis are defined in Section 3.2.2 in Tables 3.3 and 3.4. Table 5.1 shows values of the constant held parameters while the other parameter is varied in the blast-loading event. A standoff distance of 5 meters is used, instead of 0 meters, throughout the analyses because it is assumed that the vehicle bomb is not at the front of the vehicle and that the vehicle rebounds off of the bridge pier at impact due to the force.

Table 5.1: Constant Blast Parameters in Blast Sensitivity Analysis

Variable	Mean
Pier Radius	0.25 m (0.82 ft)
Pier Height	5 m (16.4 ft)
Bar Number	7
Axial Load	75%P_{allow} kN
Standoff Distance	5 m (16.4 ft)
Coefficient of Variation	0.33
Mean-to-Nominal Ratio	1.0

5.1.1 Sensitivity Analysis of Reinforcement Ratio

The reinforcement ratio is the ratio of the reinforcement steel area to the gross area of the bridge pier shown in Equation 4.1. As seen in Table 5.1, the constant pier radius is taken as 0.25 meters (9.8 in). With this radius, the gross area of the bridge pier is calculated as 1,964 cm^2 (304.4 in^2). In the sensitivity analysis of the reinforcement ratio, the steel reinforcing area is increased while the additional variables are kept constant. The bar numbers and their corresponding cross-sectional areas can be seen in Table 4.3. The reinforcement ratio is increased by considering the eight reinforcing bars in the bridge pier and increasing the bar number with each iteration.

The reliability curves for the sensitivity analysis of the reinforcement ratio due to blast loading are displayed in Figures 5.1 and 5.2. The different curves demonstrate the analysis of the multiple charge weights, from 11.3 kilograms (25 pounds) of TNT to 453 kilograms (1,000 pounds) of TNT. Each sensitivity analysis for the specific parameters will be completed for each of the charge weights.

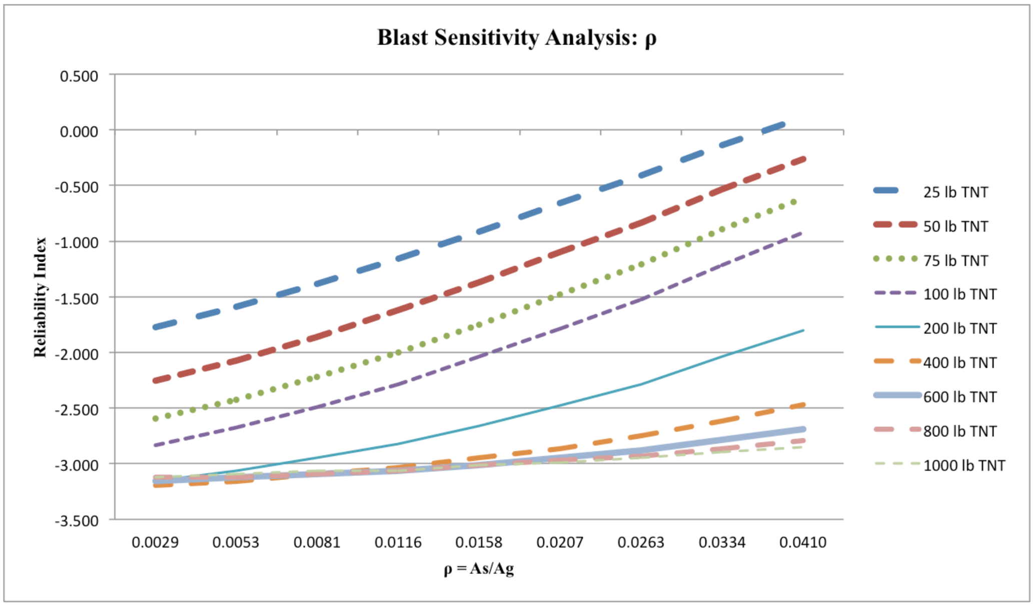

Figure 5.1: Reinforcement Ratio Reliability Index Curve – Blast

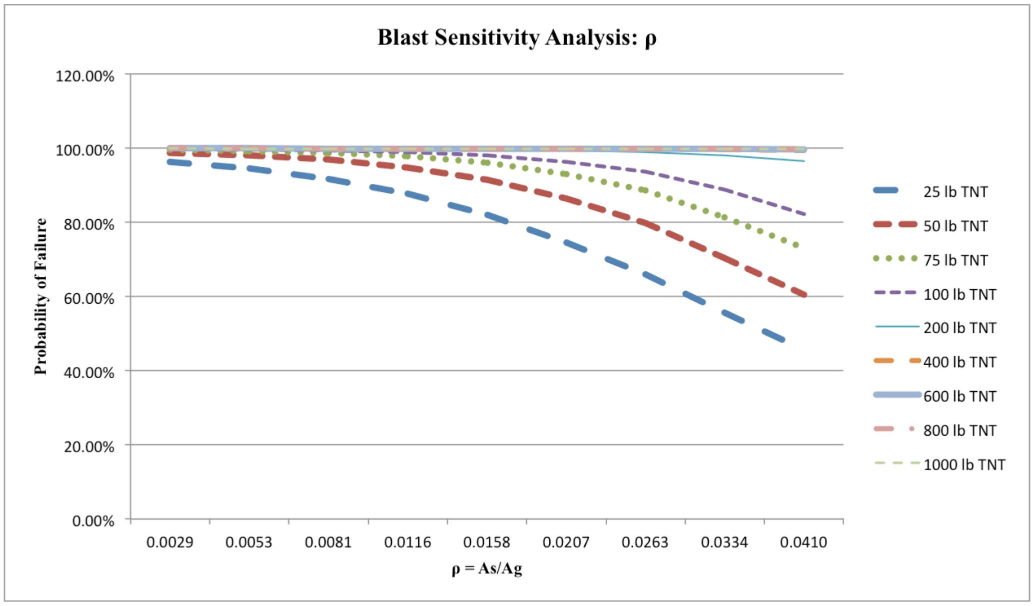

Figure 5.2: Reinforcement Ratio Fragility Curve - Blast

The reliability curves corresponding to the different charge weights generally follow the same trend. The reliability index consistently increases as the reinforcement ratio increases, and therefore, the probability of failure consistently decreases as the reinforcement ratio increases. Table 5.2 provides the values of the largest decrease in the probability of failure for the different charge weights and at which change of reinforcement ratio the maximum decrease occurs (e.g. the maximum change in the failure probability occurs from the use of a number 11 bar rather than a number 10 bar).

Table 5.2: Maximum Incremental Reinforcement Ratio Percentage Change

Reinforcement Ratio Incremental % Change			
Charge Weight	**Maximum % Change**	**From:**	**To:**
25 lb TNT	-18.02%	#10 Bar	#11 Bar
50 lb TNT	-14.03%	#10 Bar	#11 Bar
75 lb TNT	-10.28%	#10 Bar	#11 Bar
100 lb TNT	-7.40%	#10 Bar	#11 Bar
200 lb TNT	-1.53%	#10 Bar	#11 Bar
400 lb TNT	-0.23%	#10 Bar	#11 Bar
600 lb TNT	-0.09%	#10 Bar	#11 Bar
800 lb TNT	-0.05%	#10 Bar	#11 Bar
1000 lb TNT	-0.03%	#10 Bar	#11 Bar

Table 5.2 demonstrates that the fragility curves get steeper as the bar numbers get higher. This means that the decrease of failure probability becomes larger with each increase in bar size. However, this is more evident in the smaller vehicles, as the larger vehicles display a much flatter curve. The percentages representing the largest decrease in failure probability, provided in Table 5.2, indicate that as the vehicle mass is increased, the change in failure probability is lesser and the fragility curves are flatter than that of a smaller mass vehicle. The curves representing charge weights of 90.7 kilograms (200 pounds) of TNT and above indicate minimal variation in failure probability with increasing reinforcement area. This is due to the probabilities of failure of the larger charge weights being very high, regardless of the reinforcement ratio.

Table 5.3 presents the percentage change in the probability of failure of the bridge pier with a percentage increase in the reinforcement ratio. Tables for each parameter undergoing a sensitivity analysis are provided to allow for the most influential resistance and loading parameters to be identified. For uniformity and ease of understanding, a percentage increase in the resistance and loading parameters will be held at ten percent.

Table 5.3: Reinforcement Ratio Percentage Change in Failure Probability - Blast

Charge Weight	Percentage Change in Reinforcement Ratio	Percentage Change in Probability of Failure
25 lb TNT	10%	-0.40%
50 lb TNT	10%	-0.29%
75 lb TNT	10%	-0.20%
100 lb TNT	10%	-0.13%
200 lb TNT	10%	-0.03%
400 lb TNT	10%	0.00%
600 lb TNT	10%	0.00%
800 lb TNT	10%	0.00%
1000 lb TNT	10%	0.00%

The values in Table 5.3 demonstrate that the a ten percent increase in the reinforcement ratio can results in up to a 0.40% decrease in the probability of failure of the bridge pier. The values in the table indicate that the reinforcement ratio influences the probability of failure of the bridge pier, but very minimally for charge weights of 90.7 kilograms (200 pounds) of TNT and above.

5.1.2 Sensitivity Analysis of Pier Radius

In the sensitivity analysis of the pier radius, the pier radius is increased from 0.15 meters (5.9 in) to 0.35 meters (13.8 in), in increments of 0.05 meters (2 in), while all other variables are kept constant. The reliability curves for the sensitivity analysis of the pier radius due to blast loading are displayed in Figures 5.3 and 5.4.

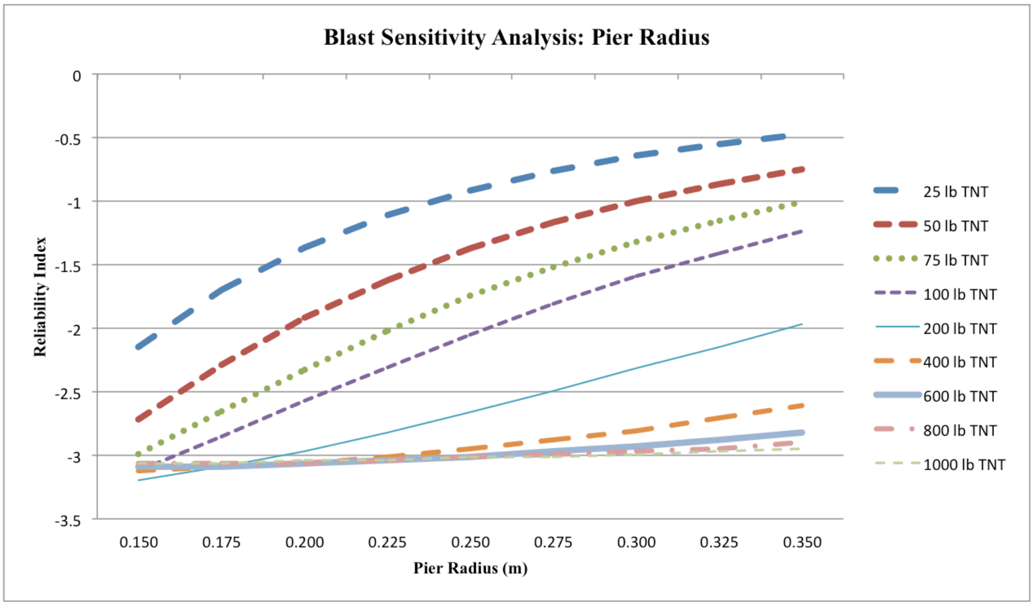

Figure 5.3: Pier Radius Reliability Index Curve - Blast

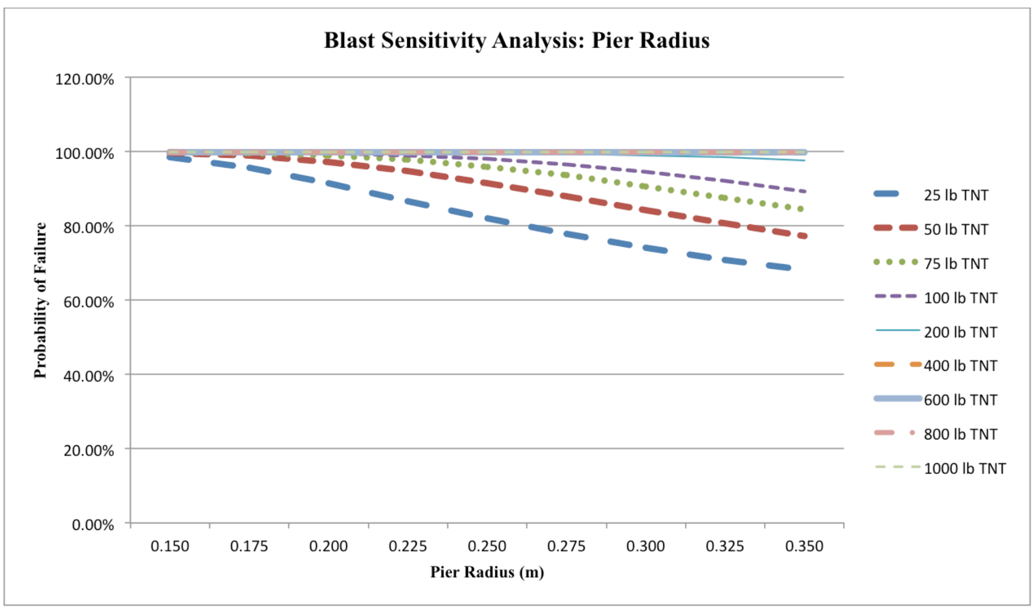

Figure 5.4: Pier Radius Fragility Curve - Blast

The reliability curves corresponding to the different charge weights generally follow the same trend. The reliability index consistently increases as the pier radius increases, and therefore, the probability of failure consistently decreases as the reinforcement ratio increases. Table 5.4 provides the values of the largest decrease in the probability of failure for the different charge weights and at which change of pier radius the maximum decrease occurs.

Table 5.4: Maximum Incremental Pier Radius Percentage Change

Pier Incremental % Change			
Charge Weight	**Maximum % Change**	**From:**	**To:**
25 lb TNT	-5.34%	0.225 meters	0.250 meters
50 lb TNT	-4.21%	0.300 meters	0.325 meters
75 lb TNT	-3.61%	0.325 meters	0.350 meters
100 lb TNT	-3.08%	0.325 meters	0.350 meters
200 lb TNT	-0.87%	0.325 meters	0.350 meters
400 lb TNT	-0.12%	0.325 meters	0.350 meters
600 lb TNT	-0.04%	0.325 meters	0.350 meters
800 lb TNT	-0.03%	0.325 meters	0.350 meters
1000 lb TNT	-0.01%	0.325 meters	0.350 meters

These values show that the lesser charge weights display a steeper decrease in failure probability at smaller pier radii. The curves representing charge weights of 90.7 kilograms (200 pounds) of TNT and above indicate minimal variation in failure probability with increasing reinforcement area. This is due to the probabilities of failure of the larger charge weights being very high, regardless of the pier radius. These changes in failure probability are fairly small, indicating flatter curves, even for the smaller charge weights. This confirms that the pier radius is influential on the probability of failure of the reinforced concrete bridge pier when subject to blast loading of 45.4 kilograms (100 pounds) of TNT or less at small standoff distances.

Table 5.5 presents the percentage change in the probability of failure of the bridge pier with a ten percent increase in the pier radius.

Table 5.5: Pier Radius Percentage Change in Failure Probability - Blast

Charge Weight	Percentage Change in Pier Radius	Percentage Change in Probability of Failure
25 lb TNT	10%	-2.31%
50 lb TNT	10%	-1.69%
75 lb TNT	10%	-1.17%
100 lb TNT	10%	-0.80%
200 lb TNT	10%	-0.18%
400 lb TNT	10%	-0.03%
600 lb TNT	10%	-0.01%
800 lb TNT	10%	-0.01%
1000 lb TNT	10%	0.00%

The values in Table 5.5 demonstrate that the a ten percent increase in the pier radius can results in up to a 2.31% decrease in the probability of failure of the bridge pier. The values in the table indicate that the pier radius influences the probability of failure of the bridge pier, but very minimally for charge weights of 181.4 kilograms (400 pounds) of TNT and above.

5.1.3 Sensitivity Analysis of Pier Height

In the sensitivity analysis of the pier height, the pier height is increased from 4.5 meters (14.8 ft) to 8.5 meters (27.9 ft), in increments of 0.50 meters (1.6 ft), while all other variables are kept constant. The reliability curves for the sensitivity analysis of the pier height due to blast loading are displayed in Figures 5.5 and 5.6.

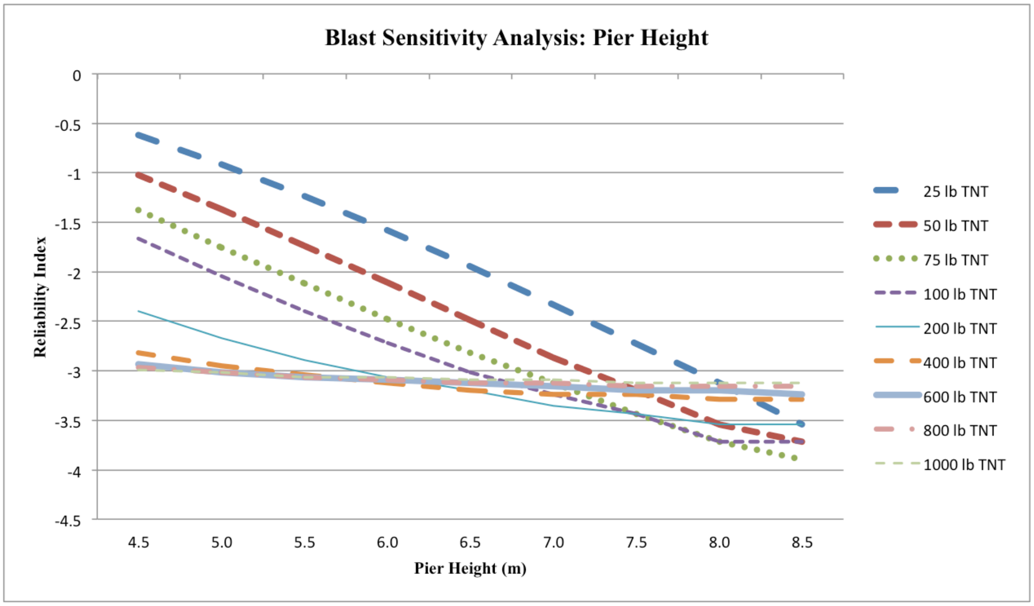

Figure 5.5: Pier Height Reliability Index Curve - Blast

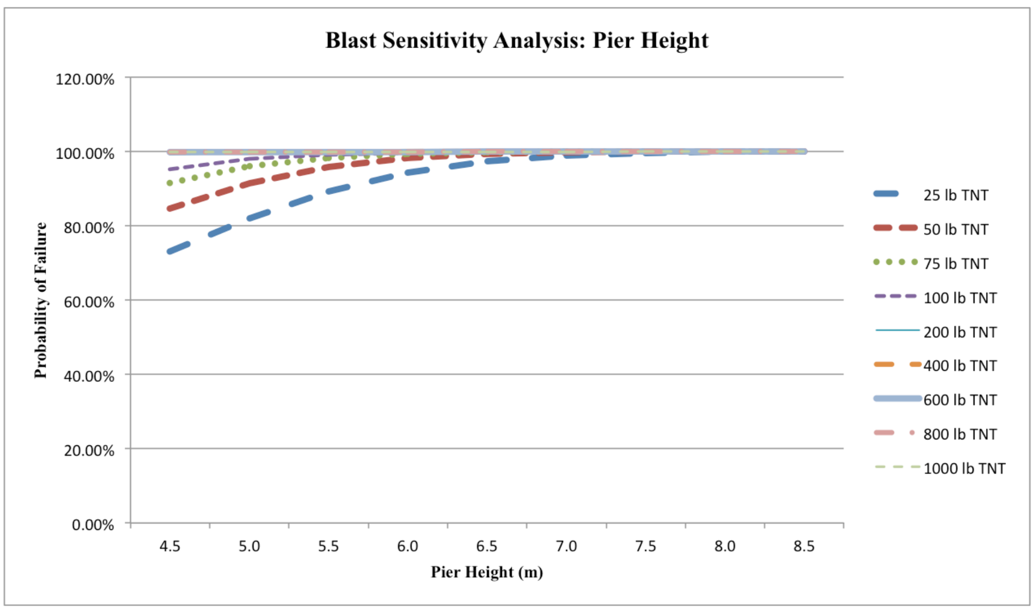

Figure 5.6: Pier Height Fragility Curve - Blast

For the smaller charge weights, the reliability curves corresponding to the different charge weights generally follow the same trend. The reliability index consistently decreases as the pier height increases. The fragility curves increase at the beginning but as the pier height is increased, the curves flatten out, reaching close to

100% probability of failure. Table 5.6 provides the values of the largest increase in the probability of failure for the different charge weights and at which change of pier height the maximum increase occurs.

Table 5.6: Maximum Incremental Pier Height Percentage Change

Pier Height Incremental % Change			
Charge Weight	**Maximum % Change**	**From:**	**To:**
25 lb TNT	12.14%	4.5 meters	5.0 meters
50 lb TNT	8.05%	4.5 meters	5.0 meters
75 lb TNT	4.91%	4.5 meters	5.0 meters
100 lb TNT	2.88%	4.5 meters	5.0 meters
200 lb TNT	0.44%	4.5 meters	5.0 meters
400 lb TNT	0.08%	4.5 meters	5.0 meters
600 lb TNT	0.04%	4.5 meters	5.0 meters
800 lb TNT	0.02%	4.5 meters	5.0 meters
1000 lb TNT	0.02%	5.0 meters	5.5 meters

These values confirm that the lesser charge weights display a steeper increase in failure probability at smaller pier heights. The curves representing charge weights of 90.7 kilograms (200 pounds) of TNT and above indicate minimal variation in failure probability with increasing pier heights. This is due to the probabilities of failure of the larger charge weights being very high, regardless of the pier height. These changes in failure probability are fairly small, indicating flat curves, even for the smaller charge weights. This confirms that the pier height is influential on the probability of failure of the reinforced concrete bridge pier when subject to blast loading of 45.4 kilograms (100 pounds) of TNT or less at small standoff distances.

Table 5.7 presents the percentage change in the probability of failure of the bridge pier with a ten percent increase in the pier height.

Table 5.7: Pier Height Percentage Change in Failure Probability - Blast

Charge Weight	Percentage Change in Pier Height	Percentage Change in Probability of Failure
25 lb TNT	10%	4.14%
50 lb TNT	10%	2.05%
75 lb TNT	10%	1.04%
100 lb TNT	10%	0.56%
200 lb TNT	10%	0.09%
400 lb TNT	10%	0.02%
600 lb TNT	10%	0.01%
800 lb TNT	10%	0.01%
1000 lb TNT	10%	0.01%

The values in Table 5.7 demonstrate that the a ten percent increase in the pier height can results in up to a 4.14% increase in the probability of failure of the bridge pier. The values in the table indicate that the pier height influences the probability of failure of the bridge pier, but very minimally for charge weights of 90.7 kilograms (200 pounds) of TNT and above.

5.1.4 Sensitivity Analysis of Axial Load

In the sensitivity analysis of the axial load, the axial load is increased from 15% of the allowable axial load to the 95% of the allowable axial load, while the additional variables are kept constant. The reliability curves for the sensitivity analysis of the axial load due to blast loading are displayed in Figures 5.7 and 5.8.

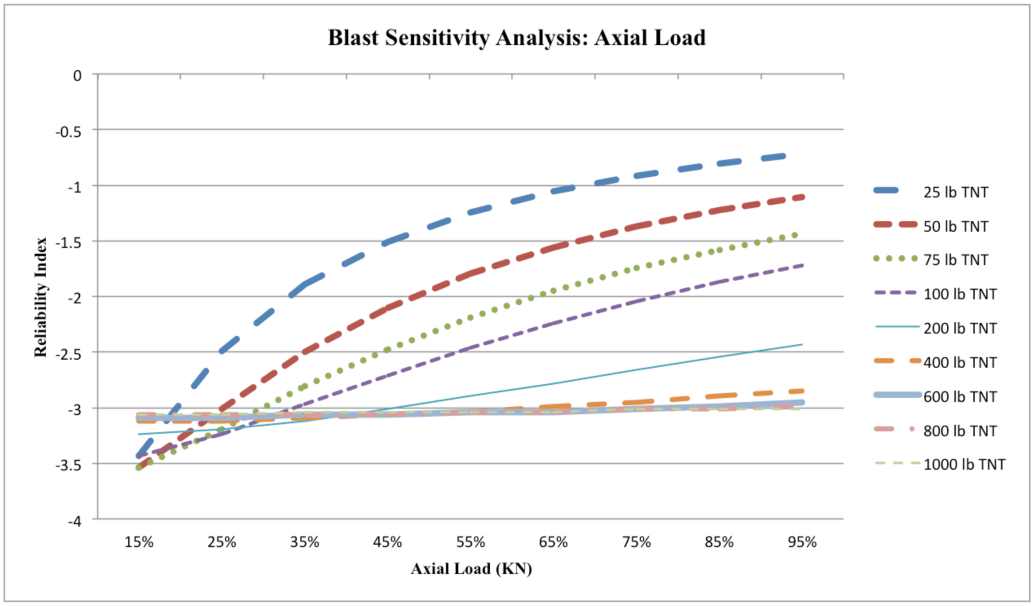

Figure 5.7: Axial Load Reliability Index Curve - Blast

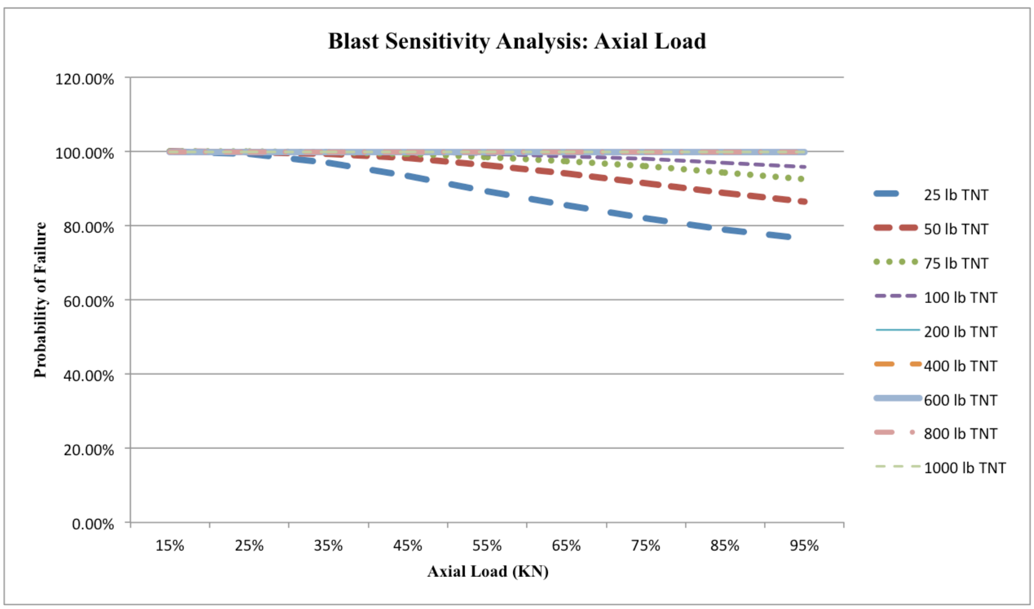

Figure 5.8: Axial Load Fragility Curve - Blast

The reliability curves corresponding to the different charge weights generally follow the same trend. The reliability index consistently increases as the axial load increases, and therefore, the probability of failure consistently decreases as the axial load increases. Table 5.8 provides the values of the largest decrease in the probability of failure for the different charge weights and at which change of axial load the maximum decrease occurs.

Table 5.8: Maximum Incremental Axial Load Percentage Change

Axial Load Incremental % Change			
Charge Weight	**Maximum % Change**	**From:**	**To:**
25 lb TNT	-4.40%	45%	55%
50 lb TNT	-2.79%	65%	75%
75 lb TNT	-1.96%	85%	95%
100 lb TNT	-1.24%	85%	95%
200 lb TNT	-0.21%	85%	95%
400 lb TNT	-0.03%	85%	95%
600 lb TNT	-0.02%	85%	95%
800 lb TNT	-0.01%	85%	95%
1000 lb TNT	-0.01%	65%	75%

These values show that the smaller charge weights display a steeper decrease in failure probability at smaller axial loads than the larger charge weights. The curves representing charge weights of 90.7 kilograms (200 pounds) of TNT and above indicate minimal variation in failure probability with increasing axial load. This is due to the probabilities of failure of the larger charge weights being very high, regardless of the axial load. These changes in failure probability are fairly small, indicating flat curves, even for the smaller charge weights. This confirms that the axial is marginally influential on the probability of failure of the reinforced concrete bridge pier when subject to blast loading of 45.4 kilograms (100 pounds) of TNT or less at small standoff distances.

Table 5.9 presents the percentage change in the probability of failure of the bridge pier with a ten percent increase in the axial load.

Table 5.9: Axial Load Percentage Change in Failure Probability - Blast

Charge Weight	Percentage Change in Axial Load	Percentage Change in Probability of Failure
25 lb TNT	10%	-0.44%
50 lb TNT	10%	-0.25%
75 lb TNT	10%	-0.14%
100 lb TNT	10%	-0.08%
200 lb TNT	10%	-0.01%
400 lb TNT	10%	0.00%
600 lb TNT	10%	0.00%
800 lb TNT	10%	0.00%
1000 lb TNT	10%	0.00%

The values in Table 5.9 demonstrate that the a ten percent increase in the axial load can results in up to a 0.44% decrease in the probability of failure of the bridge pier. The values in the table indicate that the axial load influences the probability of failure of the bridge pier, but very minimally for charge weights of 45.4 kilograms (100 pounds) of TNT and above.

5.1.5 Sensitivity Analysis of Standoff Distance

In the sensitivity analysis of the standoff distance, the standoff distance is increased from 4.0 meters (13.1 ft) to 20.0 meters (65.6 ft), while the additional variables are kept constant. The reliability curves for the sensitivity analysis of the standoff distance due to blast loading are displayed in Figures 5.9 and 5.10.

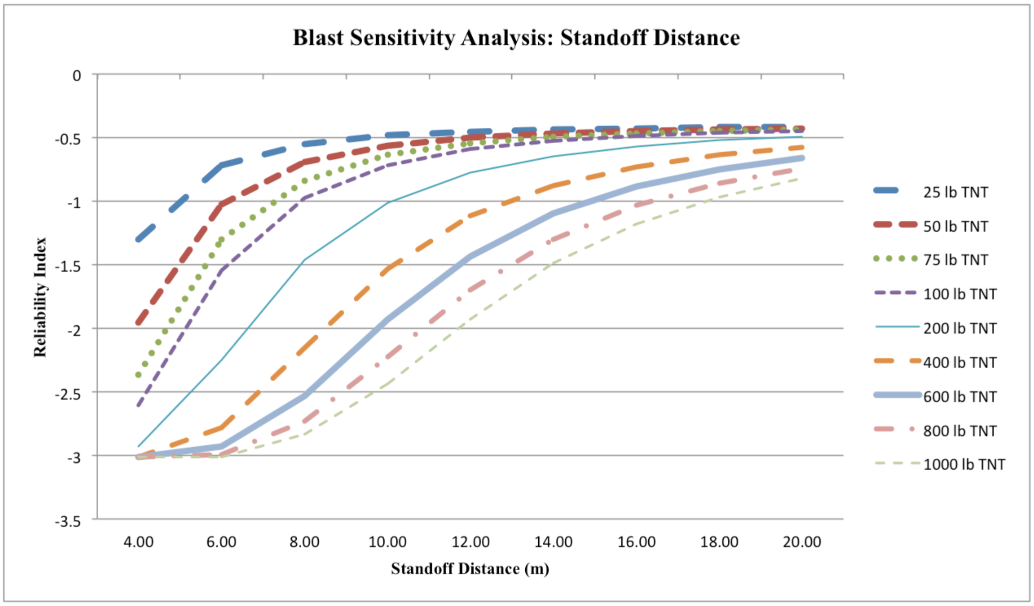

Figure 5.9: Standoff Distance Reliability Index Curve - Blast

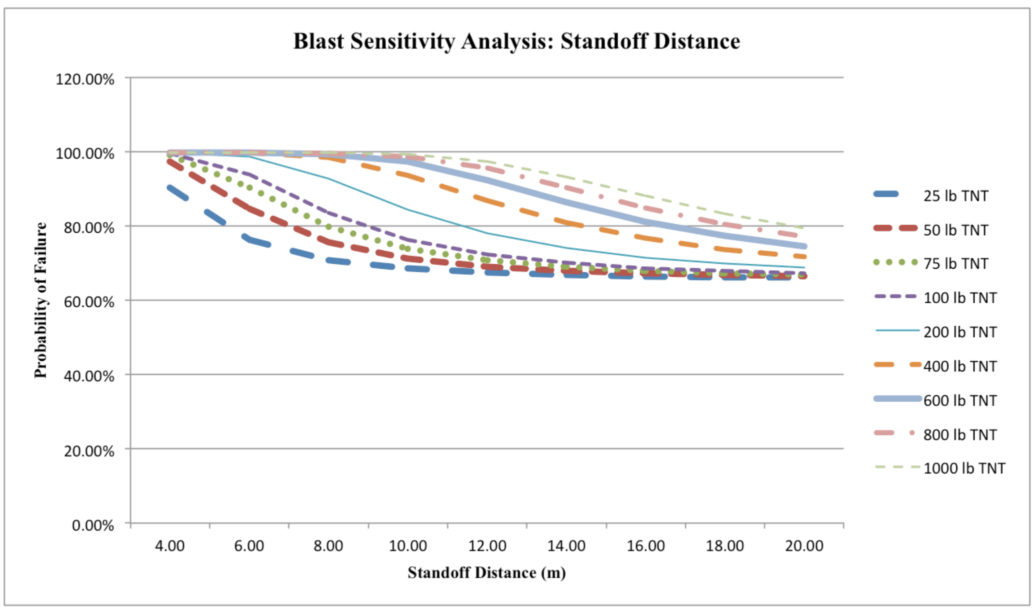

Figure 5.10: Standoff Distance Fragility Curve - Blast

The reliability curves corresponding to the different charge weights generally follow the same trend. The reliability index consistently increases and then flattens out as the standoff distance increases. Consequently, the probability of failure consistently decreases and then flattens out as the standoff distance increases. Table 5.10 provides the values of the largest decrease in the probability of failure for the different charge weights and at which change of standoff distance the maximum decrease occurs.

Table 5.10: Maximum Incremental Standoff Distance Percentage Change

Standoff Distance Incremental % Change			
Charge Weight	**Maximum % Change**	**From:**	**To:**
25 lb TNT	-15.48%	4.0 meters	6.0 meters
50 lb TNT	-13.13%	4.0 meters	6.0 meters
75 lb TNT	-11.56%	6.0 meters	8.0 meters
100 lb TNT	-11.08%	6.0 meters	8.0 meters
200 lb TNT	-8.99%	8.0 meters	10.0 meters
400 lb TNT	-7.40%	10.0 meters	12.0 meters
600 lb TNT	-6.60%	12.0 meters	14.0 meters
800 lb TNT	-6.08%	14.0 meters	16.0 meters
1000 lb TNT	-5.47%	14.0 meters	16.0 meters

These values show that as the charge weight increases, the maximum change in failure probability occurs at a larger standoff distance. It is right after this location that the reliability index and probability of failure curves begin to flatten. Thus, the fragility curves representing smaller charge weights flatten out more quickly than the fragility curves representing larger charge weights. With this concept and the values in Table 5.10, it can be seen that standoff distance influences the failure probability of the bridge pier with smaller charge weights at closer distances and then dissipates at larger distances. The standoff distance influences the failure probability of the bridge pier with larger charge weights at larger distances. Still, the maximum percentage decreases in the probability of failure with changing standoff distances are larger for smaller charge weights than larger charge weights. This implies that a change in standoff distances has greater influence with smaller charge weights.

Table 5.11 presents the percentage change in the probability of failure of the bridge pier with a ten percent increase in the standoff distance.

Table 5.11: Standoff Distance Percentage Change in Failure Probability - Blast

Charge Weight	Percentage Change in Standoff Distance	Percentage Change in Probability of Failure
25 lb TNT	10%	-0.67%
50 lb TNT	10%	-0.79%
75 lb TNT	10%	-0.81%
100 lb TNT	10%	-0.81%
200 lb TNT	10%	-0.78%
400 lb TNT	10%	-0.70%
600 lb TNT	10%	-0.64%
800 lb TNT	10%	-0.57%
1000 lb TNT	10%	-0.51%

The values in Table 5.11 demonstrate that the a ten percent increase in the standoff distance can results in up to a 0.81% decrease in the probability of failure of the bridge pier. The values in the table indicate that the standoff distance influences the probability of failure of the bridge pier for all charge weights considered.

5.1.6 Sensitivity Analysis of Charge Weight

The percentage change of the probability of failure between the different charge weights is calculated for each of the parameter's individual sensitivity analysis. For each analysis, the percentage changes in the probability of failure of the bridge pier are calculated and then averaged for a ten percent increase in charge weight. Table 5.12 presents the percentage change in the probability of failure of the bridge pier with a ten percent increase in the charge weight.

Table 5.12: Charge Weight Percentage Change in Failure Probability - Blast

Analysis	**% Change in Charge Weight**	**% Change in Probability of Failure**
Reinforcement Ratio	10%	0.10%
Pier Radius	10%	0.06%
Pier Height	10%	0.02%
Axial Load	10%	0.03%
Standoff Distance	10%	0.08%

The values in Table 5.12 demonstrate that a ten percent increase in the charge weight can results in up to a 0.10% increase in the probability of failure of the bridge pier. The values in the table indicate that the charge weight influences the probability of failure of the bridge pier, but has less influence than the standoff distance.

5.2 Blast Statistical Parameters

Typical design codes do not account for blast loading. Due to the limited information regarding blast loading, there are not statistical parameters regarding this loading. Because of this, a value for the coefficient of variation is assumed for the blast loading moment and a sensitivity analysis is performed to determine the importance and probable value of this parameter. The reliability curves for the sensitivity analysis of the coefficient of variation due to blast loading are displayed in Figures 5.11 and 5.12.

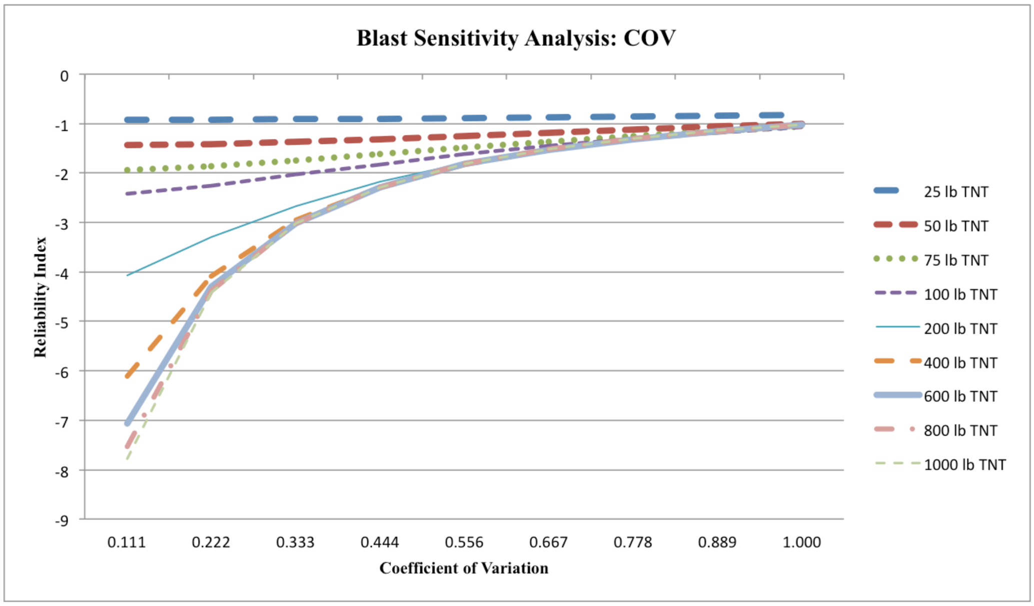

Figure 5.11: Coefficient of Variation Reliability Index Curve - Blast

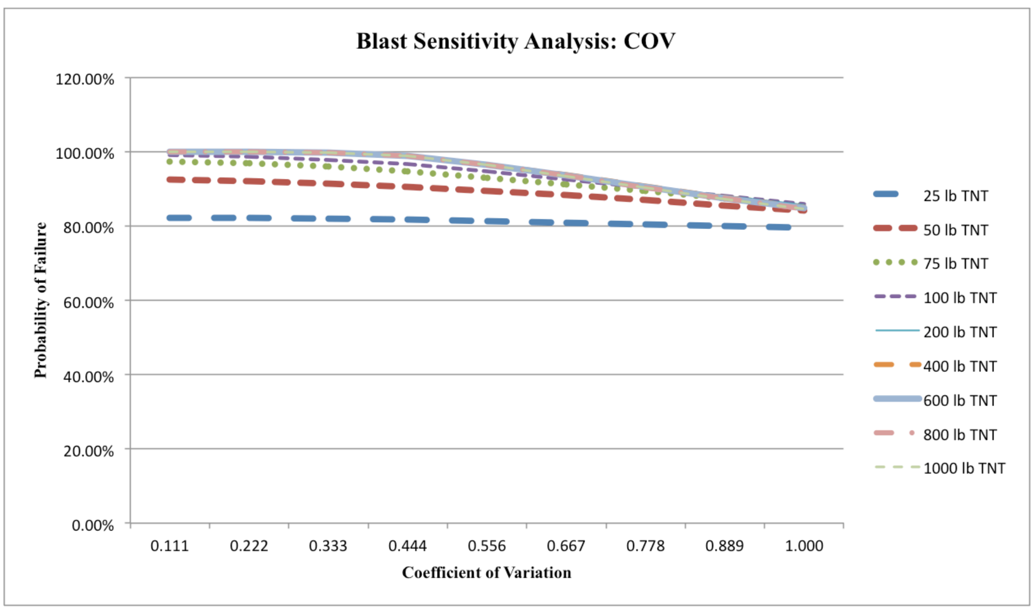

Figure 5.12: Coefficient of Variation Fragility Curve - Blast

The coefficient of variation is assumed to be 0.33 throughout the study. In looking at the figures, this assumption is a good estimate of what the value should be for the blast coefficient of variation. At a value of 0.33, the curves start to flatten out but still have variation. It is important to understand that variation in blast can be a result of several blast characteristics, including the type of blast, chemical properties of the blast, origin of the blast, and surrounding area of the blast location.

Like the coefficient of variation, a value for the mean-to-nominal value is assumed for the blast loading moment and a sensitivity analysis is performed to determine the importance and probable value of this parameter. The reliability curves for the sensitivity analysis of the mean-to-nominal due to blast loading are displayed in Figures 5.13 and 5.14.

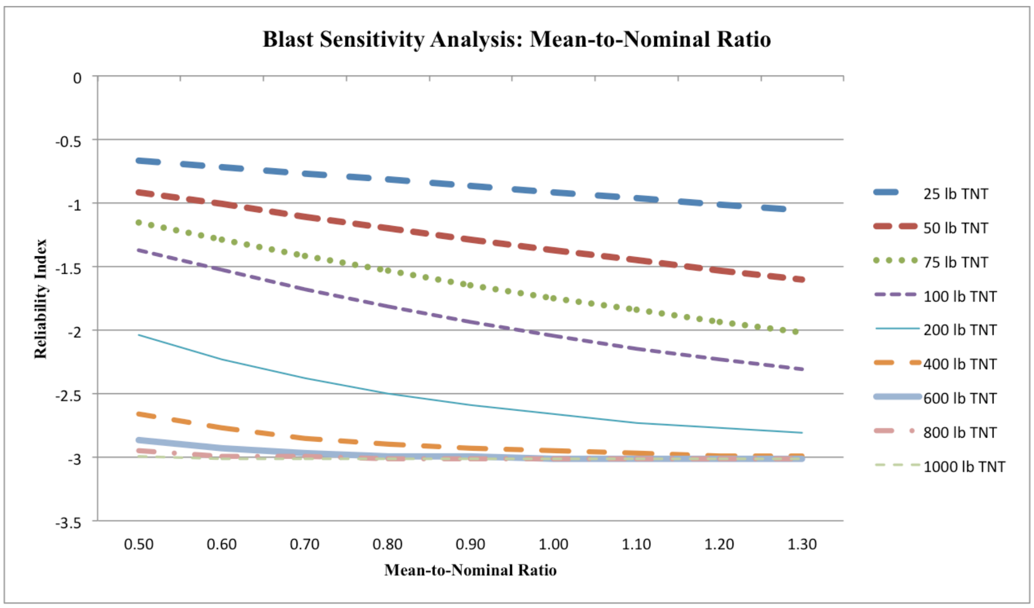

Figure 5.13: Mean-to-Nominal Ratio Reliability Index Curve - Blast

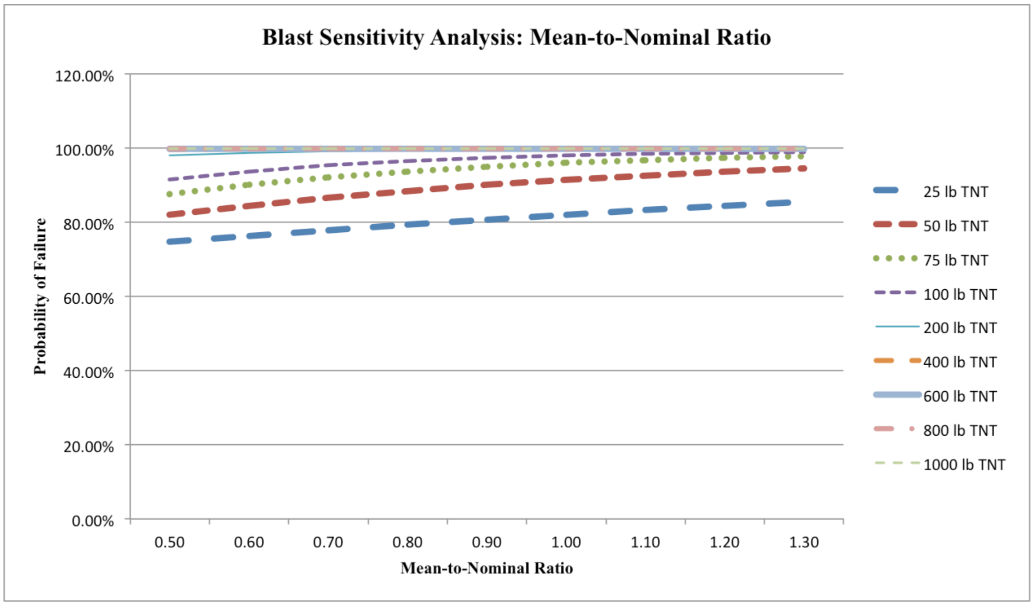

Figure 5.14: Mean-to-Nominal Ratio Fragility Curve - Blast

The mean-to-nominal ratio is assumed to be 1.0 throughout the study. In looking at the figures, this assumption is a good estimate of what the value should be for the blast mean-to-nominal ratio. At a value of 1.0, the curves start to flatten out but still have variation.

5.3 Conclusions

A summary of the results from the blast loading is presented in Table 5.13. The table presents the percentage change in the probability of failure of the bridge pier with a ten percent increase in resistance and loading parameters. This allows for the parameters that most contribute to the probability of failure to be identified and arranged according to their level of influence.

Table 5.13A: Probability of Failure Overview for the Blast Analysis

% Change in Probability of Failure due to Blast Loading: Resistance Parameters		
Reinforcement Ratio		
Charge Weight	% Change in Reinforcement Ratio	% Change in Probability of Failure
25 lb TNT	10%	-0.40%
50 lb TNT	10%	-0.29%
75 lb TNT	10%	-0.20%
100 lb TNT	10%	-0.13%
Pier Radius		
Charge Weight	% Change in Pier Radius	% Change in Probability of Failure
25 lb TNT	10%	-2.31%
50 lb TNT	10%	-1.69%
75 lb TNT	10%	-1.17%
100 lb TNT	10%	-0.80%
Pier Height		
Charge Weight	% Change in Pier Height	% Change in Probability of Failure
25 lb TNT	10%	4.14%
50 lb TNT	10%	2.05%
75 lb TNT	10%	1.04%
100 lb TNT	10%	0.56%
Axial Load		
Charge Weight	% Change in Axial Load	% Change in Probability of Failure
25 lb TNT	10%	-0.44%
50 lb TNT	10%	-0.25%
75 lb TNT	10%	-0.14%
100 lb TNT	10%	-0.08%

Table 5.13B: Probability of Failure Overview for the Blast Analysis

% Change in Probability of Failure due to Blast Loading: Loading Parameters		
Standoff Distance		
Charge Weight	% Change in Standoff Distance	% Change in Probability of Failure
25 lb TNT	10%	-0.67%
50 lb TNT	10%	-0.79%
75 lb TNT	10%	-0.81%
100 lb TNT	10%	-0.81%
Vehicle Mass		
Analysis	% Change in Charge Weight	% Change in Probability of Failure
Reinforcement Ratio	10%	0.10%
Pier Radius	10%	0.06%
Pier Height	10%	0.02%
Axial Load	10%	0.03%
Standoff Distance	10%	0.08%

The investigation led to the identification of the following pier resistance factors, in descending order, that most likely contribute to failure in the blast loading event: 1) pier height 2) pier radius 3) reinforcement ratio and 4) axial load applied to the pier. It should be understood that a decrease in the pier height decreases the probability of failure of the bridge pier whereas an increase in the other pier resistance factors decrease the probability of failure of the bridge pier.

The investigation also led to the identification of the following blast loading factors, in descending order, that most likely contribute to failure: 1) standoff distance and 2) charge weight. It should be understood that an increase in the standoff distance decreases the probability of failure of the bridge pier whereas a decrease in the charge weight decreases the probability of failure of the bridge pier.

Current countermeasures are typically intended to increase the standoff distance. According to the results, this method of reducing the accessibility and vulnerability of the bridge pier lowers the probability of failure by a substantial amount. Design countermeasures to reduce the probability of failure include decreasing the pier height, increasing the diameter of the pier to provide a larger gross area of concrete, and increasing the reinforcement ratio by either adding more vertical reinforcing bars or increasing the bar size. Another countermeasure is to provide protection surrounding the bridge pier, such as barriers, to reduce the accessibility and vulnerability of the bridge piers and increase the standoff distance.

CHAPTER 6

MULTI-HAZARD ANALYSIS

Multi-hazard engineering is a growing field as the possibility of multiple threats to structures becomes more apparent to structural engineers (Bell & Glade, 2004). Multi-hazard analysis has several advantages including the possibility for more accurate estimation of structural resiliency, or recovery, from intense loading, a better prediction of lifecycle cost of the structure, and structural health monitoring to increase structural efficiency and economic analysis (Agrawal, et. al., 2007). Hazards produce intense demands on structures because of the different loading types and intensities and there exists a real possibility that a structure will undergo multiple short-duration, high-intensity consecutive loadings.

The reliability analysis of the bridge pier subject to the impact and blast loading successively follows the methodology outlined in Section 3.1.2. Using the procedures and equations defined in Sections 3.2 and 3.3, the reliability and sensitivity analyses are completed with a MATLAB code, included in Appendix C, developed for the analysis of a circular reinforced concrete bridge pier subject to intentional vehicular impact and blast loading, successively. The results of the multi-hazard reliability and sensitivity analyses are presented hereafter.

6.1 Multi-Hazard Analysis

The principal focus of the multi-hazard segment of this study is on intentional vehicular impact followed by blast loading, using a vehicle bomb at a small standoff distance. The standoff distance is taken as minimal to consider maximum disruption to the reinforced concrete bridge pier, which is the intention of terrorism. The variables and their corresponding statistical parameters used in the multi-hazard analysis are defined in Section 3.2.2, Tables 3.3 and 3.4. Table 6.1 shows the values of the constantly held parameters while the vehicle mass and charge weights are varied.

Table 6.1: Constant Parameters in Multi-Hazard Sensitivity Analysis

Variable	Mean
Pier Radius	0.25 m (0.82 ft)
Pier Height	5 m (16.4 ft)
Bar Number	7
Axial Load	75%P_{allow} kN
Standoff Distance	5 m (16.4 ft)
Coefficient of Variation	0.33
Mean-to-Nominal Ratio	1.0

In the multi-hazard reliability analysis, the probability of failure is first determined from the vehicular impact. Based on this probability of failure, the moment resistance of the bridge pier is reduced and used in the reliability analysis with the blast loading. Table 6.2 provides the resistance reduction factors corresponding to the probability of failure values from the vehicle impact reliability analysis. The resistance reduction factors were developed in this thesis based on Ellingwood's findings.

Table 6.2: Pier Resistance Reduction

Probability of Failure from Vehicle Impact	Reduction
0% < P_f ≤ 12%	1σ
12% < P_f ≤ 24%	2σ
24% < P_f ≤ 36%	3σ
36% < P_f ≤ 48%	4σ
48% < P_f ≤ 60%	5σ
60% < P_f ≤ 72%	6σ
72% < P_f ≤ 84%	7σ
84% < P_f ≤ 100%	8σ

As explained in Section 3.2.1, Ellingwood defines the coefficient of variation of reinforced concrete, with Grade 60 steel, in flexure as 0.11. The standard deviation (σ) used in the resistance reduction is defined as the moment resistance found in the impact reliability analysis multiplied by the coefficient of variation defined by Ellingwood. The fragility curves for the multi-hazard analysis are displayed in Figure 6.1. In Figure 6.1, only two lines are visible because the four largest vehicle classes display probabilities of failure of 100% for each charge weight.

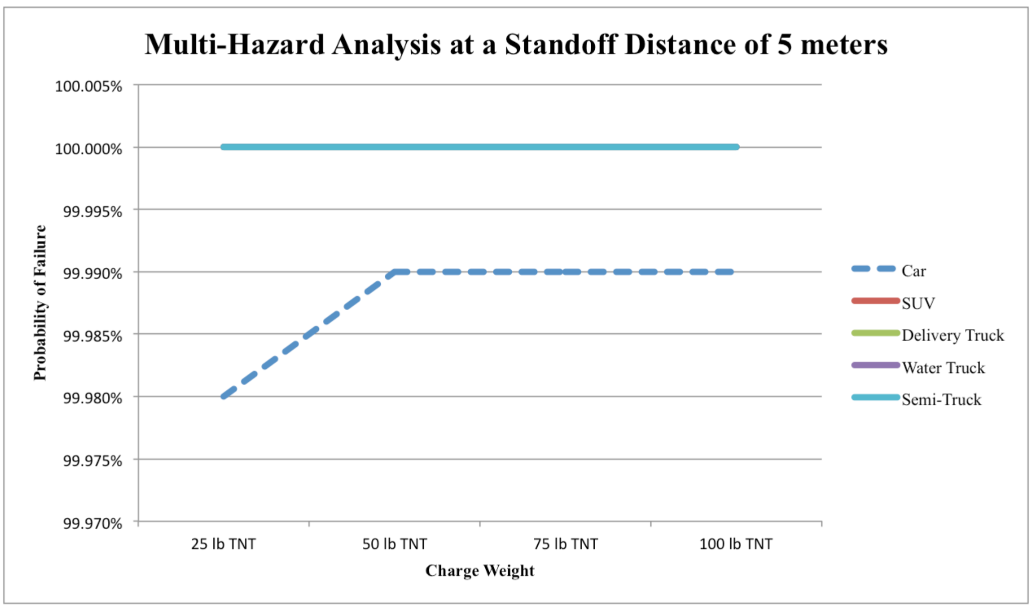

Figure 6.1: Multi-Hazard Analysis Fragility Curve

The SUV, Delivery Truck, Water Truck, and Semi-Truck vehicle classes reach 100% probability of failure for all charge weights considered. The multi-hazard loading event with the car vehicle class did not reach 100% probability of failure but was not less than 99% in the multi-hazard scenario. Table 6.3 provides the probabilities of failure of the multi-hazardous events.

Table 6.3: Multi-Hazard Analysis with Car Vehicle Class

Probability of Failure with Car Vehicle Class				
Standoff Distance	25 lb TNT	50 lb TNT	75 lb TNT	100 lb TNT
5 meters	99.98%	99.99%	99.99%	99.99%

The fragility curves in Figure 6.1 and values provided in Table 6.3 demonstrate that a multi-hazard event, involving vehicular impact and blast loading, is extremely detrimental to a circular reinforced concrete bridge pier.

6.2 Multi-Hazard Resistance Reduction Sensitivity Analysis

In the sensitivity analysis of the multi-hazard analysis resistance reduction, the moment resistance of the bridge pier is reduced from 10% to 90%, while all other variables are kept constant. The reliability curves for the sensitivity analysis of the bridge pier resistance reduction due to multi-hazard loading are displayed in Figures 6.2 and 6.3.

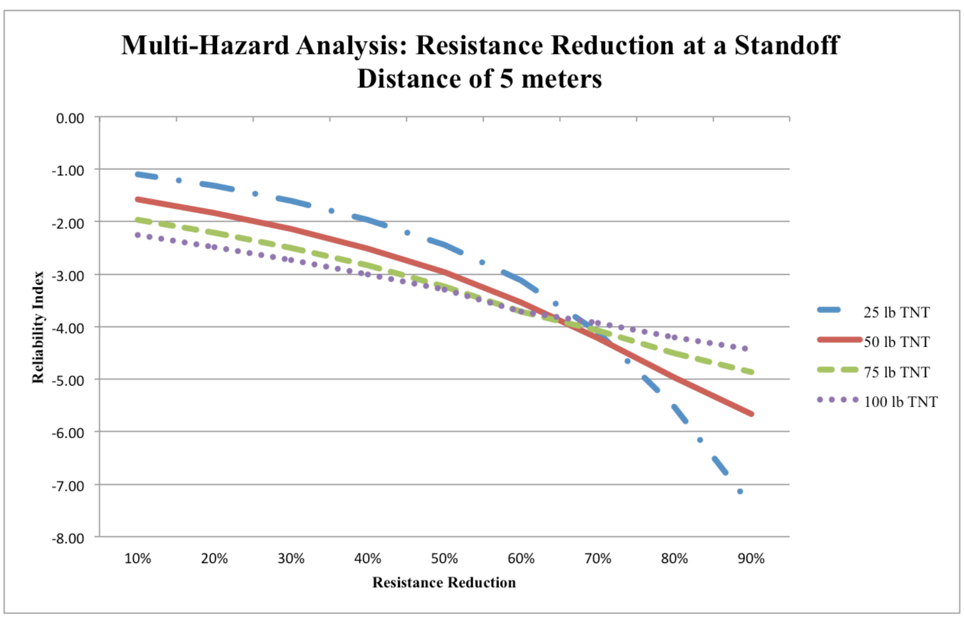

Figure 6.2: Multi-Hazard Sensitivity Analysis Reliability Curve

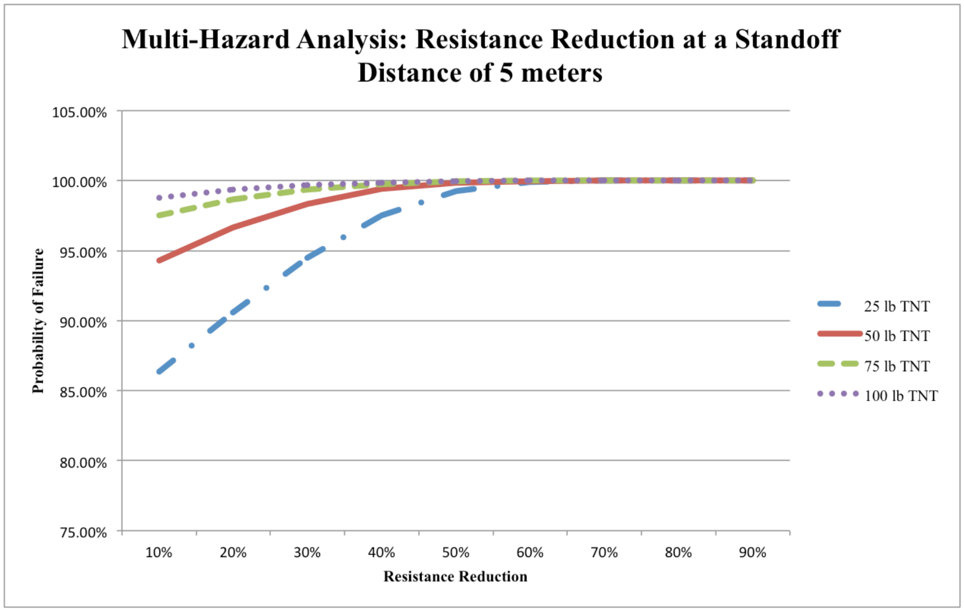

Figure 6.3: Multi-Hazard Sensitivity Analysis Fragility Curve

The reliability curves corresponding to the different charge weights generally follow the same trend. Naturally, reliability index consistently decreases as the resistance reduction is increased, and therefore, the probability of failure consistently increases as the resistance reduction increases. The fragility curves signifying the larger charge weights are much flatter than those of the smaller charge weights due to exceptionally high probabilities of failure of the bridge pier regardless of the reduction. Furthermore, all of the fragility curves flatten out at a 100% probability of failure around a 50% resistance reduction

6.3 Multi-Hazard Fault Tree Analysis

The fault tree analysis, described in 3.2.1.3, is performed for all five vehicle classes and different charge weights. The failure probabilities determined in the impact and blast analyses are used as the probabilities of failure of the individual events in Equation. The constant parameters shown in Table 6.1 are used in this analysis. Table 6.4 shows the results of the multi-hazard fault tree analysis.

Table 6.4: Multi-Hazard Fault Tree Analysis

Probability of Failure			
Analysis Parameter: Resistance Reduction (5 meters)			
Charge Weight of 25 lb of TNT			
Vehicle	**Impact**	**Blast**	**Multi-Hazard**
Car	63.36%	81.93%	93.38%
SUV	90.03%	81.93%	98.20%
Delivery Truck	98.94%	81.93%	99.81%
Water Truck	99.85%	81.93%	99.97%
Semi-Truck	99.98%	81.93%	100.00%
Charge Weight of 50 lb of TNT			
Vehicle	**Impact**	**Blast**	**Multi-Hazard**
Car	63.36%	91.48%	96.88%
SUV	90.03%	91.48%	99.15%
Delivery Truck	98.94%	91.48%	99.91%
Water Truck	99.85%	91.48%	99.99%
Semi-Truck	99.98%	91.48%	100.00%
Charge Weight of 75 lb of TNT			
Vehicle	**Impact**	**Blast**	**Multi-Hazard**
Car	63.36%	96.01%	98.54%
SUV	90.03%	96.01%	99.60%
Delivery Truck	98.94%	96.01%	99.96%
Water Truck	99.85%	96.01%	99.99%
Semi-Truck	99.98%	96.01%	100.00%
Charge Weight of 100 lb of TNT			
Vehicle	**Impact**	**Blast**	**Multi-Hazard**
Car	63.36%	97.93%	99.24%
SUV	90.03%	97.93%	99.79%
Delivery Truck	98.94%	97.93%	99.98%
Water Truck	99.85%	97.93%	100.00%
Semi-Truck	99.98%	97.93%	100.00%

The values provided in Table 6.4 demonstrate lower values than those of the proposed multi-hazard analysis methodology developed in this study and provided in Section 6.1. Table 6.5 shows a comparison of the two methods and the resulting multi-hazard probabilities of failure.

Table 6.5: Multi-Hazard Method Comparison

Multi-Hazard Analysis Probability of Failure Comparison (25 lb TNT)		
Vehicle Class	**Fault Tree Analysis**	**Proposed Method Analysis**
Car	93.38%	99.99%
SUV	98.20%	100.00%
Delivery Truck	99.81%	100.00%
Water Truck	99.97%	100.00%
Semi-Truck	100.00%	100.00%

Table 6.5 indicates that the conventional method of multi-hazard analysis using the fault tree provides less conservative results than performing the first-order, second-moment reliability analysis for both loading events and reducing the bridge pier resistance. However, both analyses result in very high probabilities of failure, confirming that a multi-hazard event, involving vehicular impact and blast loading, is extremely detrimental to a circular reinforced concrete bridge pier.

6.4 Threat Assessment

Chapters 4 and 5 validate that both vehicular impact and blast are detrimental to circular reinforced concrete bridge piers. With the multi-hazard analysis, it is valuable to perform a threat assessment as well. The assessment allows for the two loadings in the multi-hazardous event to be contrasted and the loading with the most significance on the bridge pier to be identified.

In looking at Chapter 5, a charge weight of 11.3 kilograms (25 pounds) of TNT results in a high probability of failure. Table 6.6 identifies the probabilities of failure of the bridge pier subject to smaller charge weights determined using the proposed multi-hazard analysis methodology. Due to the small standoff distance and variations in the charge weight, the probabilities of failure are still substantial but increase notably with an increase in charge weight.

Table 6.6: Blast Analysis with Small Charge Weights

Analysis of Small Blast Loading					
Charge Weight	**5 lb TNT**	**10 lb TNT**	**15 lb TNT**	**20 lb TNT**	**25 lb TNT**
Probability of Failure	69.48%	72.98%	76.27%	79.27%	82.00%

Table 6.7 compares the probabilities of failure of the bridge pier for each of the vehicle classes of the impact loading and the multi-hazardous loading with a small charge weight of 2.3 kilograms (5 pounds) of TNT determined using the proposed multi-hazard analysis methodology. Referring to Figure 3.1 in Section 3.1.1, 2.3 kilograms (5 pounds) of TNT is equivalent to a pipe bomb.

Table 6.7: Multi-Hazard Analysis with 5 pounds of TNT

Probability of Failure					
Impact Loading Compared with Multi-Hazard Analysis (5 lb of TNT)					
Vehicle	**Car**	**SUV**	**Delivery Truck**	**Water Truck**	**Semi-Truck**
Impact Loading	63.42%	90.02%	98.94%	99.84%	99.98%
Multi-Hazard Loading	99.49%	100.00%	100.00%	100.00%	100.00%
Percentage Increase	56.87%	11.09%	1.07%	0.16%	0.02%

The values in Table 6.6 indicate that for the smaller vehicle classes, car and SUV, the blast loading significantly increases the probability of failure compared to that of the impact loading alone. With larger mass vehicles, the probability of failure of the bridge pier is nearly 100% from the vehicular impact loading alone. It is concluded that with a vehicle of 4,536 kilograms (10,000 pounds) or less, the vehicular impact and blast loading are both equally important threats to protect against to ensure the safety of the bridge pier. For large mass vehicles, with masses above 4,536 kilograms (10,000 pounds), the vehicular impact is the primary threat to hinder. Though the potential charge weights in the larger vehicles is immense, the large mass in the impact loading is sufficient to cause extremely high probabilities of failure without the blast loading.

In looking at the analyses, it is concluded that large mass vehicles and high charge weights cause immense amounts of damage alone. If these significant loadings reach the bridge pier, there is little an engineer can do to protect against failure of the bridge pier. This leads to the conclusion that protection around the bridge pier needs to be utilized in order to decrease the vulnerability of the bridge pier to protect against these massive loadings.

The other threat concluded from the threat assessment is a smaller vehicle with a small charge weight. Table 6.7 shows that a multi-hazard event involving a car vehicle class and 5 pounds of TNT, equivalent to a pipe bomb, results in a probability of failure of 99.49%. Smaller vehicles with less charge weight capacity are more difficult to detect but have the ability to cause almost 100% probability of failure. Protection against smaller vehicles and charge weights is also a necessity to improve the safety of bridge piers.

6.5 Conclusions

Multi-hazard loading events are extremely detrimental to circular reinforced concrete bridge piers. The countermeasures explained in Chapters 4 and 5 can be used to reduce the probability of failure of the bridge pier subject to the multi-hazard loadings. These countermeasures include: increase in the gross area of concrete, increase in the reinforcement ratio, and protection surrounding the bridge pier, such as to reduce the accessibility and vulnerability of the bridge piers and increase the standoff distance.

Though impact and blast are both detrimental, it may be more beneficial to focus on preventing the initial hazardous loading, vehicular impact, especially for larger mass vehicles. It is also confirmed that traditional methods of multi-hazard analysis do not adequately consider sequential loading and the structural resistance reduction methodology developed in this study is a better indicator of the reliability of the bridge pier subject to two hazardous, sequential loadings.

CHAPTER 7

SUMMARY, CONCLUSIONS, AND FUTURE WORK

7.1 Summary and Conclusions

7.1.1 Methodology Summary

This study determines the probability of failure of a circular reinforced concrete bridge pier that experiences vehicular impact loading, blast loading, and multi-hazardous loading; specifically vehicular impact loading followed by blast loading. In order to accomplish the objectives of this study, a numerical model is developed in MATLAB employing Monte Carlo simulation and a first order, second moment reliability analysis.

Cizmar and others studied the reliability of rectangular concrete piers under vehicle impact loading and provide useful information about probabilistic and deterministic modeling of reinforced concrete piers subject to vehicle impact (Cizmar et. al., 2008). The research performed by Cizmar and others serves as the foundation for this study and is built upon by considering: 1) circular instead of square piers, 2) terroristic intention (i.e. acceleration vs. deceleration), 3) strength reduction versus fault tree analysis and 4) sensitivity analysis to determine those design factors that most contribute to high probabilities of failure and as such can be modified to decrease probabilities of failure.

The performance functions represent the flexural capacity of the bridge pier and the flexural application of the impact and blast loading. The pier resistance and impact loading equations used in this study are identified in the foundational study provided by Cizmar and others. The blast performance function includes the already defined resistance equation and utilizes the method of superposition and assumption of a trapezoidal loading on the bridge pier to determine the demand of the reinforced bridge pier due to the blast pressure.

The first-order, second-moment reliability analysis is used to determine the probabilities of failure due to the impact load alone, the blast load alone, and sequential impact and blast loads. Several pier resistance and loading event scenarios are considered and sensitivity analysis is carried out for the purpose of identifying the most influential parameters of the impact and blast loadings. In the sensitivity analysis, one parameter is adjusted while the others stay constant to analyze the influence the changing parameter has on the reliability. Fragility curves are generated in Microsoft Excel to provide a graphical representation of the sensitivity analysis.

7.1.2 Results

Objective 1 of this study was to determine the probability of failure and residual strength of a bridge pier due to an impact event. The probabilities of failure of the reinforced concrete bridge pier for various scenarios were determined and found to be extremely high with a vehicular impact-loading event. Current countermeasures are typically intended to slow the vehicle or increase the distance between the roadway and pier. According to the results, this method of reducing the accessibility and vulnerability of the bridge pier lowers the probability of failure by a substantial amount. Design countermeasures to reduce the probability of failure include increasing the diameter of the pier radius to provide a larger gross area of concrete and increasing the reinforcement ratio by either adding more vertical reinforcing bars or increasing the bar size. Another countermeasure is to provide protection surrounding the bridge pier, such as barriers, to reduce the accessibility and vulnerability of the bridge piers.

Objective 2 of this study was to determine the probability of failure and residual strength of a bridge pier due to a blast event. The probabilities of failure of the reinforced concrete bridge pier for various scenarios were determined and found to be extremely high with a blast-loading event. Current countermeasures are typically intended to increase the standoff distance. According to the results, this method of reducing the accessibility and vulnerability of the bridge pier lowers the probability of failure by a substantial amount. Design countermeasures to reduce the probability of failure include decreasing the pier height, increasing the diameter of the pier to provide a larger gross area of concrete, and increasing the reinforcement ratio by either adding more vertical reinforcing bars or increasing the bar size. Another countermeasure is to provide protection surrounding the bridge pier, such as barriers, to reduce the accessibility and vulnerability of the bridge piers and increase the standoff distance.

Objective 3 of this study was to determine a range of resistance reduction factors corresponding to associated probabilities of failure to be used in the multi-hazardous reliability analysis after the impact event. Resistance reduction factors corresponding to the probability of failure values from the vehicle impact reliability analysis were identified using the standard deviation of the reinforced concrete bridge pier provided by Ellingwood. Further research should be performed to determine accurate reduction ranges for the reduction values according to the condition of the bridge pier after the first hazardous loading.

Objective 4 of this study was to determine the probability of failure and residual strength of a bridge pier due to a blast load following an impact load. The investigation of the multi-hazard loading led to the conclusion that multi-hazardous events are extremely detrimental to circular reinforced concrete bridge piers. Most of the multi-hazardous scenarios resulted in a probability of failure of 100%. Because the multi-hazardous events are extremely detrimental, a threat analysis was completed to allow for the two loadings in the multi-hazardous event to be contrasted and the loading with the most significance on the bridge pier to be identified. It is concluded that with a vehicle of 4,536 kilograms (10,000 pounds) or less, the vehicular impact and blast loading are both equally important threats to protect against to ensure the safety of the bridge pier. For large mass vehicles, with masses above 4,536 kilograms (10,000 pounds), the vehicular impact is the primary threat to hinder. Though the potential charge weights in the larger vehicles is immense, the large mass in the impact loading is sufficient to cause extremely high probabilities of failure without the blast loading.

Objective 5 of this study was to perform a sensitivity analysis and develop sets of fragility curves corresponding to the impact, blast, and multi-hazardous loading imposed on different concrete bridge pier resistance scenarios. Fragility curves were developed in *Microsoft Excel* for various scenarios and contributed in the identification of factors contributing to high probabilities of failure for each of the loadings.

Objective 6 was to identify the factors that most contribute to high probabilities of failure and identify countermeasures to reduce the probabilities of failure. The investigation of the vehicular impact loading led to the identification of the following pier resistance factors, in descending order, that most likely contribute to failure in the intentional and accidental impact event: 1) pier radius 2) axial load in the pier 3) reinforcement ratio and 4) pier length. The investigation also led to the identification of the following impact loading factors, in descending order, that most likely contribute to failure in the impact event with the smaller vehicle classes: 1) vehicle speed 2) vehicle mass and 3) vehicle acceleration. For the larger vehicle classes, the following impact loading factors, in descending order, that most contribute to failure in the impact event are identified: 1) vehicle mass 2) vehicle speed and 3) vehicle acceleration.

The investigation of the blast loading led to the identification of the following pier resistance factors, in descending order, that most likely contribute to failure in the blast loading event: 1) pier length 2) pier radius 3) reinforcement ratio and 4) axial load applied to the pier. It should be understood that a decrease in the pier length decreases the probability of failure of the bridge pier whereas an increase in the other pier resistance factors decrease the probability of failure of the bridge pier. The investigation also led to the identification of the following blast loading factors, in descending order, that most likely contribute to failure in the blast loading event: 1) standoff distance and 2) charge weight. It should be understood that an increase in the standoff distance decreases the probability of failure of the bridge pier whereas a decrease in the charge weight decreases the probability of failure of the bridge pier.

7.2 Recommendations for Future Research

Based on the finding of this research, several future research projects are possible. Since the traditional methods of multi-hazard analysis do not adequately consider sequential loading and the structural resistance reduction methodology developed in this study is a better indicator of the reliability of the bridge pier subject to two hazardous, sequential loadings, further research should be performed on this new method. Reduction values for the bridge pier resistance after the impact loading are assumed. Further research should be performed to determine accurate reduction ranges for the reduction values according to the condition of the bridge pier after the first hazardous loading. Structural programs, such as *ANSYS*, could be utilized to determine the reductions.

There is limited information regarding the statistics of a blast loading and it would be extremely valuable to continue research on this subject. This study assumes a normal distribution, mean-to-nominal ratio, and coefficient of variation for the blast loading. It will be very useful to continue studying and come to optimal values for these blast statistical parameters. In addition to the blast statistics, this study assumes a trapezoidal blast distribution on the bridge pier and uses the law of superposition. This is an approximation and an analysis of the actual loading distribution on the bridge pier will contribute to the understanding of this loading on a structural element. A better understanding of explosive loading will assist in preventing terroristic mayhem. A continuation of this can be used with programs provided by the Protective Design Center, such as *Single-degree-of-freedom Blast Effects Design Spreadsheet* (SBEDS) and *Column Blast Analysis and Retrofit Design* (CBARD).

This study focuses on the flexural capacity and demand of the reinforced concrete bridge pier. It will be beneficial to continue this study and consider the deflection capacity and demand. The shear reinforcement is also assumed to be adequate to resist against shear. The analysis of shear capacity and demand should also be considered as a continuation of this study. Also, this study only considers bridge piers with circular cross-sections. A beneficial continuation would be investigating multiple cross-sections, rather than just circular, to determine if the cross-sectional shape affects the probability of failure of the bridge pier. Various arrangements of steel reinforcing should be considered, including vertical shear reinforcement, and additional flexural steel.

BIBLIOGRAPHY

Agrawal, A.K. & Chen, C. (2008). Bridge vehicle impact assessment. *University Transportation Research Consortium New York State Department of Transportation,* 1-28.

Agrawal, A., Alampalli, S., & Ettouney, M.M. (2007). Theory of Multi-Hazards: Theory of Multi-Hazards: A Quantification Procedure to the Process. *Symposium on Emerging Developments in Multi-Hazard Engineering.*

Al-Manaseer, A. & Hassoun, M.N. (2012). *Structural Concrete Theory and Design. (5 ed.).* New Jersey: John Wiley & Sons, Inc.

Alexander, D. (2003). Application of monte carlo simulations to system reliability analysis. *Proceedings of the Twentieth International Pump Users Symposium,* 91-94.

Ambrosini, R.D., Danesi, R.F., & Luccioni, B.M. (2004). Analysis of building collapse under blast loads. *Engineering Structures, 26,* 63-71.

Ambrosini, D., Danesi, R., Jacinto, A., & Luccioni, B. (2005). Location and mass of explosive from structural damage. *Engineering Structures, 27,* 167-176.

American Society of Civil Engineers. (2010). Minimum design loads of buildings and other Structures. *American Society of Civil Engineers, 7.*

Applied R&M Manual for Defence Systems (2011). Monte-Carlo simulation. *Part D – Supporting Theory,* 1-8.

Asprone, D., Jalayer, F., Manfredi, G., & Prota, A. (2009). Proposal of probabilistic model for multi-hazard risk assessment of structures in seismic zones subjected to blast for the limit state of collapse. *Structural Safety,* 1-10.

Ayyub, B.M., Kaminskiy, M., & McGill, W.L. (2007). Critical asset and portfolio risk analysis: an all-hazards framework. *Risk Analysis, 27,* (4) 789-801.

Ayyub, B.M. & McCuen, R.H. (2011). *In Probability, statistics, and reliability for engineers and scientists (3 ed.)*. Florida: Taylor & Francis Group.

Banerjee, S. & Prasad, G.G. (2011) Analysis of bridge performance under the combined effect of earthquake and flood-induced scour. *Vulnerability, Uncertainty, and Risk,* 889-896.

Bao, X. & Li, B. (2009). Residual strength of blast damaged reinforced concrete columns. *International Journal of Impact Engineering,* 1-14.

Bell, R. & Glade, T. (2004). Multi-hazard analysis in natural risk assessments. *International Conference on Computer Simulation Risk Analysis and Hazard Mitigation,* 197-206.

Bridge Terms Definitions. *Retrieved from* *http://www.dot.state.oh.us/Divisions/Communications/BridgingtheGap/Pages/BridgeTermDefinitions.aspx*

Brode, H. (1955). Numerical solutions of spherical blast waves. *Journal of Applied Physics, 26,* 766-775.

Chapman, S.J. (2008). *MATLAB Programming for Engineers (4 ed).* Thomson Learning.

Ching, J. (2011). Practical Monte-Carlo based reliability analysis and design methods of geotechnical problems. *Applications of Monte Carlo Method in Science and Engineering, 31,* 757-780.

Cizmar, D., Mestrovic, D., & Miculinic, L. (2008). Reliability of concrete columns under vehicle impact. *Structures Under Shock and Impact X, 98,* 157-165.

Collins, K.R. & Nowak, A.S. (2000). *Reliability of Structures.* Boston: McGraw-Hill Higher Education.

Darwin, D., Dolan, C.W., & Nilson, A.H. (2010). *Design of Concrete Structures (14 ed).* Boston: McGraw-Hill Higher Education.

DeHann, J.D. (2012). Deflagrations vs. detonations. *Retrieved from* *http://www.interfire.org/*

Doege, T. & Gebbeken, N. (n.d.) Residual load-carrying capacity of masonry walls subjected to blast loads. *JCSS and IABSE Workshop on Robustness of Structures,* 1-10.

Eamon, C.D. (2007). Reliability of concrete masonry unit walls subjected to explosive loads. *Journal of Structural Engineering,* 935-944.

El-Tawil, S. (2004). Vulnerability of bridge piers to impact by heavy vehicles. *Simulation Technology, 2,* (7), 13-20.

Ellingwood, B.R. (2007). Assessment and mitigation of risk from competing low probability, high- consequence hazards. *Symposium on Emerging Developments in Multi-Hazard Engineering.*

Ellingwood, B., Galambos, T.V., MacGregor, J.G., & Cornell, C.A. (1980). Development of a probability based load criterion for American National Standard A58. *NBS Special Publication 577.*

Elliot, C.L., Jackson, P., Jenkinson, R.J., Mairs, D., Mays, G.C., Smith, P.D., ...Veale, J.R. (1995). In *Blast effects on buildings.* Retrieved from http://books.google.com/books?hl=en&lr=&id=t2Zlxs0pBC4C&oi=fnd&pg=PA1&dq=what+is+dynamic+blast+loading&ots=AuH2jO7Nf3&sig=jqjT542K-WsqcRSbTU0hIRmSZPM#v=onepage&q=what%20is%20dynamic%20blast%20loading&f=false

Exponent Engineering and Scientific Consulting. (2010). Explosions, deflagrations, &detonations. *Exponent Engineering and Scientific Consulting.*

Faber, M.H. (2001) Probabilistic model code. *JCSS Publication.*

Galati, N., Nanni, A., Quintero, R., & Wei, J. (2007). Failure modeling of bridge components subjected to blast loading part II: estimation of the capacity and critical charge. *International Journal of Concrete Structures and Materials, 1,* (1) 29-36.

Gedeon, G. (n.d.). Explosive blast. *Building terrorism mitigation-blast and CBR measures* (pp.1-20). Retrieved from: http://www.cedengineering.com/upload/FEMA%20426%20Chapters%204%20&%205.pdf

Gupta, A., Mendis, P., Ngo, T., & Ramsay, J. (2007). Blast loading and blast effects on structures – an overview. *Electronic Journal of Science Engineering Special Issue: Loading on Structures,* 76-91.

Haugh, M. (2004). Overview of monte carlo simulation, probability review and introduction to matlab. *Monte Carlo Simulation: IEOR E4703,* 1-11.

Inkester, J.E. & Watson, A.J. (n.d.) Impact loading of a reinforced concrete beam-to-column joint. *Special Publication, 73,* 143-164.

Law, K.H. & Soh, H. (2000). Bayesian probabilistic damage detection of a reinforced concrete bridge column. *Earthquake Engineering and Structural Damage, 29,* 1131-1152.

Longinow, A. & Mniszewski, K.R. (1996). Protecting buildings against vehicle bomb attacks. *Practice Periodical of Structural Design and Construction,* 51-54.

Lu, B. & Silva, P.F. (2009). Blast resistance capacity of reinforced concrete slabs. *Journal of Structural Engineering,* 708-716.

Mainstone, R.J. (n.d.). Properties of materials at high rates of straining or loading. *Materials and Structures, 8,* 102-116.

MCEER (2007). Leading experts present emerging developments in multi-hazard engineering at AEI-MCEER symposium. *Symposium on Emerging Developments in Multi-Hazard Engineering.*

Melchers, R. E. (2002). Safety and risk in structural engineering. *Project Structural Engineering Matter, 4,* 193-202.

Notteboom, T. & Rodrigue, J.-P. (2012). Transportation and economic development. *The Geography of Transportation Systems.*

Ruiz, G., Tarifa, M., Yu, R.C., & Zhang, X.X. (2009). Fracture behavior of high-strength Concrete at a wide range of loading rates. *International Journal of Impact Engineering, 36,* 1204-1209.

Starossek, U. (2006). Progressive collapse of structures. *2006 Annual Conference of the Structural Engineering Committee of the Korean Society of Civil Engineers,* 1-7.

US Department of Energy (2012). Maps and Data. Alternative Fuels Data Center.

Van Hecke, G.R. (1999). What is an exothermic reaction? *Retrieved from http://www.scientificamerican.com/article.cfm?id=what-is-an-exothermic-rea*

Woo, G. (2002) Quantitative terrorism risk assessment. *The Journal of Risk Finance, 4,* 7-14.

Yallop, H.J. (1964). Investigation of the causes of explosions. *Firearms and Explosives,* 6-10.

APPENDIX A

```
%Prompt user for column parameters (concrete and reinforcement details)
disp('The column dimensions and reinforcement details are needed for
the analysis.')
disp(' ')
disp('This code only analyzes circular columns with spiral
reinforcement.')
disp('It is assumed that the vertical reinforcing consist of 8 bars
that are')
disp('evenly spaced in the column. It is also assumed that the spiral')
disp('reinforcement is adequate to support against shear.')
disp(' ')
column_radius = input('Enter the radius of the reinforced concerete
bridge column in meters: ');
disp(' ')
column_length = input('Enter the length of the reinforced concrete
brige column in meters: ');
disp(' ')
vertical_barsize = input('Enter the bar size for the vertical
reinforcement, such as 3,4,etc.:','s');
disp(' ')
bar_count = 8; %input('Enter the number of bars in the vertical
reinforcement: ');
disp(' ')


%Column Parameter Calculations
Ag = pi*((column_radius*100)^2); %square centimeters
compressive_strength = 3*1.04; %KN/(cm^2)
column_diameter = 2*column_radius; %meters

if strcmp(vertical_barsize, '3')
    bar_diameter = 0.95; %centimeters
    bar_area = 0.710; %square centimeters
elseif strcmp(vertical_barsize, '4')
    bar_diameter = 1.27; %centimeters
    bar_area = 1.29; %square centimeters
elseif strcmp(vertical_barsize, '5')
    bar_diameter = 1.59; %centimeters
    bar_area = 2.0; %square centimeters
elseif strcmp(vertical_barsize, '6')
    bar_diameter = 1.91; %centimeters
    bar_area = 2.84; %square centimeters
elseif strcmp(vertical_barsize, '7')
    bar_diameter = 2.22; %centimeters
    bar_area = 3.87; %square centimeters
elseif strcmp(vertical_barsize, '8')
    bar_diameter = 2.54; %centimeters
    bar_area = 5.09; %square centimeters
elseif strcmp(vertical_barsize, '9')
    bar_diameter = 2.87; %centimeters
    bar_area = 6.45; %square centimeters
elseif strcmp(vertical_barsize, '10')
    bar_diameter = 3.23; %centimeters
    bar_area = 8.19; %square centimeters
elseif strcmp(vertical_barsize, '11')
```

```
    bar_diameter = 3.58; %centimeters
    bar_area = 10.06; %square centimeters
else
  disp('error, please enter a valid response (3,4,...,11)')
end

As = bar_area*bar_count; %square centimeters
fy = 50; %KN/(cm^2)
E = 57000*sqrt(compressive_strength); %KN/cm^2
row = As/Ag;
y2 = (column_radius*100)*2-2*3.8; %centimeters (1.5 inches cover to
rebar)

%Find Allowable Axial Load
%fixed fixed, so k = 0.5

I = pi()*((column_radius*100)^4)/4; %cm^4
rg = sqrt(I/Ag); %cm
slenderness = 0.5*(column_length*100)/rg;

%Pallowable
if slenderness > 40
    disp('slender column, please choose different column properties')
else
    P_allowable = 0.85*(0.85*compressive_strength*(Ag-As)+As*fy); %KN
end

N = 0.75*P_allowable; %KN

%Monte Carlo Method for Resistance

n = 10000;

%Deterministic Value
gammaM = 1; %resistance uncertainty, unitless

%Nondeterministic Values

%Steel Area is Normal

As1_rand = rand(n,1);
As2_rand = rand(n,1);
As1i = -qfuncinv(As1_rand);
As2i = -qfuncinv(As2_rand);

As1 = 3*bar_area; %square centimeters
As2 = 2*bar_area; %square centimeters

gamma_As = 1.02;
mean_As1 = gamma_As*As1; %square centimeters
mean_As2 = gamma_As*As2; %square centimeters

sigma_As1 = .05*mean_As1; %square centimeters
sigma_As2 = .05*mean_As2; %square centimeters
```

```
%yield strength is lognormal

fy_rand = rand(n,1);
fyi = -qfuncinv(fy_rand);

gamma_fy = 1.1;
mean_fy = gamma_fy*fy; %KN/(cm^2)

sigma_fy = 0.05*mean_fy; %KN/(cm^2)

V_fy = sigma_fy/mean_fy;
sigma_lnfy =(log10(V_fy^2+1))^0.5;
mu_lnfy = log10(mean_fy)-0.5*(sigma_lnfy^2);

%Moment Arm is Normal

y2_rand = rand(n,1);
y2i = -qfuncinv(y2_rand);

sigma_y2 = .05*y2;

%Axial Load is Lognormal
N_rand = rand(n,1);
Ni = -qfuncinv(N_rand);

sigma_N = 0.1*N;

V_N = sigma_N/N;
sigma_lnN =(log10(V_N^2+1))^0.5;
mu_lnN = log10(N)-0.5*(sigma_lnN^2);

%Values of Random Variable
As1_mc = mean(mean_As1+As1i*sigma_As1);
As2_mc = mean(mean_As2+As2i*sigma_As2);
fy_mc = mean(exp(mu_lnfy+fyi*sigma_lnfy));
y2_mc = mean(y2+y2i*sigma_y2);
N_mc = mean(exp(mu_lnN+Ni*sigma_lnN));

M_resistance =
(gammaM*(As2_mc*fy_mc*y2_mc+2*As1_mc*fy_mc*(y2_mc/2)+N_mc*(y2_mc/2)))/1
00; %KN-m

%Prompt the user for vehicle speed
disp(' ')
v = input('Enter the velocity of the vehicle in km/h for the
reliability analysis: ')*(1000/60); %meters/second
disp(' ')
a = input('Enter the acceleration of the vehicle in m/s^2 at impact for
the reliability analysis: ');

%vehicle = input('Enter the type of vehicle from the choices
above:','s');
%disp(' ')

%Define parameters for each type of vehicle
```

```
%Parameters for All Vehicles
  k = 300; %KN/m
  %a = -5; %meters/square second
  r =23; %meters

%Monte Carlo Method for Loading

n = 10000;

%Nondeterministic Values

%Vehicle Stiffness is lognormal
k_rand = rand(n,1);
ki = -qfuncinv(k_rand);

sigma_k = 0.2*k;

V_k = sigma_k/k;
sigma_lnk =(log10(V_k^2+1))^0.5;
mu_lnk = log10(k)-0.5*(sigma_lnk^2);

%Vehicle Acceleration is Lognormal
a_rand = rand(n,1);
ai = -qfuncinv(a_rand);

sigma_a = 0.325*a;

V_a = sigma_a/a;
sigma_lna =(log10(V_a^2+1))^0.5;
mu_lna = log10(a)-0.5*(sigma_lna^2);

%Vehicle is a Car
  h_impact_car = 0.61; %meters
  m_car = 2270; %kg

%Vehicle is a SUV
  h_impact_SUV = 0.91; %meters
  m_SUV = 4540; %kg

%Vehicle is a small moving van/delivery truck
  h_impact_DT = 1.22; %meters
  m_DT = 8170; %kg

%Vehicle is a van/water truck
  h_impact_WT = 1.5; %meters
  m_WT = 11800; %kg

%Vehicle is a semi-truck/trailer
  h_impact_ST = 1.8; %meters
  m_ST = 19100; %kg

%vehicle speed is lognormal
%vehicle mass is normal
```

```
v_rand = rand(n,1);
m_car_rand = rand(n,1);
m_SUV_rand = rand(n,1);
m_DT_rand = rand(n,1);
m_WT_rand = rand(n,1);
m_ST_rand = rand(n,1);

vi = -qfuncinv(v_rand);
mi_car = -qfuncinv(m_car_rand);
mi_SUV = -qfuncinv(m_SUV_rand);
mi_DT = -qfuncinv(m_DT_rand);
mi_WT = -qfuncinv(m_WT_rand);
mi_ST = -qfuncinv(m_ST_rand);

sigma_v = 0.15*v;

sigma_m_car = 0.33*m_car;
sigma_m_SUV = 0.33*m_SUV;
sigma_m_DT = 0.33*m_DT;
sigma_m_WT = 0.33*m_WT;
sigma_m_ST = 0.33*m_ST;

%lognormal calcs to calculate v_mc
V_v = sigma_v/v;
sigma_lnv = (log10(V_v^2+1))^2;
mu_lnv = log10(v)-0.5*(sigma_lnv^2);

%Values of Random Variables
k_mc = mean(exp(mu_lnk+ki*sigma_lnk)); %kN/m
a_mc = mean(exp(mu_lna+ai*sigma_lna)); %meters/s^2
v_mc = mean(exp(mu_lnv+vi*sigma_lnv)); %meters/s
m_car_mc = mean(m_car+mi_car*sigma_m_car)/1000; %1Mg=1000kg
m_SUV_mc = mean(m_SUV+mi_SUV*sigma_m_SUV)/1000;
m_DT_mc = mean(m_DT+mi_DT*sigma_m_DT)/1000;
m_WT_mc = mean(m_WT+mi_WT*sigma_m_WT)/1000;
m_ST_mc = mean(m_ST+mi_ST*sigma_m_ST)/1000;

%Impact Force Calculations
Fimpact_car = sqrt(k_mc*m_car_mc*((v_mc^2)-2*(-a_mc)*r)); %KN
Fimpact_SUV = sqrt(k_mc*m_SUV_mc*((v_mc^2)-2*(-a_mc)*r)); %KN
Fimpact_DT = sqrt(k_mc*m_DT_mc*((v_mc^2)-2*(-a_mc)*r)); %KN
Fimpact_WT = sqrt(k_mc*m_WT_mc*((v_mc^2)-2*(-a_mc)*r)); %KN
Fimpact_ST = sqrt(k_mc*m_ST_mc*((v_mc^2)-2*(-a_mc)*r)); %KN

%Applied Moment Calculation
M_impact_car = h_impact_car*Fimpact_car; %KN-m
M_impact_SUV = h_impact_SUV*Fimpact_SUV; %KN-m
M_impact_DT = h_impact_DT*Fimpact_DT; %KN-m
M_impact_WT = h_impact_WT*Fimpact_WT; %KN-m
M_impact_ST = h_impact_ST*Fimpact_ST; %KN-m

%Impact Performance Equation

muz_impact_car = M_resistance-M_impact_car;
muz_impact_SUV = M_resistance-M_impact_SUV;
muz_impact_DT = M_resistance-M_impact_DT;
```

```
muz_impact_WT = M_resistance-M_impact_WT;
muz_impact_ST = M_resistance-M_impact_ST;


%Column Resistance Sigma Calculations

%Partial Derivative Calculations
syms gammaM1 As2_mc1 As1_mc1 fy_mc1 y2_mc1 N_mc1
Fr=(gammaM1*(As2_mc1*fy_mc1*y2_mc1+2*As1_mc1*fy_mc1*(y2_mc1/2)+N_mc1*(y
2_mc1/2))/100); %KN-m
pd_gammaM1 = diff(Fr,gammaM1);
pd_As2_mc1 = diff(Fr,As2_mc1);
pd_As1_mc1 = diff(Fr,As1_mc1);
pd_fy_mc1 = diff(Fr,fy_mc1);
pd_y2_mc1 = diff(Fr,y2_mc1);
pd_N_mc1 = diff(Fr,N_mc1);

gammaM1 = gammaM;
As2_mc1 = As2_mc;
As1_mc1 = As1_mc;
fy_mc1 = fy_mc;
y2_mc1 = y2_mc;
N_mc1 = N_mc;

pd_gammaM = subs(pd_gammaM1);
pd_As2_mc = subs(pd_As2_mc1);
pd_As1_mc = subs(pd_As1_mc1);
pd_fy_mc = subs(pd_fy_mc1);
pd_y2_mc = subs(pd_y2_mc1);
pd_N_mc = subs(pd_N_mc1);

%Partial Derivatives Squared
pd_gammaM_sq = pd_gammaM^2;
pd_As2_mc_sq = pd_As2_mc^2;
pd_As1_mc_sq = pd_As1_mc^2;
pd_fy_mc_sq = pd_fy_mc^2;
pd_y2_mc_sq = pd_y2_mc^2;
pd_N_mc_sq = pd_N_mc^2;

%Standard Deviations
std_gammaM = 0; %Deterministic
std_As2_mc = 0.05*As2_mc;
std_As1_mc = 0.05*As1_mc;
std_fy_mc = 0.05*fy_mc;
std_y2_mc = 0.05*y2;
std_N_mc = 0.1*N;

%Standard Deviations Squared
std_gammaM_sq = std_gammaM^2;
std_As2_mc_sq = std_As2_mc^2;
std_As1_mc_sq = std_As1_mc^2;
std_fy_mc_sq = std_fy_mc^2;
std_y2_mc_sq = std_y2_mc^2;
std_N_mc_sq = std_N_mc^2;

%Resistance SigmaZ Calculations
```

```
sigma_sq_gammaM = pd_gammaM_sq*std_gammaM_sq;
sigma_sq_As2_mc = pd_As2_mc_sq*std_As2_mc_sq;
sigma_sq_As1_mc = pd_As1_mc_sq*std_As1_mc_sq;
sigma_sq_fy_mc = pd_fy_mc_sq*std_fy_mc_sq;
sigma_sq_y2_mc = pd_y2_mc_sq*std_y2_mc_sq;
sigma_sq_N_mc = pd_N_mc_sq*std_N_mc_sq;

%Impact Loading Sigma Calculations

%VEHICLE = CAR

%Car Partial Derivative Calculations
syms h_impact_car1 k_mc1 m_car_mc1 v_mc1 a_mc1 r1
Fi_car=h_impact_car1*sqrt(k_mc1*m_car_mc1*((v_mc1^2)-2*(-a_mc1)*r1));
pd_h_impact_car1 = diff(Fi_car,h_impact_car1);
pd_k_mc1 = diff(Fi_car,k_mc1);
pd_m_car_mc1 = diff(Fi_car,m_car_mc1);
pd_v_mc1 = diff(Fi_car,v_mc1);
pd_a_mc1 = diff(Fi_car,a_mc1);
pd_r1 = diff(Fi_car,r1);

h_impact_car1 = h_impact_car;
k_mc1 = k_mc;
m_car_mc1 = m_car_mc;
v_mc1 = v_mc;
a_mc1 = a_mc;
r1 = r;

pd_h_impact_car = subs(pd_h_impact_car1);
pd_k_mc = subs(pd_k_mc1);
pd_m_car_mc = subs(pd_m_car_mc1);
pd_v_mc = subs(pd_v_mc1);
pd_a_mc = subs(pd_a_mc1);
pd_r = subs(pd_r1);

%Car Partial Derivatives Squared
pd_h_impact_car_sq = pd_h_impact_car^2;
pd_k_mc_sq = pd_k_mc^2;
pd_m_car_mc_sq = pd_m_car_mc^2;
pd_v_mc_sq = pd_v_mc^2;
pd_a_mc_sq = pd_a_mc^2;
pd_r_sq = pd_r^2;

%Car Standard Deviations
std_h_impact_car = 0; %Deterministic
std_k_mc = 0.2*k_mc;
std_m_car_mc = 0.33*m_car_mc;
std_v_mc = 0.15*v_mc;
std_a_mc = 0.325*a_mc; %Deterministic
std_r = 0; %Deterministic

%Car Standard Deviations Squared
std_h_impact_car_sq = std_h_impact_car^2;
std_k_mc_sq = std_k_mc^2;
std_m_car_mc_sq = std_m_car_mc^2;
std_v_mc_sq = std_v_mc^2;
std_a_mc_sq = std_a_mc^2;
```

```
std_r_sq = std_r^2;

%Car Impact SigmaZ Calculations
sigma_sq_h_impact_car = pd_h_impact_car_sq*std_h_impact_car_sq;
sigma_sq_k_mc = pd_k_mc_sq*std_k_mc_sq;
sigma_sq_m_car_mc = pd_m_car_mc_sq*std_m_car_mc_sq;
sigma_sq_v_mc = pd_v_mc_sq*std_v_mc_sq;
sigma_sq_a_mc = pd_a_mc_sq*std_a_mc_sq;
sigma_sq_r = pd_r_sq*std_r_sq;

sigmaz_impact_car_sq =
sigma_sq_gammaM+sigma_sq_As2_mc+sigma_sq_As1_mc+sigma_sq_fy_mc+sigma_sq
_y2_mc+sigma_sq_N_mc+sigma_sq_h_impact_car+sigma_sq_k_mc+sigma_sq_m_car
_mc+sigma_sq_v_mc+sigma_sq_a_mc+sigma_sq_r;

sigmaz_impact_car = sqrt(sigmaz_impact_car_sq);

rindex_impact_car = muz_impact_car/sigmaz_impact_car;

reliability_impact_car = (1/2)*erfc(-rindex_impact_car/sqrt(2));

failure_prob_impact_car = 1-reliability_impact_car;

%Car Output

disp(' ')
disp('If the vehicle type in the impact event is a car (average mass')
disp('of 2,270 kilograms and impact height of 0.61 meters), then: ')
disp(' ')
disp('The reliability index of the reinforced concrete bridge pier
subject to impact is: ')
disp(rindex_impact_car)

%disp(' ')
%disp('The reliability of the reinforced concrete bridge pier subject
to impact is: ')
%disp(reliability_impact_car)

disp(' ')
disp('The probability of failure of the reinforced concrete bridge pier
subject to impact is: ')
disp(failure_prob_impact_car)

%VEHICLE = SUV

%SUV Partial Derivative Calculations
syms h_impact_SUV1 k_mc1 m_SUV_mc1 v_mc1 a_mc1 r1
Fi_SUV=h_impact_SUV1*sqrt(k_mc1*m_SUV_mc1*((v_mc1^2)-2*(-a_mc1)*r1));
pd_h_impact_SUV1 = diff(Fi_SUV,h_impact_SUV1);
pd_k_mc1 = diff(Fi_SUV,k_mc1);
pd_m_SUV_mc1 = diff(Fi_SUV,m_SUV_mc1);
pd_v_mc1 = diff(Fi_SUV,v_mc1);
pd_a_mc1 = diff(Fi_SUV,a_mc1);
pd_r1 = diff(Fi_SUV,r1);

h_impact_SUV1 = h_impact_SUV;
```

```
k_mc1 = k_mc;
m_SUV_mc1 = m_SUV_mc;
v_mc1 = v_mc;
a_mc1 = a_mc;
r1 = r;

pd_h_impact_SUV = subs(pd_h_impact_SUV1);
pd_k_mc = subs(pd_k_mc1);
pd_m_SUV_mc = subs(pd_m_SUV_mc1);
pd_v_mc = subs(pd_v_mc1);
pd_a_mc = subs(pd_a_mc1);
pd_r = subs(pd_r1);

%SUV Partial Derivatives Squared
pd_h_impact_SUV_sq = pd_h_impact_SUV^2;
pd_k_mc_sq = pd_k_mc^2;
pd_m_SUV_mc_sq = pd_m_SUV_mc^2;
pd_v_mc_sq = pd_v_mc^2;
pd_a_mc_sq = pd_a_mc^2;
pd_r_sq = pd_r^2;

%SUV Standard Deviations
std_h_impact_SUV = 0; %Determinsitic
std_k_mc = 0.2*k_mc;
std_m_SUV_mc = 0.33*m_SUV_mc;
std_v_mc = 0.15*v_mc;
std_a_mc = 0.325*a_mc; %Deterministic
std_r = 0; %Deterministic

%SUV Standard Deviations Squared
std_h_impact_SUV_sq = std_h_impact_SUV^2;
std_k_mc_sq = std_k_mc^2;
std_m_SUV_mc_sq = std_m_SUV_mc^2;
std_v_mc_sq = std_v_mc^2;
std_a_mc_sq = std_a_mc^2;
std_r_sq = std_r^2;

%SUV Impact SigmaZ Calculations
sigma_sq_h_impact_SUV = pd_h_impact_SUV_sq*std_h_impact_SUV_sq;
sigma_sq_k_mc = pd_k_mc_sq*std_k_mc_sq;
sigma_sq_m_SUV_mc = pd_m_SUV_mc_sq*std_m_SUV_mc_sq;
sigma_sq_v_mc = pd_v_mc_sq*std_v_mc_sq;
sigma_sq_a_mc = pd_a_mc_sq*std_a_mc_sq;
sigma_sq_r = pd_r_sq*std_r_sq;

sigmaz_impact_SUV_sq =
sigma_sq_gammaM+sigma_sq_As2_mc+sigma_sq_As1_mc+sigma_sq_fy_mc+sigma_sq
_y2_mc+sigma_sq_N_mc+sigma_sq_h_impact_SUV+sigma_sq_k_mc+sigma_sq_m_SUV
_mc+sigma_sq_v_mc+sigma_sq_a_mc+sigma_sq_r;

sigmaz_impact_SUV = sqrt(sigmaz_impact_SUV_sq);

rindex_impact_SUV = muz_impact_SUV/sigmaz_impact_SUV;

reliability_impact_SUV = (1/2)*erfc(-rindex_impact_SUV/sqrt(2));
```

```
failure_prob_impact_SUV = 1-reliability_impact_SUV;

%SUV Output
disp(' ')
disp('If the vehicle type in the impact event is an SUV (average mass')
disp('of 4,540 kilograms and impact height of 0.91 meters), then: ')
disp(' ')
disp('The reliability index of the reinforced concrete bridge pier
subject to impact is: ')
disp(rindex_impact_SUV)

%disp(' ')
%disp('The reliability of the reinforced concrete bridge pier subject
to impact is: ')
%disp(reliability_impact_SUV)

disp(' ')
disp('The probability of failure of the reinforced concrete bridge pier
subject to impact is: ')
disp(failure_prob_impact_SUV)

%VEHICLE = SMALL MOVING VAN/DELIVERTY TRUCK

%DT Partial Derivative Calculations
syms h_impact_DT1 k_mc1 m_DT_mc1 v_mc1 a_mc1 r1
Fi_DT=h_impact_DT1*sqrt(k_mc1*m_DT_mc1*((v_mc1^2)-2*(-a_mc1)*r1));
pd_h_impact_DT1 = diff(Fi_DT,h_impact_DT1);
pd_k_mc1 = diff(Fi_DT,k_mc1);
pd_m_DT_mc1 = diff(Fi_DT,m_DT_mc1);
pd_v_mc1 = diff(Fi_DT,v_mc1);
pd_a_mc1 = diff(Fi_DT,a_mc1);
pd_r1 = diff(Fi_DT,r1);

h_impact_DT1 = h_impact_DT;
k_mc1 = k_mc;
m_DT_mc1 = m_DT_mc;
v_mc1 = v_mc;
a_mc1 = a_mc;
r1 = r;

pd_h_impact_DT = subs(pd_h_impact_DT1);
pd_k_mc = subs(pd_k_mc1);
pd_m_DT_mc = subs(pd_m_DT_mc1);
pd_v_mc = subs(pd_v_mc1);
pd_a_mc = subs(pd_a_mc1);
pd_r = subs(pd_r1);

%DT Partial Derivatives Squared
pd_h_impact_DT_sq = pd_h_impact_DT^2;
pd_k_mc_sq = pd_k_mc^2;
pd_m_DT_mc_sq = pd_m_DT_mc^2;
pd_v_mc_sq = pd_v_mc^2;
pd_a_mc_sq = pd_a_mc^2;
pd_r_sq = pd_r^2;

%DT Standard Deviations
```

```
std_h_impact_DT = 0; %Deterministic
std_k_mc = 0.2*k_mc;
std_m_DT_mc = 0.33*m_DT_mc;
std_v_mc = 0.15*v_mc;
std_a_mc = 0.325*a_mc; %Deterministic
std_r = 0; %Deterministic

%DT Standard Deviations Squared
std_h_impact_DT_sq = std_h_impact_DT^2;
std_k_mc_sq = std_k_mc^2;
std_m_DT_mc_sq = std_m_DT_mc^2;
std_v_mc_sq = std_v_mc^2;
std_a_mc_sq = std_a_mc^2;
std_r_sq = std_r^2;

%DT Impact SigmaZ Calculations
sigma_sq_h_impact_DT = pd_h_impact_DT_sq*std_h_impact_DT_sq;
sigma_sq_k_mc = pd_k_mc_sq*std_k_mc_sq;
sigma_sq_m_DT_mc = pd_m_DT_mc_sq*std_m_DT_mc_sq;
sigma_sq_v_mc = pd_v_mc_sq*std_v_mc_sq;
sigma_sq_a_mc = pd_a_mc_sq*std_a_mc_sq;
sigma_sq_r = pd_r_sq*std_r_sq;

sigmaz_impact_DT_sq =
sigma_sq_gammaM+sigma_sq_As2_mc+sigma_sq_As1_mc+sigma_sq_fy_mc+sigma_sq
_y2_mc+sigma_sq_N_mc+sigma_sq_h_impact_DT+sigma_sq_k_mc+sigma_sq_m_DT_m
c+sigma_sq_v_mc+sigma_sq_a_mc+sigma_sq_r;

sigmaz_impact_DT = sqrt(sigmaz_impact_DT_sq);

rindex_impact_DT = muz_impact_DT/sigmaz_impact_DT;

reliability_impact_DT = (1/2)*erfc(-rindex_impact_DT/sqrt(2));

failure_prob_impact_DT = 1-reliability_impact_DT;

%DT Output
disp(' ')
disp('If the vehicle type in the impact event is a small moving
van/delivery truck (average mass')
disp('of 8,170 kilograms and impact height of 1.22 meters), then: ')
disp(' ')
disp('The reliability index of the reinforced concrete bridge pier
subject to impact is: ')
disp(rindex_impact_DT)

%disp(' ')
%disp('The reliability of the reinforced concrete bridge pier subject
to impact is: ')
%disp(reliability_impact_DT)

disp(' ')
disp('The probability of failure of the reinforced concrete bridge pier
subject to impact is: ')
disp(failure_prob_impact_DT)
```

```
%VEHICLE = MOVING VAN/WATER TRUCK

%WT Partial Derivative Calculations
syms h_impact_WT1 k_mc1 m_WT_mc1 v_mc1 a_mc1 r1
Fi_WT=h_impact_WT1*sqrt(k_mc1*m_WT_mc1*((v_mc1^2)-2*(-a_mc1)*r1));
pd_h_impact_WT1 = diff(Fi_WT,h_impact_WT1);
pd_k_mc1 = diff(Fi_WT,k_mc1);
pd_m_WT_mc1 = diff(Fi_WT,m_WT_mc1);
pd_v_mc1 = diff(Fi_WT,v_mc1);
pd_a_mc1 = diff(Fi_WT,a_mc1);
pd_r1 = diff(Fi_WT,r1);

h_impact_WT1 = h_impact_WT;
k_mc1 = k_mc;
m_WT_mc1 = m_WT_mc;
v_mc1 = v_mc;
a_mc1 = a_mc;
r1 = r;

pd_h_impact_WT = subs(pd_h_impact_WT1);
pd_k_mc = subs(pd_k_mc1);
pd_m_WT_mc = subs(pd_m_WT_mc1);
pd_v_mc = subs(pd_v_mc1);
pd_a_mc = subs(pd_a_mc1);
pd_r = subs(pd_r1);

%WT Partial Derivatives Squared
pd_h_impact_WT_sq = pd_h_impact_WT^2;
pd_k_mc_sq = pd_k_mc^2;
pd_m_WT_mc_sq = pd_m_WT_mc^2;
pd_v_mc_sq = pd_v_mc^2;
pd_a_mc_sq = pd_a_mc^2;
pd_r_sq = pd_r^2;

%WT Standard Deviations
std_h_impact_WT = 0; %Deterministic
std_k_mc = 0.2*k_mc;
std_m_WT_mc = 0.33*m_WT_mc;
std_v_mc = 0.15*v_mc;
std_a_mc = 0.325*a_mc; %Deterministic
std_r = 0; %Deterministic

%WT Standard Deviations Squared
std_h_impact_WT_sq = std_h_impact_WT^2;
std_k_mc_sq = std_k_mc^2;
std_m_WT_mc_sq = std_m_WT_mc^2;
std_v_mc_sq = std_v_mc^2;
std_a_mc_sq = std_a_mc^2;
std_r_sq = std_r^2;

%WT Impact SigmaZ Calculations
sigma_sq_h_impact_WT = pd_h_impact_WT_sq*std_h_impact_WT_sq;
sigma_sq_k_mc = pd_k_mc_sq*std_k_mc_sq;
sigma_sq_m_WT_mc = pd_m_WT_mc_sq*std_m_WT_mc_sq;
sigma_sq_v_mc = pd_v_mc_sq*std_v_mc_sq;
sigma_sq_a_mc = pd_a_mc_sq*std_a_mc_sq;
sigma_sq_r = pd_r_sq*std_r_sq;
```

```
sigmaz_impact_WT_sq =
sigma_sq_gammaM+sigma_sq_As2_mc+sigma_sq_As1_mc+sigma_sq_fy_mc+sigma_sq
_y2_mc+sigma_sq_N_mc+sigma_sq_h_impact_WT+sigma_sq_k_mc+sigma_sq_m_WT_m
c+sigma_sq_v_mc+sigma_sq_a_mc+sigma_sq_r;

sigmaz_impact_WT = sqrt(sigmaz_impact_WT_sq);

rindex_impact_WT = muz_impact_WT/sigmaz_impact_WT;

reliability_impact_WT = (1/2)*erfc(-rindex_impact_WT/sqrt(2));

failure_prob_impact_WT = 1-reliability_impact_WT;

%WT Output
disp(' ')
disp('If the vehicle type in the impact event is a moving van/water
truck (average mass')
disp('of 11,800 kilograms and impact height of 1.50 meters), then: ')
disp(' ')
disp('The reliability index of the reinforced concrete bridge pier
subject to impact is: ')
disp(rindex_impact_WT)

%disp(' ')
%disp('The reliability of the reinforced concrete bridge pier subject
to impact is: ')
%disp(reliability_impact_WT)

disp(' ')
disp('The probability of failure of the reinforced concrete bridge pier
subject to impact is: ')
disp(failure_prob_impact_WT)

%VEHCILE = SEMI-TRUCK/TRAILER

%ST Partial Derivative Calculations
syms h_impact_ST1 k_mc1 m_ST_mc1 v_mc1 a_mc1 r1
Fi_ST=h_impact_ST1*sqrt(k_mc1*m_ST_mc1*((v_mc1^2)-2*(-a_mc1)*r1));
pd_h_impact_ST1 = diff(Fi_ST,h_impact_ST1);
pd_k_mc1 = diff(Fi_ST,k_mc1);
pd_m_ST_mc1 = diff(Fi_ST,m_ST_mc1);
pd_v_mc1 = diff(Fi_ST,v_mc1);
pd_a_mc1 = diff(Fi_ST,a_mc1);
pd_r1 = diff(Fi_ST,r1);

h_impact_ST1 = h_impact_ST;
k_mc1 = k_mc;
m_ST_mc1 = m_ST_mc;
v_mc1 = v_mc;
a_mc1 = a_mc;
r1 = r;

pd_h_impact_ST = subs(pd_h_impact_ST1);
pd_k_mc = subs(pd_k_mc1);
pd_m_ST_mc = subs(pd_m_ST_mc1);
```

```
pd_v_mc = subs(pd_v_mc1);
pd_a_mc = subs(pd_a_mc1);
pd_r = subs(pd_r1);

%ST Partial Derivatives Squared
pd_h_impact_ST_sq = pd_h_impact_ST^2;
pd_k_mc_sq = pd_k_mc^2;
pd_m_ST_mc_sq = pd_m_ST_mc^2;
pd_v_mc_sq = pd_v_mc^2;
pd_a_mc_sq = pd_a_mc^2;
pd_r_sq = pd_r^2;

%ST Standard Deviations
std_h_impact_ST = 0; %Deterministic
std_k_mc = 0.2*k_mc;
std_m_ST_mc = 0.33*m_ST_mc;
std_v_mc = 0.15*v_mc;
std_a_mc = 0.325*a_mc; %Deterministic
std_r = 0; %Deterministic

%ST Standard Deviations Squared
std_h_impact_ST_sq = std_h_impact_ST^2;
std_k_mc_sq = std_k_mc^2;
std_m_ST_mc_sq = std_m_ST_mc^2;
std_v_mc_sq = std_v_mc^2;
std_a_mc_sq = std_a_mc^2;
std_r_sq = std_r^2;

%ST Impact SigmaZ Calculations
sigma_sq_h_impact_ST = pd_h_impact_ST_sq*std_h_impact_ST_sq;
sigma_sq_k_mc = pd_k_mc_sq*std_k_mc_sq;
sigma_sq_m_ST_mc = pd_m_ST_mc_sq*std_m_ST_mc_sq;
sigma_sq_v_mc = pd_v_mc_sq*std_v_mc_sq;
sigma_sq_a_mc = pd_a_mc_sq*std_a_mc_sq;
sigma_sq_r = pd_r_sq*std_r_sq;

sigmaz_impact_ST_sq =
sigma_sq_gammaM+sigma_sq_As2_mc+sigma_sq_As1_mc+sigma_sq_fy_mc+sigma_sq
_y2_mc+sigma_sq_N_mc+sigma_sq_h_impact_ST+sigma_sq_k_mc+sigma_sq_m_ST_m
c+sigma_sq_v_mc+sigma_sq_a_mc+sigma_sq_r;

sigmaz_impact_ST = sqrt(sigmaz_impact_ST_sq);

rindex_impact_ST = muz_impact_ST/sigmaz_impact_ST;

reliability_impact_ST = (1/2)*erfc(-rindex_impact_ST/sqrt(2));

failure_prob_impact_ST = 1-reliability_impact_ST;

%ST Output
%disp(' ')
disp('If the vehicle type in the impact event is a semi-truck/trailer
(average mass')
disp('of 19,100 kilograms and impact height of 1.80 meters), then: ')
disp(' ')
disp('The reliability index of the reinforced concrete bridge pier
```

```
subject to impact is: ')
disp(rindex_impact_ST)

%disp(' ')
%disp('The reliability of the reinforced concrete bridge pier subject
to impact is: ')
%disp(reliability_impact_ST)

disp(' ')
disp('The probability of failure of the reinforced concrete bridge pier
subject to impact is: ')
disp(failure_prob_impact_ST)
```

APPENDIX B

```
%Prompt user for column parameters (concrete and reinforcement details)
disp('The column dimensions and reinforcement details are needed for
the analysis.')
disp(' ')
disp('This code only analyzes circular columns with spiral
reinforcement.')
disp('It is assumed that the vertical reinforcing consist of 8 bars
that are')
disp('evenly spaced in the column. It is also assumed that the spiral')
disp('reinforcement is adequate to support against shear.')
disp(' ')
%column_radius = input('Enter the radius of the reinforced concerete
bridge column in meters: ');
column_radius = .25; %meters
disp(' ')
%column_length = input('Enter the length of the reinforced concrete
brige column in meters: ');
column_length = 5; %meters
disp(' ')
vertical_barsize = input('Enter the bar size for the vertical
reinforcement, such as 3,4,etc.:','s');
disp(' ')
bar_count = 8; %input('Enter the number of bars in the vertical
reinforcement: ');
disp(' ')


%Column Parameter Calculations
Ag = pi*((column_radius*100)^2); %square centimeters
compressive_strength = 3; %KN/(cm^2)
column_diameter = 2*column_radius; %meters


if strcmp(vertical_barsize, '3')
    bar_diameter = 0.95; %centimeters
    bar_area = 0.710; %square centimeters
elseif strcmp(vertical_barsize, '4')
    bar_diameter = 1.27; %centimeters
    bar_area = 1.29; %square centimeters
elseif strcmp(vertical_barsize, '5')
    bar_diameter = 1.59; %centimeters
    bar_area = 2.0; %square centimeters
elseif strcmp(vertical_barsize, '6')
    bar_diameter = 1.91; %centimeters
    bar_area = 2.84; %square centimeters
elseif strcmp(vertical_barsize, '7')
    bar_diameter = 2.22; %centimeters
    bar_area = 3.87; %square centimeters
elseif strcmp(vertical_barsize, '8')
    bar_diameter = 2.54; %centimeters
    bar_area = 5.09; %square centimeters
elseif strcmp(vertical_barsize, '9')
    bar_diameter = 2.87; %centimeters
    bar_area = 6.45; %square centimeters
elseif strcmp(vertical_barsize, '10')
```

```
    bar_diameter = 3.23; %centimeters
    bar_area = 8.19; %square centimeters
elseif strcmp(vertical_barsize, '11')
    bar_diameter = 3.58; %centimeters
    bar_area = 10.06; %square centimeters
else
  disp('error, please enter a valid response (3,4,...,11)')
end

As = bar_area*bar_count; %square centimeters
fy = 50; %KN/(cm^2)
E = 57000*sqrt(compressive_strength); %KN/cm^2
row = As/Ag;
y2 = (column_radius*100)*2-2*3.8; %centimeters (1.5 inches cover to
rebar)

%Find Allowable Axial Load
%fixed fixed, so k = 0.5

I = pi()*((column_radius*100)^4)/4; %cm^4
rg = sqrt(I/Ag); %cm
slenderness = 0.5*(column_length*100)/rg;

%Pallowable
if slenderness > 40
    disp('slender column, please choose different column properties')
else
    P_allowable = 0.85*(0.85*compressive_strength*(Ag-As)+As*fy); %KN
end

%percentage = input('enter percentage: ');
%N = percentage*P_allowable; %KN
N = .75*P_allowable; %KN

%Monte Carlo Method for Resistance

n = 10000;

%Deterministic Value
gammaM = 1; %resistance uncertainty, unitless

%Nondeterministic Values

%Steel Area is Normal

As1_rand = rand(n,1);
As2_rand = rand(n,1);
As1i = -qfuncinv(As1_rand);
As2i = -qfuncinv(As2_rand);

As1 = 3*bar_area; %square centimeters
As2 = 2*bar_area; %square centimeters

gamma_As = 1.02;
mean_As1 = gamma_As*As1; %square centimeters
mean_As2 = gamma_As*As2; %square centimeters
```

```
sigma_As1 = .05*mean_As1; %square centimeters
sigma_As2 = .05*mean_As2; %square centimeters

%yield strength is lognormal

fy_rand = rand(n,1);
fyi = -qfuncinv(fy_rand);

gamma_fy = 1.1;
mean_fy = gamma_fy*fy; %KN/(cm^2)

sigma_fy = 0.05*mean_fy; %KN/(cm^2)

V_fy = sigma_fy/mean_fy;
sigma_lnfy =(log10(V_fy^2+1))^0.5;
mu_lnfy = log10(mean_fy)-0.5*(sigma_lnfy^2);

%Moment Arm is Normal

y2_rand = rand(n,1);
y2i = -qfuncinv(y2_rand);

sigma_y2 = .05*y2;

%Axial Load is Lognormal
N_rand = rand(n,1);
Ni = -qfuncinv(N_rand);

sigma_N = 0.1*N;

V_N = sigma_N/N;
sigma_lnN =(log10(V_N^2+1))^0.5;
mu_lnN = log10(N)-0.5*(sigma_lnN^2);

%Values of Random Variable
As1_mc = mean(mean_As1+As1i*sigma_As1);
As2_mc = mean(mean_As2+As2i*sigma_As2);
fy_mc = mean(exp(mu_lnfy+fyi*sigma_lnfy));
y2_mc = mean(y2+y2i*sigma_y2);
N_mc = mean(exp(mu_lnN+Ni*sigma_lnN));
fds = 1.23*fy_mc;

M_resistance =
gammaM*(As2_mc*fds*y2_mc+2*As1_mc*fds*(y2_mc/2)+N_mc*(y2_mc/2))/100;
%KN-m

%Prompt the user for the standoff distance
%R = input('Enter the standoff distance in meters for the reliability
analysis: '); %meters
R = 5; %meters
R_max = R; %meters
R_min = sqrt(((R_max)^2)+((column_length)^2)); %meters

W_lb = input('Enter the charge weight in lb of TNT: ');
```

```
W = W_lb/2.2; %kg of TNT
%gam = input ('enter gamma: ');
gam = 1.0;
%W = gam*200/2.2; %kg of TNT
n = 10000;

%Assume charge weight is Normal
W_rand = rand(n,1);

Wi = -qfuncinv(W_rand);

COV_CW = .33;
%COV_CW = input ('enter COV: ');
sigma_W = W*COV_CW;

W_mc = mean(W+Wi*sigma_W); %kg of TNT

%Use law of super-position to determine max moment with x_max
assumption
M_blast =
(((((6.7*W_mc)/(R_min^3))+1)*98066.5)*column_diameter*(column_length^2)
/12+(((((6.7*W_mc)/(R_max^3))+1)*98066.5)-
((((6.7*W_mc)/(R_min^3))+1)*98066.5))*column_diameter*(column_length^2)
/20)/1000; %KN-m

%Blast Performance Equation

muz_blast = M_resistance-M_blast;

%Column Resistance Sigma Calculations

%Partial Derivative Calculations
syms gammaM1 As2_mc1 As1_mc1 fds1 y2_mc1 N_mc1
Fr=(gammaM1*(As2_mc1*fds1*y2_mc1+2*As1_mc1*fds1*(y2_mc1/2)+N_mc1*(y2_mc
1/2))/100); %KN-m
pd_gammaM1 = diff(Fr,gammaM1);
pd_As2_mc1 = diff(Fr,As2_mc1);
pd_As1_mc1 = diff(Fr,As1_mc1);
pd_fds1 = diff(Fr,fds1);
pd_y2_mc1 = diff(Fr,y2_mc1);
pd_N_mc1 = diff(Fr,N_mc1);

gammaM1 = gammaM;
As2_mc1 = As2_mc;
As1_mc1 = As1_mc;
fds1 = fds;
y2_mc1 = y2_mc;
N_mc1 = N_mc;

pd_gammaM = subs(pd_gammaM1);
pd_As2_mc = subs(pd_As2_mc1);
pd_As1_mc = subs(pd_As1_mc1);
pd_fds = subs(pd_fds1);
pd_y2_mc = subs(pd_y2_mc1);
pd_N_mc = subs(pd_N_mc1);
```

```
%Partial Derivatives Squared
pd_gammaM_sq = pd_gammaM^2;
pd_As2_mc_sq = pd_As2_mc^2;
pd_As1_mc_sq = pd_As1_mc^2;
pd_fds_sq = pd_fds^2;
pd_y2_mc_sq = pd_y2_mc^2;
pd_N_mc_sq = pd_N_mc^2;

%Standard Deviations
std_gammaM = 0; %Deterministic
std_As2_mc = 0.05*As2_mc;
std_As1_mc = 0.05*As1_mc;
std_fds = 0.05*fds;
std_y2_mc = 0.05*y2;
std_N_mc = 0.1*N;

%Standard Deviations Squared
std_gammaM_sq = std_gammaM^2;
std_As2_mc_sq = std_As2_mc^2;
std_As1_mc_sq = std_As1_mc^2;
std_fds_sq = std_fds^2;
std_y2_mc_sq = std_y2_mc^2;
std_N_mc_sq = std_N_mc^2;

%Resistance SigmaZ Calculations
sigma_sq_gammaM = pd_gammaM_sq*std_gammaM_sq;
sigma_sq_As2_mc = pd_As2_mc_sq*std_As2_mc_sq;
sigma_sq_As1_mc = pd_As1_mc_sq*std_As1_mc_sq;
sigma_sq_fds = pd_fds_sq*std_fds_sq;
sigma_sq_y2_mc = pd_y2_mc_sq*std_y2_mc_sq;
sigma_sq_N_mc = pd_N_mc_sq*std_N_mc_sq;

%Blast Loading Sigma Calculations
syms W_mc1 R_min1 column_diameter1 column_length1 R_max1
Fi=(((((6.7*W_mc1)/(R_min1^3))+1)*98066.5)*column_diameter1*(column_len
gth1^2)/12+(((((6.7*W_mc1)/(R_max1^3))+1)*98066.5)-
((((6.7*W_mc1)/(R_min1^3))+1)*98066.5))*column_diameter1*(column_length
1^2)/20)/1000; %KN-m
pd_W_mc1 = diff(Fi,W_mc1);
pd_R_min1 = diff(Fi,R_min1);
pd_column_diameter1 = diff(Fi, column_diameter1);
pd_column_length1 = diff(Fi,column_length1);
pd_R_max1 = diff(Fi,R_max1);

W_mc1 = W_mc;
R_min1 = R_min;
column_diameter1 = column_diameter;
column_length1 = column_length;
R_max1 = R_max;

pd_W_mc = subs(pd_W_mc1);
pd_R_min = subs(pd_R_min1);
pd_column_diameter = subs(pd_column_diameter1);
pd_column_length = subs(pd_column_length1);
pd_R_max = subs(pd_R_max1);

%Car Partial Derivatives Squared
```

```
pd_W_mc_sq = pd_W_mc^2;
pd_R_min_sq = pd_R_min^2;
pd_column_diameter_sq = pd_column_diameter^2;
pd_column_length_sq = pd_column_length^2;
pd_R_max_sq = pd_R_max^2;

%Car Standard Deviations
std_W_mc = COV_CW*W_mc;
std_R_min = 0; %Deterministic
std_column_diameter = 0.05*column_diameter;
std_column_length = 0; %Deterministic
std_R_max = 0; %Deterministic

%Car Standard Deviations Squared
std_W_mc_sq = std_W_mc^2;
std_R_min_sq = std_R_min^2;
std_column_diameter_sq = std_column_diameter^2;
std_column_length_sq = std_column_length^2;
std_R_max_sq = std_R_max^2;

%Car Blast SigmaZ Calculations
sigma_sq_W_mc = pd_W_mc_sq*std_W_mc_sq;
sigma_sq_R_min = pd_R_min_sq*std_R_min_sq;
sigma_sq_column_diameter =
pd_column_diameter_sq*std_column_diameter_sq;
sigma_sq_column_length = pd_column_length_sq*std_column_length_sq;
sigma_sq_R_max = pd_R_max_sq*std_R_max_sq;

sigmaz_blast_sq =
sigma_sq_gammaM+sigma_sq_As2_mc+sigma_sq_As1_mc+sigma_sq_fds+sigma_sq_y
2_mc+sigma_sq_N_mc+sigma_sq_W_mc+sigma_sq_R_min+sigma_sq_column_diamete
r+sigma_sq_column_length+sigma_sq_R_max;

sigmaz_blast = sqrt(sigmaz_blast_sq);

rindex_blast = muz_blast/sigmaz_blast

reliability_blast = (1/2)*erfc(-rindex_blast/sqrt(2));

failure_prob_blast = 1-reliability_blast
```

APPENDIX C

```
%Prompt user for column parameters (concrete and reinforcement details)
disp('The column dimensions and reinforcement details are needed for
the analysis.')
disp(' ')
disp('This code only analyzes circular columns with spiral
reinforcement.')
disp('It is assumed that the vertical reinforcing consist of 8 bars
that are')
disp('evenly spaced in the column. It is also assumed that the spiral')
disp('reinforcement is adequate to support against shear.')
disp(' ')
%column_radius = input('Enter the radius of the reinforced concerete
bridge column in meters: ');
column_radius = 0.25; %meters
disp(' ')
%column_length = input('Enter the length of the reinforced concrete
brige column in meters: ');
column_length = 5; %meters
disp(' ')
vertical_barsize = input('Enter the bar size for the vertical
reinforcement, such as 3,4,etc.:','s');
disp(' ')
bar_count = 8; %input('Enter the number of bars in the vertical
reinforcement: ');
disp(' ')


%Column Parameter Calculations
Ag = pi*((column_radius*100)^2); %square centimeters
compressive_strength = 3*1.04; %KN/(cm^2)
column_diameter = 2*column_radius; %meters

if strcmp(vertical_barsize, '3')
    bar_diameter = 0.95; %centimeters
    bar_area = 0.710; %square centimeters
elseif strcmp(vertical_barsize, '4')
    bar_diameter = 1.27; %centimeters
    bar_area = 1.29; %square centimeters
elseif strcmp(vertical_barsize, '5')
    bar_diameter = 1.59; %centimeters
    bar_area = 2.0; %square centimeters
elseif strcmp(vertical_barsize, '6')
    bar_diameter = 1.91; %centimeters
    bar_area = 2.84; %square centimeters
elseif strcmp(vertical_barsize, '7')
    bar_diameter = 2.22; %centimeters
    bar_area = 3.87; %square centimeters
elseif strcmp(vertical_barsize, '8')
    bar_diameter = 2.54; %centimeters
    bar_area = 5.09; %square centimeters
elseif strcmp(vertical_barsize, '9')
    bar_diameter = 2.87; %centimeters
    bar_area = 6.45; %square centimeters
elseif strcmp(vertical_barsize, '10')
    bar_diameter = 3.23; %centimeters
```

```
    bar_area = 8.19; %square centimeters
elseif strcmp(vertical_barsize, '11')
    bar_diameter = 3.58; %centimeters
    bar_area = 10.06; %square centimeters
else
  disp('error, please enter a valid response (3,4,...,11)')
end

As = bar_area*bar_count; %square centimeters
fy = 50; %KN/(cm^2)
E = 57000*sqrt(compressive_strength); %KN/cm^2
row = As/Ag;
y2 = (column_radius*100)*2-2*3.8; %centimeters (1.5 inches cover to
rebar)

%Find Allowable Axial Load
%fixed fixed, so k = 0.5

I = pi()*((column_radius*100)^4)/4; %cm^4
rg = sqrt(I/Ag); %cm
slenderness = 0.5*(column_length*100)/rg;

%Pallowable
if slenderness > 40
    disp('slender column, please choose different column properties')
else
    P_allowable = 0.85*(0.85*compressive_strength*(Ag-As)+As*fy); %KN
end

N = 0.75*P_allowable; %KN

%Monte Carlo Method for Resistance

n = 10000;

%Deterministic Value
gammaM = 1; %resistance uncertainty, unitless

%Nondeterministic Values

%Steel Area is Normal

As1_rand = rand(n,1);
As2_rand = rand(n,1);
As1i = -qfuncinv(As1_rand);
As2i = -qfuncinv(As2_rand);

As1 = 3*bar_area; %square centimeters
As2 = 2*bar_area; %square centimeters

gamma_As = 1.02;
mean_As1 = gamma_As*As1; %square centimeters
mean_As2 = gamma_As*As2; %square centimeters

sigma_As1 = .05*mean_As1; %square centimeters
```

```
sigma_As2 = .05*mean_As2; %square centimeters

%yield strength is lognormal

fy_rand = rand(n,1);
fyi = -qfuncinv(fy_rand);

gamma_fy = 1.1;
mean_fy = gamma_fy*fy; %KN/(cm^2)

sigma_fy = 0.05*mean_fy; %KN/(cm^2)

V_fy = sigma_fy/mean_fy;
sigma_lnfy =(log10(V_fy^2+1))^0.5;
mu_lnfy = log10(mean_fy)-0.5*(sigma_lnfy^2);

%Moment Arm is Normal

y2_rand = rand(n,1);
y2i = -qfuncinv(y2_rand);

sigma_y2 = .05*y2;

%Axial Load is Lognormal
N_rand = rand(n,1);
Ni = -qfuncinv(N_rand);

sigma_N = 0.1*N;

V_N = sigma_N/N;
sigma_lnN =(log10(V_N^2+1))^0.5;
mu_lnN = log10(N)-0.5*(sigma_lnN^2);

%Values of Random Variable
As1_mc = mean(mean_As1+As1i*sigma_As1);
As2_mc = mean(mean_As2+As2i*sigma_As2);
fy_mc = mean(exp(mu_lnfy+fyi*sigma_lnfy));
y2_mc = mean(y2+y2i*sigma_y2);
N_mc = mean(exp(mu_lnN+Ni*sigma_lnN));

M_resistance =
(gammaM*(As2_mc*fy_mc*y2_mc+2*As1_mc*fy_mc*(y2_mc/2)+N_mc*(y2_mc/2)))/1
00; %KN-m

%Prompt user for vehicle type
disp(' ')
disp('The type of vehicle in the impact event is needed. Input the
vehicle type using the terms below.')
disp('If the vehicle is a car, enter 1.')
disp('If the vehicle is an SUV/van, enter 2.')
disp('If the vehicle is a small moving van/delivery truck, enter 3.')
disp('If the vehicle is a moving van/water truck, enter 4.')
disp('If the vehicle is a semi-truck/trailer, enter 5.')
disp(' ')
```

```
vehicle = input('Enter the vehicle in the impact event:','s');

if strcmp(vehicle, '1')
  h_impact = 0.61; %meters
  m = 2270; %kg
elseif strcmp(vehicle, '2')
  h_impact = 0.91; %meters
  m= 4540; %kg
elseif strcmp(vehicle, '3')
  h_impact = 1.22; %meters
  m = 8170; %kg
elseif strcmp(vehicle, '4')
  h_impact = 1.5; %meters
  m = 11800; %kg
elseif strcmp(vehicle, '5')
  h_impact = 1.8; %meters
  m = 19100; %kg
else
  disp('error, please enter a valid response')
end

%Prompt the user for vehicle speed
disp(' ')
%v = input('Enter the velocity of the vehicle in km/h for the
reliability analysis: ')*(1000/60); %meters/second
v = 110*(1000/60); %meters/second
disp(' ')
%a = input('Enter the acceleration of the vehicle in m/s^2 at impact
for the reliability analysis: ');

%vehicle = input('Enter the type of vehicle from the choices
above:','s');
%disp(' ')

%Define parameters for each type of vehicle

%Parameters for All Vehicles
  k = 300; %KN/m
  a = 3; %meters/square second
  r =23; %meters

%Monte Carlo Method for Loading

n = 10000;

%Nondeterministic Values

%Vehicle Stiffness is lognormal
k_rand = rand(n,1);
ki = -qfuncinv(k_rand);

sigma_k = 0.2*k;

V_k = sigma_k/k;
sigma_lnk =(log10(V_k^2+1))^0.5;
mu_lnk = log10(k)-0.5*(sigma_lnk^2);
```

```
%Vehicle Acceleration is Lognormal
a_rand = rand(n,1);
ai = -qfuncinv(a_rand);

sigma_a = 0.325*a;

V_a = sigma_a/a;
sigma_lna =(log10(V_a^2+1))^0.5;
mu_lna = log10(a)-0.5*(sigma_lna^2);

%vehicle speed is lognormal
%vehicle mass is normal

v_rand = rand(n,1);
m_rand = rand(n,1);

vi = -qfuncinv(v_rand);
mi = -qfuncinv(m_rand);

sigma_v = 0.15*v;

sigma_m = 0.33*m;


%lognormal calcs to calculate v_mc
V_v = sigma_v/v;
sigma_lnv = (log10(V_v^2+1))^2;
mu_lnv = log10(v)-0.5*(sigma_lnv^2);

%Values of Random Variables
k_mc = mean(exp(mu_lnk+ki*sigma_lnk)); %kN/m
a_mc = mean(exp(mu_lna+ai*sigma_lna)); %meters/s^2
v_mc = mean(exp(mu_lnv+vi*sigma_lnv)); %meters/s
m_mc = mean(m+mi*sigma_m)/1000; %1Mg=1000kg

%Impact Force Calculations
Fimpact = sqrt(k_mc*m_mc*((v_mc^2)-2*(-a_mc)*r)); %KN

%Applied Moment Calculation
M_impact = h_impact*Fimpact; %KN-m

%Impact Performance Equation

muz_impact = M_resistance-M_impact;

%Column Resistance Sigma Calculations

%Partial Derivative Calculations
syms gammaM1 As2_mc1 As1_mc1 fy_mc1 y2_mc1 N_mc1
Fr=(gammaM1*(As2_mc1*fy_mc1*y2_mc1+2*As1_mc1*fy_mc1*(y2_mc1/2)+N_mc1*(y
2_mc1/2))/100); %KN-m
pd_gammaM1 = diff(Fr,gammaM1);
pd_As2_mc1 = diff(Fr,As2_mc1);
pd_As1_mc1 = diff(Fr,As1_mc1);
```

```
pd_fy_mc1 = diff(Fr,fy_mc1);
pd_y2_mc1 = diff(Fr,y2_mc1);
pd_N_mc1 = diff(Fr,N_mc1);

gammaM1 = gammaM;
As2_mc1 = As2_mc;
As1_mc1 = As1_mc;
fy_mc1 = fy_mc;
y2_mc1 = y2_mc;
N_mc1 = N_mc;

pd_gammaM = subs(pd_gammaM1);
pd_As2_mc = subs(pd_As2_mc1);
pd_As1_mc = subs(pd_As1_mc1);
pd_fy_mc = subs(pd_fy_mc1);
pd_y2_mc = subs(pd_y2_mc1);
pd_N_mc = subs(pd_N_mc1);

%Partial Derivatives Squared
pd_gammaM_sq = pd_gammaM^2;
pd_As2_mc_sq = pd_As2_mc^2;
pd_As1_mc_sq = pd_As1_mc^2;
pd_fy_mc_sq = pd_fy_mc^2;
pd_y2_mc_sq = pd_y2_mc^2;
pd_N_mc_sq = pd_N_mc^2;

%Standard Deviations
std_gammaM = 0; %Deterministic
std_As2_mc = 0.05*As2_mc;
std_As1_mc = 0.05*As1_mc;
std_fy_mc = 0.05*fy_mc;
std_y2_mc = 0.05*y2;
std_N_mc = 0.1*N;

%Standard Deviations Squared
std_gammaM_sq = std_gammaM^2;
std_As2_mc_sq = std_As2_mc^2;
std_As1_mc_sq = std_As1_mc^2;
std_fy_mc_sq = std_fy_mc^2;
std_y2_mc_sq = std_y2_mc^2;
std_N_mc_sq = std_N_mc^2;

%Resistance SigmaZ Calculations
sigma_sq_gammaM = pd_gammaM_sq*std_gammaM_sq;
sigma_sq_As2_mc = pd_As2_mc_sq*std_As2_mc_sq;
sigma_sq_As1_mc = pd_As1_mc_sq*std_As1_mc_sq;
sigma_sq_fy_mc = pd_fy_mc_sq*std_fy_mc_sq;
sigma_sq_y2_mc = pd_y2_mc_sq*std_y2_mc_sq;
sigma_sq_N_mc = pd_N_mc_sq*std_N_mc_sq;

%Impact Loading Sigma Calculations

%Partial Derivative Calculations
syms h_impact1 k_mc1 m_mc1 v_mc1 a_mc1 r1
Fi=h_impact1*sqrt(k_mc1*m_mc1*((v_mc1^2)-2*(-a_mc1)*r1));
pd_h_impact1 = diff(Fi,h_impact1);
pd_k_mc1 = diff(Fi,k_mc1);
```

```
pd_m_mc1 = diff(Fi,m_mc1);
pd_v_mc1 = diff(Fi,v_mc1);
pd_a_mc1 = diff(Fi,a_mc1);
pd_r1 = diff(Fi,r1);

h_impact1 = h_impact;
k_mc1 = k_mc;
m_mc1 = m_mc;
v_mc1 = v_mc;
a_mc1 = a_mc;
r1 = r;

pd_h_impact = subs(pd_h_impact1);
pd_k_mc = subs(pd_k_mc1);
pd_m_mc = subs(pd_m_mc1);
pd_v_mc = subs(pd_v_mc1);
pd_a_mc = subs(pd_a_mc1);
pd_r = subs(pd_r1);

%Partial Derivatives Squared
pd_h_impact_sq = pd_h_impact^2;
pd_k_mc_sq = pd_k_mc^2;
pd_m_mc_sq = pd_m_mc^2;
pd_v_mc_sq = pd_v_mc^2;
pd_a_mc_sq = pd_a_mc^2;
pd_r_sq = pd_r^2;

%Standard Deviations
std_h_impact = 0; %Deterministic
std_k_mc = 0.2*k_mc;
std_m_mc = 0.33*m_mc;
std_v_mc = 0.15*v_mc;
std_a_mc = 0.325*a_mc; %Deterministic
std_r = 0; %Deterministic

%Standard Deviations Squared
std_h_impact_sq = std_h_impact^2;
std_k_mc_sq = std_k_mc^2;
std_m_mc_sq = std_m_mc^2;
std_v_mc_sq = std_v_mc^2;
std_a_mc_sq = std_a_mc^2;
std_r_sq = std_r^2;

%Impact SigmaZ Calculations
sigma_sq_h_impact = pd_h_impact_sq*std_h_impact_sq;
sigma_sq_k_mc = pd_k_mc_sq*std_k_mc_sq;
sigma_sq_m_mc = pd_m_mc_sq*std_m_mc_sq;
sigma_sq_v_mc = pd_v_mc_sq*std_v_mc_sq;
sigma_sq_a_mc = pd_a_mc_sq*std_a_mc_sq;
sigma_sq_r = pd_r_sq*std_r_sq;

sigmaz_impact_sq =
sigma_sq_gammaM+sigma_sq_As2_mc+sigma_sq_As1_mc+sigma_sq_fy_mc+sigma_sq
_y2_mc+sigma_sq_N_mc+sigma_sq_h_impact+sigma_sq_k_mc+sigma_sq_m_mc+sigm
a_sq_v_mc+sigma_sq_a_mc+sigma_sq_r;

sigmaz_impact = sqrt(sigmaz_impact_sq);
```

```
rindex_impact = muz_impact/sigmaz_impact;

reliability_impact = (1/2)*erfc(-rindex_impact/sqrt(2));

failure_prob_impact = 1-reliability_impact;

%REDUCTION
COV_Mr = .11;
sigma_Mr = COV_Mr*M_resistance;

if failure_prob_impact <= 0.12
    reduce = 1-1*(sigma_Mr/M_resistance);
elseif failure_prob_impact > 0.12 & failure_prob_impact <= 0.24
    reduce = 1-2*(sigma_Mr/M_resistance);
elseif failure_prob_impact > 0.24 & failure_prob_impact <= 0.36
    reduce = 1-3*(sigma_Mr/M_resistance);
elseif failure_prob_impact > 0.36 & failure_prob_impact <= 0.48
    reduce = 1-4*(sigma_Mr/M_resistance);
elseif failure_prob_impact > 0.48 & failure_prob_impact <= 0.60
    reduce = 1-5*(sigma_Mr/M_resistance);
elseif failure_prob_impact > 0.60 & failure_prob_impact <= 0.72
    reduce = 1-6*(sigma_Mr/M_resistance);
elseif failure_prob_impact > 0.72 & failure_prob_impact <= 0.84
    reduce = 1-7*(sigma_Mr/M_resistance);
elseif failure_prob_impact > 0.84
    reduce = 1-8*(sigma_Mr/M_resistance);
else
  disp('error, please enter a valid response (3,4,...,11)')
end

%Monte Carlo Method for Resistance

n = 10000;

%Deterministic Value
gammaM = 1; %resistance uncertainty, unitless

%Nondeterministic Values

%Steel Area is Normal

As1_rand = rand(n,1);
As2_rand = rand(n,1);
As1i = -qfuncinv(As1_rand);
As2i = -qfuncinv(As2_rand);

As1 = 3*bar_area; %square centimeters
As2 = 2*bar_area; %square centimeters

gamma_As = 1.02;
mean_As1 = gamma_As*As1; %square centimeters
mean_As2 = gamma_As*As2; %square centimeters

sigma_As1 = .05*mean_As1; %square centimeters
```

```
sigma_As2 = .05*mean_As2; %square centimeters

%yield strength is lognormal

fy_rand = rand(n,1);
fyi = -qfuncinv(fy_rand);

gamma_fy = 1.1;
mean_fy = gamma_fy*fy; %KN/(cm^2)

sigma_fy = 0.05*mean_fy; %KN/(cm^2)

V_fy = sigma_fy/mean_fy;
sigma_lnfy =(log10(V_fy^2+1))^0.5;
mu_lnfy = log10(mean_fy)-0.5*(sigma_lnfy^2);

%Moment Arm is Normal

y2_rand = rand(n,1);
y2i = -qfuncinv(y2_rand);

sigma_y2 = .05*y2;

%Axial Load is Lognormal
N_rand = rand(n,1);
Ni = -qfuncinv(N_rand);

sigma_N = 0.1*N;

V_N = sigma_N/N;
sigma_lnN =(log10(V_N^2+1))^0.5;
mu_lnN = log10(N)-0.5*(sigma_lnN^2);

%Values of Random Variable
As1_mc = mean(mean_As1+As1i*sigma_As1);
As2_mc = mean(mean_As2+As2i*sigma_As2);
fy_mc = mean(exp(mu_lnfy+fyi*sigma_lnfy));
y2_mc = mean(y2+y2i*sigma_y2);
N_mc = mean(exp(mu_lnN+Ni*sigma_lnN));
fds = 1.23*fy_mc;

M_resistance =
reduce*gammaM*(As2_mc*fds*y2_mc+2*As1_mc*fds*(y2_mc/2)+N_mc*(y2_mc/2))/
100; %KN-m

%Prompt the user for the standoff distance
%R = input('Enter the standoff distance in meters for the reliability
analysis: '); %meters
R = 15; %meters
R_max = R; %meters
R_min = sqrt(((R_max)^2)+((column_length)^2)); %meters



%gam = input ('enter gamma: ');
```

```
gam = 1.0;
W_lb = input('Enter the charge weight in lb of TNT: ');
W = gam*W_lb/2.2; %kg of TNT
%W = gam*25/2.2; %kg of TNT
n = 10000;

%Assume charge weight is Normal
W_rand = rand(n,1);

Wi = -qfuncinv(W_rand);

COV_CW = .33;
%COV_CW = input ('enter COV: ');
sigma_W = W*COV_CW;

W_mc = mean(W+Wi*sigma_W); %kg of TNT

%Use law of super-position to determine max moment with x_max
assumption
M_blast =
(((((6.7*W_mc)/(R_min^3))+1)*98066.5)*column_diameter*(column_length^2)
/12+(((((6.7*W_mc)/(R_max^3))+1)*98066.5)-
((((6.7*W_mc)/(R_min^3))+1)*98066.5))*column_diameter*(column_length^2)
/20)/1000; %KN-m

%Blast Performance Equation

muz_blast = M_resistance-M_blast;

%Column Resistance Sigma Calculations

%Partial Derivative Calculations
syms gammaM1 As2_mc1 As1_mc1 fds1 y2_mc1 N_mc1
Fr=reduce*(gammaM1*(As2_mc1*fds1*y2_mc1+2*As1_mc1*fds1*(y2_mc1/2)+N_mc1
*(y2_mc1/2))/100); %KN-m
pd_gammaM1 = diff(Fr,gammaM1);
pd_As2_mc1 = diff(Fr,As2_mc1);
pd_As1_mc1 = diff(Fr,As1_mc1);
pd_fds1 = diff(Fr,fds1);
pd_y2_mc1 = diff(Fr,y2_mc1);
pd_N_mc1 = diff(Fr,N_mc1);

gammaM1 = gammaM;
As2_mc1 = As2_mc;
As1_mc1 = As1_mc;
fds1 = fds;
y2_mc1 = y2_mc;
N_mc1 = N_mc;

pd_gammaM = subs(pd_gammaM1);
pd_As2_mc = subs(pd_As2_mc1);
pd_As1_mc = subs(pd_As1_mc1);
pd_fds = subs(pd_fds1);
pd_y2_mc = subs(pd_y2_mc1);
pd_N_mc = subs(pd_N_mc1);
```

```
%Partial Derivatives Squared
pd_gammaM_sq = pd_gammaM^2;
pd_As2_mc_sq = pd_As2_mc^2;
pd_As1_mc_sq = pd_As1_mc^2;
pd_fds_sq = pd_fds^2;
pd_y2_mc_sq = pd_y2_mc^2;
pd_N_mc_sq = pd_N_mc^2;

%Standard Deviations
std_gammaM = 0; %Deterministic
std_As2_mc = 0.05*As2_mc;
std_As1_mc = 0.05*As1_mc;
std_fds = 0.05*fds;
std_y2_mc = 0.05*y2;
std_N_mc = 0.1*N;

%Standard Deviations Squared
std_gammaM_sq = std_gammaM^2;
std_As2_mc_sq = std_As2_mc^2;
std_As1_mc_sq = std_As1_mc^2;
std_fds_sq = std_fds^2;
std_y2_mc_sq = std_y2_mc^2;
std_N_mc_sq = std_N_mc^2;

%Resistance SigmaZ Calculations
sigma_sq_gammaM = pd_gammaM_sq*std_gammaM_sq;
sigma_sq_As2_mc = pd_As2_mc_sq*std_As2_mc_sq;
sigma_sq_As1_mc = pd_As1_mc_sq*std_As1_mc_sq;
sigma_sq_fds = pd_fds_sq*std_fds_sq;
sigma_sq_y2_mc = pd_y2_mc_sq*std_y2_mc_sq;
sigma_sq_N_mc = pd_N_mc_sq*std_N_mc_sq;

%Blast Loading Sigma Calculations
syms W_mc1 R_min1 column_diameter1 column_length1 R_max1
Fi=(((((6.7*W_mc1)/(R_min1^3))+1)*98066.5)*column_diameter1*(column_len
gth1^2)/12+(((((6.7*W_mc1)/(R_max1^3))+1)*98066.5)-
((((6.7*W_mc1)/(R_min1^3))+1)*98066.5))*column_diameter1*(column_length
1^2)/20)/1000; %KN-m
pd_W_mc1 = diff(Fi,W_mc1);
pd_R_min1 = diff(Fi,R_min1);
pd_column_diameter1 = diff(Fi, column_diameter1);
pd_column_length1 = diff(Fi,column_length1);
pd_R_max1 = diff(Fi,R_max1);

W_mc1 = W_mc;
R_min1 = R_min;
column_diameter1 = column_diameter;
column_length1 = column_length;
R_max1 = R_max;

pd_W_mc = subs(pd_W_mc1);
pd_R_min = subs(pd_R_min1);
pd_column_diameter = subs(pd_column_diameter1);
pd_column_length = subs(pd_column_length1);
pd_R_max = subs(pd_R_max1);

%Car Partial Derivatives Squared
```

```
pd_W_mc_sq = pd_W_mc^2;
pd_R_min_sq = pd_R_min^2;
pd_column_diameter_sq = pd_column_diameter^2;
pd_column_length_sq = pd_column_length^2;
pd_R_max_sq = pd_R_max^2;

%Car Standard Deviations
std_W_mc = COV_CW*W_mc;
std_R_min = 0; %Deterministic
std_column_diameter = 0.05*column_diameter;
std_column_length = 0; %Deterministic
std_R_max = 0; %Deterministic

%Car Standard Deviations Squared
std_W_mc_sq = std_W_mc^2;
std_R_min_sq = std_R_min^2;
std_column_diameter_sq = std_column_diameter^2;
std_column_length_sq = std_column_length^2;
std_R_max_sq = std_R_max^2;

%Car Blast SigmaZ Calculations
sigma_sq_W_mc = pd_W_mc_sq*std_W_mc_sq;
sigma_sq_R_min = pd_R_min_sq*std_R_min_sq;
sigma_sq_column_diameter =
pd_column_diameter_sq*std_column_diameter_sq;
sigma_sq_column_length = pd_column_length_sq*std_column_length_sq;
sigma_sq_R_max = pd_R_max_sq*std_R_max_sq;

sigmaz_blast_sq =
sigma_sq_gammaM+sigma_sq_As2_mc+sigma_sq_As1_mc+sigma_sq_fds+sigma_sq_y
2_mc+sigma_sq_N_mc+sigma_sq_W_mc+sigma_sq_R_min+sigma_sq_column_diamete
r+sigma_sq_column_length+sigma_sq_R_max;

sigmaz_blast = sqrt(sigmaz_blast_sq);

rindex_blast = muz_blast/sigmaz_blast

reliability_blast = (1/2)*erfc(-rindex_blast/sqrt(2));

failure_prob_blast = 1-reliability_blast
```